Mechanisms of Mutation at Mouse Expanded Simple Tandem Repeat (ESTR) Loci

Thesis submitted for the degree of

Doctor of Philosophy

At the University of Leicester

by

Robert John Hardwick

University of Leicester

September 2007

University *of* Leicester

UMI Number: U235838

UMI

Dissertation Publishing

ProQuest

Contents

References

Abstract

Mechanisms of Mutation at Mouse
Expanded Simple Tandem Repeat (ESTR) Loci

Robert John Hardwick

Mouse expanded simple tandem repeat (ESTR) loci are non-coding, unstable arrays of short repeat units with high spontaneous mutation rates (up to 15% per gamete). Exposure to ionising radiation and some chemicals can elevate the mutation rate further, which makes them useful tools for the assessment of genomic mutation rates.

ESTRs mutate by either gaining or losing repeat units to result in the generation of differentially-sized mutant alleles. However, the mechanism by which this occurs remains unclear, and this hinders the reliable extrapolation of ESTR data to other loci. To address this issue, this thesis aimed to investigate the mechanism of mutation at the ESTR locus Ms6-hm.

Recent evidence has suggested that events at DNA replication are responsible for generating ESTR mutants. If this is the case, then it would be expected that ESTR mutation rate would increase in line with the number of cell division events in a tissue system. In this thesis, the speculated link between cell division rate and ESTR mutation rate was tested in three different tissues of varying mitotic proficiencies: brain (low mitotic index), bone marrow (intermediate mitotic index), and sperm (high mitotic index). In the first instance, spontaneous mutation rates in each of these tissues were assessed in mice of four different age groups: 12, 26, 48, and 96 weeks old; and in the second part of this thesis, in utero-irradiated mice were analysed to evaluate the mitosis-proficient process of embryogenesis.

I report increases in ESTR spontaneous mutation rate in sperm with age, but not in brain, and I also demonstrate that ESTR mutation rates are elevated in each tissue – including brain – following in utero-irradiation. I conclude that DNA replication is an important process in the generation of ESTR mutants.

Abbreviations

AP – Apurinic/Apyrimidinic site
APC – Anaphase promoting complex
ARS – Autonomously replicating sequences
ATM – Ataxia telangiectasia-mutated
ATR – ATM and Rad3-related
BER – Base excision repair
BIR – Break-induced repair
BrdU – Bromodeoxyuridine
CAF – Chromatin assembly factor
CAP – Chromatin associated protein
CDK – Cyclin-dependent kinase
DDK – Dbf-dependent kinase
DnMT – DNA methyltransferase
DSB – Double strand break
GG-NER – Global genomic NER
HAT – Histone acetyltransferase
HDAC – Histone deacetylase
HMT – Histone methyltransferase
HP1 – Heterochromatin protein 1
HSC – Haemopoeitic stem cell
MPF – M-phase promoting factor
NER – Nucleotide excision repair
NHEJ – Non-homologous end-joining
NSC – Neural stem cell
ORC – Origin recognition complex
PARP – Poly(ADP-ribose) polymerase
PCNA – Proliferating cell nuclear antigen
PcG – Polycomb Group
PIKK – phosphatidylinositol 3' kinase-like kinase
PNK – Polynucleotide kinase
pre-RC – pre-replicative complex
ROS – Reactive oxygen species
SCE – Sister-chromatid exchange
SDSA – Synthesis-dependent strand annealing
SMC – Structural maintenance of chromosome
SSA – Single-strand annealing
SSB – Single-strand break
TC-NER – Transcription-coupled NER
TLS – Translesion synthesis

Acknowledgments

Chapter 1: Introduction

1.1 General Introduction

Eukaryotic chromosomes are dynamic structures that are constantly being reconfigured to fulfil their many different roles. They must be tightly packaged to fit within the nucleus, but must also be readily accessible to a range of DNA binding proteins during DNA transactions such as replication, recombination, repair, and gene transcription. This structural fluidity is delivered by various DNA-binding proteins, epigenetic factors, and post-translational modifications.

The dual impact of the structural distortions imposed on each chromosome during these various manipulations and the vulnerability of chromosomes to errors during replication, recombination, and repair, leaves chromosomes susceptible to mutations which could potentially be very harmful to the cell. In addition, exposure to external genotoxic agents may increase the likelihood of chromosomes experiencing structural anomalies, through the harmful interactions that these agents can have with DNA molecules. If these mutations are allowed to accumulate in the cell, it could potentially lead to diseases such as cancer, and thus it is important to gather estimates of the effects of mutagenic exposure on DNA mutation frequencies in order to assess the safety of exposure to these agents.

In recent years tandemly repeated DNA loci have been used as markers for mutation induction following mutagenic exposure. One example are mouse expanded simple tandem repeat (ESTR) loci, which have provided estimates of mutation rates following ionising radiation (e.g. Dubrova, et al., 2000a) and chemical exposures (e.g. Vilarino-Guell, et al., 2003), but to date the mechanism by which they mutate remains unclear. It is the purpose of this thesis to address this issue of ESTR mutation mechanism, and in this chapter an introduction to the key chromosome manipulations and their influence on ESTR stability will be given as background for the later results and discussion chapters.

1.2 Chromosome Dynamics Through the Cell Cycle

1.2.1 Cell and Nuclear Division and the Cell Cycle

Cell and nuclear division is the fundamental biological process by which new cells (the daughter cells) are produced from existing cells (the parental cells). In higher eukaryotes this can occur by mitosis to create genetically-identical daughter cells for tissue growth, development, and cell number maintenance, or alternatively by germline-restricted meiosis to produce genetically variable haploid gametes. In each case, for the cell to successfully complete the division process, it must progress through a series of genetic and cellular transactions with periodic checkpoints to monitor the precision of these events. These checkpoints may halt this otherwise continuous cell cycle should the cell be in an unsatisfactory condition. Resumption of the cycle will occur from that checkpoint only when the necessary criteria for progression have been fulfilled.

The stages of the mitotic cell cycle are well-defined and known as S-phase (in which DNA synthesis occurs), M-phase (in which the cells complete mitosis), and the gap (G) phases G_1 (between S- and M-phase), and G_2 (between M- and S-phase). A fifth 'quiescent' state called G_0 also exists for cells that have temporarily exited the cell cycle, such as non-dividing nerve and muscle cells. Similarly, meiosis undergoes this same succession of phases before entering into a second consecutive M-phase with no intervening S-phase. These successive meiotic M-phase divisions are called meiosis I and meiosis II, and result in the production of the haploid gametes.

At the DNA level the cell cycle is responsible for directing quite dramatic structural modifications upon each chromosome in order to aid their transcription, duplication, and segregation. During interphase (the combined period of G_1, S, and G_2 phases) of both mitosis and meiosis, chromosomes exist as thin and dispersed filaments within the nucleus, experiencing constant manipulation by proteins involved in transcription and replication. As the mitotic and meiotic cycles move through G_1 and into M-phase, the chromosomes are subjected to further structural modifications acting to condense the filaments into more compact structures. In meiotic cells, the M-phase chromosomes are also permissive to modification by homologous recombination.

Whilst these various DNA modifications and transactions are critical for sustaining the viability of their host cells, they can also pose a number of problems if and when they malfunction. The significance and timing of these structural

manipulations will be discussed in the following sections, beginning with an overview of the most fundamental level of chromosome organisation: chromatin.

1.2.2 Chromatin Structure

Chromatin is the DNA-protein complex that results from interactions between the naked DNA duplex and its various DNA-binding proteins. The most abundant of these chromatin-associated proteins (CAPs) are the histones; a family of highly conserved basic proteins that are classified into five major types termed H1, H2A, H2B, H3 and H4. The other CAPs can generally be described as either remodelling proteins which change the physical chromatin structure, or modifying factors which introduce biochemical modifications to the chromatin.

The histones are amongst the first CAPs to bind to DNA to manipulate its conformation. Two copies each of the histones H2A, H2B, H3, and H4 contribute to a particulate structure called the nucleosome; a 10 nm diameter complex which consists of a precise length of 146 base pairs of DNA wrapped around an octameric assemblage of these histones (Luger, *et al.*, 1997). Long linear arrays of these nucleosomes are formed to give interphase chromatin the appearance of 'beads on a string'. The DNA connecting each nucleosome is called 'linker DNA', and it is with these DNA tracts that histone H1 associates to stabilise higher-order structures (Thoma, *et al.*, 1979).

The role of chromatin remodelling factors is to make DNA more accessible to other DNA-binding proteins by spatially and temporally manipulating nucleosomes to reveal and occlude local DNA-binding targets. At the core of chromatin remodelling factors is a catalytic ATPase which hydrolyses ATP to harvest energy for the active loosening of the DNA-histone connection. This makes nucleosomes more amenable to positional rearrangements such as histone removal (Boeger, *et al.*, 2003) and histone-variant exchange (Mizuguchi, *et al.*, 2004). ATP-dependent remodelling factors have also been linked to double-strand break repair (Morrison, *et al.*, 2004; van Attikum, *et al.*, 2004) and replication (Collins, *et al.*, 2002; Poot, *et al.*, 2004), but the significance of this is not certain.

Chromatin modifying factors catalyse the post-translational addition of chemical groups to DNA and histone protein components of the primary chromatin molecule. These modifications may be heritable through a DNA replication-dependent mechanism of incorporation (epigenetic modifications), or alternatively they can be catalysed via DNA replication-independent *de novo* events. Given the breadth of different post-translational chromatin modifications they will be described separately below.

1.2.3 Post-translational Histone Modifications

A variety of post-translational chemical modifications can be incorporated into histones via their N-terminal protruding amino acid terminal tails or at exposed sites on their C-terminal globular domains. Although the role of these modifications remains inadequately defined, in general they appear to mark histones as protein binding or non-binding sites to facilitate or restrict transcription, replication, recombination, and repair (Strahl and Allis, 2000). These histone modifications include acetylation, methylation, phosphorylation, ubiquitination, and ADP-ribosylation, and will be detailed more below.

1.2.3.1 Histone Acetylation

Reactions that catalyse the addition of acetyl groups to histones are broadly associated with transcriptional activation, although there are exceptions to this rule (De Nadal, et al., 2004). The chromatin modifying enzymes that perform these reactions are the histone acetyltransferases (HATs) which target lysine residues at the ϵ-NH_3^+ position of the histone tail to neutralise the local positive charge. However, these reactions can be reversed by histone deacetylases (HDACs). HATs are reviewed more extensively elsewhere (Roth, et al., 2001), as are HDACs (de Ruijter, et al., 2003).

1.2.3.2 Histone Methylation

Histone methylation is carried out by histone methyltransferases (HMTs), which can target both lysine and arginine residues in the histone polypeptide tail (Kouzarides, 2002; Zhang and Reinberg, 2001). Lysines can accept up to three methyl groups, giving rise to mono-, di-, and trimethylated forms, whilst arginine can be either mono- or dimethylated. These various levels of methylation can serve different functions such as transcriptional activation (Chen, et al., 1999) and repression (Briggs, et al., 2001). It also appears that differences in the methylation status of the same residue can be influential, with Santos-Rosa et al. (2002) showing that H3K4 trimethylation is restricted to active genes whilst H3K4 dimethylation may be found in both active and inactive euchromatic genes.

Histone methylation appears to be more chemically stable than acetylation and until recently was thought to be irreversible. However, deimination of arginine into citrulline has been shown to erase methylated arginines (Cuthbert, et al., 2004; Wang, et al., 2004), and demethylation of lysines has been demonstrated to occur courtesy of an amino-oxidase reaction (Shi, et al., 2004).

1.2.3.3 Histone Phosphorylation

Histone phosphorylation is mainly seen on the histone tails of H1 and H3 at residues serine 10, serine 28, and threonine 11. It appears to be involved in chromosome condensation (Mahadevan, *et al.*, 1991; Van Hooser, *et al.*, 1998; Chadee, *et al.*, 1999), gene expression (Crosio, *et al.*, 2000), and the promotion of lysine acetylation for the transcriptional activation (Lo, *et al.*, 2001).

1.2.3.4 Histone Ubiquitination

The protein ubiquitin is found in most living organisms and associated with a range of cellular processes. One such process is nucleosome modification, although its involvement in this is still not well understood.

Ubiquitin attaches to lysine residues through a cascade of enzymatic events, involving proteins belonging to three groups called E1, E2, and E3. E1 enzymes are ubiquitin-activating complexes that subsequently transfer ubiquitin to ubiquitin-conjugating E2 enzymes. Finally, ubiquitin is attached to lysine residues by the action of E3 ubiquitin ligases. Studies have shown that histone H2A is a target for ubiquitination (Nickel and Davie, 1989), that H2B can be ubiquitinated by E2 and E3 enzymes (Robzyk, *et al.*, 2000), and that H3 can be ubiquitinated in elongating spermatids of rat testes (Chen, *et al.*, 1998). Other papers suggest a certain amount of crosstalk between histone ubiquitination and histone methylation (Dover, *et al.*, 2002; Sun and Allis, 2002), and with these in mind, it is feasible that histone ubiquitination may play a role in chromatin structure and dynamics.

1.2.3.5 ADP-Ribosylation

Poly(ADP-ribosyl)ation is the attachment of ADP-ribose units onto their target histone proteins; the main targets being H1, H2A, and H2B. ADP-ribosylation is most pronounced following the introduction of strand breaks, as this event triggers the stimulation of poly(ADP-ribose) polymerase-1 (PARP-1) activity and poly(ADP-ribosyl)ation of linker histone H1. Furthermore, recent findings suggest that histone poly(ADP-ribosyl)ation also plays a role in gene transcription, chromatin organisation, and chromatin condensation (Tulin and Spradling, 2003; Kraus and Lis, 2003; Rouleau, *et al.*, 2004 [Review]).

1.2.4 The Histone Code Hypothesis

The information above demonstrates the variety of histone modifications known to exist, and prompted Strahl and Allis (2000), in their 'histone code' hypothesis, to suggest that individual histone modifications do not function in

isolation, but instead in partnerships. They speculated that signatures of histone modifications may instruct DNA-binding factors to drive specific DNA transactions including transcriptional activation and repression, chromosome condensation, or DNA replication, recombination, and repair. Strahl and Allis (2000) even proposed that the different combinations of histone modifications could achieve this through the localised changes in charge density and distribution that they would bring.

This model could help explain how the same chemical modification can have different functional consequences depending on the target residue. For example, methylation of H3 K4 is correlated with gene activation (Santos-Rosa, et al., 2002), whereas H3 K9 methylation results in repression and heterochromatin formation (Bannister, et al., 2001; Lachner, et al., 2001). It does, however, remain a hypothesis.

1.2.5 Polycomb and Trithorax Group Proteins

Another important group of chromatin modifying proteins are the transcriptionally-repressive polycomb group (PcG) and the transcriptionally-activating trithorax group (trxG) proteins, which can each epigenetically regulate gene expression. The significance of these proteins lies in their heritability, which contrasts to the post-translational *de novo* histone modifications detailed above.

The two main silencing PcG complexes are polycomb repressive complexes 1 and 2 (PRC1 and PRC2). In *Drosophila melanogaster* they interact with regulatory PcG response elements (PREs) to control their target loci (Tilib, et al., 1999), beginning with the tri-methylation of H3K27 residues at a PRE by PRC2 (Boyer, et al., 2006), and completed when PRC1 recognises this tri-methylation mark and binds to the PRE to initiate chromatin compaction. In addition, recent evidence suggests that components of the RNAi machinery may be involved in regulating the nuclear organisation of PcG chromatin targets (Grimaud, et al., 2006), but the mechanisms of this epigenetic inheritance remain unclear.

The trxG complexes possess a H3K4 tri-methylase activity (e.g. Dou, et al., 2005), and so are seemingly involved in transcription activation given that tri-methylated H3K4 is a feature associated with most active gene promoters (Kim, et al., 2005). As with the PcG proteins, the intricacies of how the trxG proteins are stably inherited through DNA replication have not been established.

1.2.6 DNA Modification by Cytosine Methylation

So far the effects of CAPs and their post-translational modifications on chromatin dynamics have been discussed, but the DNA component of chromatin is

also subject to chemical modification via sequence-specific DNA methylation. This modification can persist through DNA replication and be stably inherited (Rakyan, *et al.*, 2003), and so represents another epigenetic chromatin modification. The mechanism by which DNA is methylated is governed by several chromatin modifying factors.

In mammals, DNA methylation is almost exclusively targeted to cytosine residues located 5' to a guanine base in CpG (cytosine-phospho-guanine) dinucleotide sequences. These CpG dinucleotides tend to be clustered together in short GC-rich regions of 0.5 to 4 kb in length, and are widely known as 'CpG islands' (Bird, 2002a). CpG islands are normally found in a hypomethylated state that permits transcription of adjacent genes, but they are known to display tissue and developmental stage-specific states of methylation that act to suppress neighbouring gene expression (Bird, 2002a). These differing patterns of methylation can support a range of cellular functions and pathologies that include tissue-specific transcriptional regulation, cell differentiation, genomic imprinting, chromatin organisation, cancer, and ageing (Bird, 2002a; Robertson and Wolffe, 2000).

The covalent addition of methyl groups to cytosine bases is catalysed by various chromatin-modifying DNA methyltransferases (DNMT), which can be broadly divided into three different families: DNMT1, DNMT2, and DNMT3. The DNMT1 enzyme is involved in the copying and transmission of cellular CpG methylation patterns from parental to daughter cells, and holds a *de novo* methylating function. It has been shown to associate with replication foci (Liu, *et al.*, 1998), but will mainly target the unmethylated newly synthesised strands of sequence-specific hemimethylated CpG regions using the methylated parent strand as its template (Yoder, *et al.*, 1997). The DNMT3 family of methyltransferases comprises DNMT3a and DNMT3b, which are abundant in early embryonic cells where they perform their *de novo* methyltransferase function (Okano, *et al.*, 1998; 1999). The function of the DNMT2 family is still largely unclear.

Although CpG dinucleotides are the predominant mammalian targets for cytosine methylation, there is also evidence to suggest that non-CpG methylation (prinicipally in the form of CpA methylation) may account for between 15 and 20% of cytosine methylation in embryonic stem cells but not in somatic cells (Ramsahoye, *et al.*, 2000). However, the significance of this is not yet understood.

1.2.7 Chromatin Dynamics Through the Cell Cycle

The structural properties of chromatin have been defined in the sections above, but as previously stated, the structure as a whole is constantly changing

throughout the cell cycle. Each stage of the cell cycle directs a range of chromatin conformational changes to promote hierarchical layers of folding and other DNA transactions such as transcription, replication, recombination, and repair, and in this section the dynamic nature of chromosome structure will be illustrated in accordance with cell cycle stage.

1.2.8 G₁-Phase Chromosomes

G_1-phase chromosomes exist primarily as single protracted 10 nm chromatid fibres, but become increasingly compressed as G_1 advances. Compaction is initiated as the 10 nm fibres incorporate histone H1 proteins and commence supercoiling into bulkier fibres of 30 nm diameter (Finch and Klug, 1976). These 30 nm fibres are themselves then organised into loops which attach to strands of protruding nuclear envelope matrix protein at the loop bases. The stems of these loops are thus known as matrix attachment regions (MARs).

In parallel to this structural compaction, chromatin conformation is manipulated during the process of G_1 gene transcription. Transcription requires chromatin remodelling factors to shape a more accessible chromatin structure (Boeger, et al., 2003; Mizuguchi, et al., 2004) and to interact with the transcription machinery at cis-acting regulatory elements (Goldmark, et al., 2000; Sullivan, et al., 2001). These localised changes in chromatin structure will be distributed across the genome at any given time.

Towards the end of G_1 the DNA replication machinery begins to assemble on the chromatin in preparation for DNA synthesis. Numerous sites throughout the genome are randomly marked (or 'licensed') as replication origins by the loading of multiprotein pre-replicative complexes (pre-RCs), but these will only become activated at the forthcoming S-phase. Each pre-RC is a composite of at least four proteins: a heterohexamer complex of 'mini chromosome maintenance' proteins called Mcm2–7, a replication-origin recognition complex (ORC), and two initiator factors called Cdc6 and Cdt1. These components are loaded sequentially during pre-RC formation (Figure 1.1).

The first pre-RC component to be laid down is ORC which, in higher eukaryotes, could be orchestrated by histone acetylation (Aggarwal and Calvi, 2004), and/or an affinity for topological modifications such as negatively supercoiled DNA (Remus, et al., 2004). With ORC in position the proteins Cdc6 and Cdt1 independently associate with ORC-bound chromatin (Nishitani, et al., 2000; Maiorno, et al., 2000) to act as mediators for the binding of the Mcm2–7 unit. Mcm2–7 forms a hexameric ring structure around the DNA duplex (Fletcher, et al.

2003; Pape, *et al.* 2003), and probably operates as a replicative helicase, as suggested by *in vitro* studies of its subcomplex Mcm4-6-7 (Ishimi, 1997). In any event, the completion of pre-RC formation at numerous licensed sites together with the compaction of chromosomes into coiled 30 nm fibres signals the completion of G_1 and the transition into S-phase.

1.2.9 S-Phase Chromosomes

The defining event of S-phase is DNA replication, which begins following the conversion of dormant G_1 pre-RCs into active replication factories. This multi-step process adapts the conformations of the S-phase 10 and 30 nm chromatin fibres to allow the cellular replication machinery to access the chromatin molecule and duplicate it. The different stages of replication will be described below with respect to the effects they have on chromatin structure.

1.2.9.1 Chromatin Opening

The first structural distortion imposed on chromatin by DNA replication is duplex partitioning at each replication origin. The mechanism by which this occurs is unclear, but may involve chromatin-binding factors such as the heterochromatin remodelling complexes WSTF-ISWI (Bozhenok, *et al.*, 2002) and ACF-ISWI (Collins, *et al.*, 2002), and possibly strand repulsion induced by charge densities stemming from modified histones (Strahl and Allis, 2000). The purpose of this opening, though, is well established: it enables incoming replication proteins to bind to the chromatin (Figure 1.1).

1.2.9.2 Polymerase Loading and Replisome Establishment

Once the chromatin structure has been relaxed at each replication origin, the newly exposed single-strands of DNA and their pre-RCs become the targets for further protein assembly. This starts with the ordered recruitment of the initiator factors Mcm10 and Cdc45 to the replication origin (Wohlschlegel, *et al.*, 2002), and the subsequent recruitment of other replication proteins by Cdc45 to establish the replication machinery (Mimura, *et al.*, 2000).

The first role of Cdc45 is to interact with DNA polymerase α (DNA pol α) and assist the binding of this enzyme to DNA (Mimura, *et al.*, 2000). DNA pol α then directs the synthesis of short RNA primers on each of the single-stranded leading and lagging strands, and once these primers are in place, the sliding-clamp protein 'proliferating cell nuclear antigen' (PCNA) will engage with the primed DNA (Mimura, *et al.*, 2000). The recruitment of PCNA is facilitated by the dual action of the clamp-

loading protein Replication Factor C (RFC) and interaction with Cdc45 (Aparicio, *et al.*, 1999).

The proteins PCNA and Cdc45 provide a platform on which the DNA polymerases δ and ε (DNA pols δ and ε) can engage with the origin and replace DNA pol α. This process is called 'polymerase switching' (Tsurimoto and Stillman, 1991). Cdc45 again has a role here, providing a physical link between the pre-RC and DNA pol ε (Walter and Newport, 2000). Both DNA pol δ and ε use the primers laid down by DNA pol α as double-stranded initiating points for elongation synthesis. Unlike DNA pol α, DNA pol δ and ε possess a 5′→ 3′ proofreading function which makes them adept at long-range DNA synthesis, and the correction of any errors accrued over these greater distances.

The core tetra-complex amalgamation of DNA pol δ and ε, PCNA, and RFC is called the 'replicase' and represents the principal structure responsible for DNA synthesis. When additional replication factors associate with the replicase it creates a larger 'replisome' complex. Many of these proteins are regulated by post-translational modifications, such as ubiquitination and sumolynation of PCNA (Hoege *et al.*, 2002) (Figure 1.1).

1.2.9.3 Establishment of Replication Forks

With fully operational replicases now assembled, the duplex strands on each side of each replication origin are portioned to create branched chromatin structures called 'replication forks'. The replicases residing at the branch junctures will migrate in opposite directions on their opposite template strands to permit bidirectional DNA synthesis (Figure 1.1).

The bidirectional passage of replication forks away from replication origins incurs continual downstream structural fluidity on the chromatin as the duplex is unwound. The newly exposed single DNA strands are stabilised by the single-strand binding protein replication protein A (RPA), which links in with the replicase via Cdc45 (Zou and Stillman, 2000). RPA protects the single-stranded DNA from degradation, and also prevents hairpin formation. Nucleosomes that impede replication fork movement are disassembled into their component parts of H3-H4 tetramers and two H2A-H2B dimers. Once the fork has passed, these histones are then reassembled into nucleosomes along with freshly synthesised histones to occupy both the existing and the nascent DNA strands at that region (Gruss, *et al.*, 1993; Verreault, *et al.*, 1996). The bidirectional movement of forks means that replisomes will inevitably encounter each other, and when this occurs the replisomes are disbanded and the process halted.

10

The completion of DNA replication during late S-phase produces an identical partnering chromatin filament to the original template chromatin. These chromatin companions are at this stage renamed as sister chromatids. Further replication from the replication origins at this point is prevented by cyclin-dependent kinases (CDKs) which inhibit replication from here and through to G_2 and M-phase (Dahmann, et al., 1995; Piatti, et al., 1996). They may achieve this by targeting Cdt1 for proteolysis (Nishitani, et al., 2001) or inhibition by germinin (McGarry and Kirschner, 1998), and through inhibitory phosphorylation of ORC (Nguyen, et al., 2001; Li, et al., 2004). These concerted events ensure that only one copy of each DNA strand is synthesised as the cell approaches G_2 phase.

1.2.10 G_2-Phase Chromosomes

Each chromosome entering G_2 phase comprises two adhered sister chromatids. The chromatin is still in a highly extended state at this point, with a mixture of 10 and 30 nm fibres, and transcription continues in the same manner as in S-phase. Further hierarchical organisation and compaction of chromosomes may occur during G_2 phase, but these events are still poorly understood.

1.2.11 M-Phase Chromosomes

After completion of G_2, cycling cells enter into M-phase. M-phase consists of various stages of nuclear division: prophase, prometaphase, metaphase, anaphase and telophase, followed by cell division (cytokinesis).

Somatic cells and germline stem cells divide via mitosis and so progress through a single round of M-phase, whereas differentiating germ cells progress through meiosis and its two successive M-phases (meiosis I and II) with no second intervening S-phase. Given the many similarities between mitosis and meiosis II, the primarily focus of this section will be mitosis.

1.2.12 Mitosis

1.2.12.1 Prophase and Prometaphase

In early prophase any 10 nm fibres remaining from G_2-phase are condensed by multiprotein complexes called condensins to yield a total chromosome complement of 30 nm fibres (Kimura, et al., 1999). These fibres are further manipulated following the modification of the nuclear matrix strands into more substantial scaffold filaments, and the spiralling of 30 nm nucleosome arrays around the scaffold into tight solenoid arrangements. These solenoid structures are characterised by the location of histone H1s at their centre (Thoma, et al., 1979),

and by the presence of protruding looped 30 nm domains which are anchored to the scaffold at scaffold association regions (SARs – formerly MARs in previous phases). In addition, sister chromatids begin to sever their connections with the loosening of catenations and cohesin degradation (Giménez-Abián, et al., 1995). All these chromosome configuration modifications act to cease most gene transcription – possibly in relation to the coinciding events of histone deacetylation and the loss of transcription factors (Martínez-Balbás, et al., 1995).

In parallel with these chromosomal modifications, the cell experiences a series of morphological changes during prophase and prometaphase. The most important of these are the dismantling of the nuclear membrane into small vesicles, the migration of centrosomes to opposite poles of the cell, and the formation of the mitotic spindle. In the final act of prometaphase cohesin proteins mediate the attachment of sister chromatids to the spindle microtubules (Tanaka, et al., 2000) to allow these fibres to begin pulling the chromosomes towards the centre of the cell – a process that continues into the subsequent metaphase.

1.2.12.2 Metaphase

As the cell advances into metaphase the chromosomes are compressed to their optimal compaction states through a final series of higher-order modifications that possibly involve condensin proteins (Kimura, et al., 1999). By now, the chromosomes have aligned independently and in procession across the cell's equatorial plane (or metaphase plate). This positioning – equidistant from each centrosome pole – is the result of a counterbalance between the pulls generated from opposing kinetochores. In this state, the chromosomes are ready for their next round of manipulation in anaphase

1.2.12.3 Anaphase

Anaphase officially begins when an E3 ubiquitin ligase complex called the anaphase-promoting complex (APC) is activated to direct proteolysis of various anaphase inhibitors (Sudakin, et al., 1995). This initiates events geared towards sister chromatid separation into independent chromosomes, including irreversible cohesin disruption (Uhlmann, et al., 2000), catenation removal, and centromere division. The sister chromosomes then move to opposite poles of the spindle apparatus through the shortening of kinetochore microtubules. This is in contrast to polar microtubules, which continue to increase in length in conjunction with the elongation of the cell.

1.2.12.4 Telophase and Cytokinesis

In telophase, the cell continues to expand and begins to reverse the effects of the preceding mitotic events. New nuclear envelopes are formed around the polarised sister chromosomes, and the higher-order layers of chromatin coiling and compaction are relaxed to revert the chromosomes back to elongated 10 and 30 nm chromatin fibres. Thus telophase marks another important period of chromosome structural modification. The cell then completes the division process in cytokinesis as marked by the appearance of a cleavage furrow at the site of the former metaphase plate. From these cleavage furrows the cytoplasm is then physically divided to yield two daughter cells; each of which will enter into G_1 phase for another round of the cell cycle.

1.2.13 Meiosis

Meiosis produces haploid gametes by moving through two successive M-phases (meiosis I and meiosis II). Meiosis II is essentially identical in operation to mitosis and so will not be described in detail, but meiosis I has important differences that enable genetic diversity to be achieved. It is also the meiotic stage where chromatin compaction occurs. This section will thus focus on the chromosome transactions of meiosis I: prophase I, metaphase I, anaphase I, telophase I, and cytokinesis.

1.2.13.1 Prophase I

Prophase I of meiosis has some similarities with mitosis, but also a number of important differences. The analogies lie in chromosome condensation, with its trend towards greater compaction via higher-order chromatin organisation. However, the differences are much more pronounced, and occur within five prophase I sub-stages: leptotene, zygotene, pachytene, diplotene, and diakinesis.

1.2.13.1.1 Leptotene

Following S-phase, the chromosomes enter the first stage of prophase I, leptotene, as unpaired bipartitie structures consisting of two identical sister chromatids. Here, they condense and organise along proteinaceous axial elements to form 30 nm chromatin configurations resembling those of mitotic early prophase chromosomes wound around scaffolds. However, the meiotic chromosomes seem to be more transcriptionally active (Cook, 1997), suggesting a greater accessibility for proteins.

As well as inducing structural modifications to individual chromosomes, leptotene marks the beginning of the meiosis-specific process of homologous chromosome pairing and alignment (synapsis), by hosting their initial tentative associations. Studies in yeast have shown that synapsis initiation requires the formation of DSBs in each homologue to free the sister chromatid strands ready for eventual physical interaction and crossover (Padmore, *et al.*, 1991; Schwacha and Kleckner, 1995). These induced DSBs are generated by the highly conserved Spo11 protein in organisms such as yeast (Keeney, *et al.*, 1997), and mouse (Baudat, *et al.*, 2000; Romanienko and Camerini-Otero 2000). However, other studies have observed DSB-independent routes to pairing and alignment in yeast (Peoples, *et al.*, 2002) and in *Caenorhabditis elegans* (Dernberg, *et al.*, 1998).

1.2.13.1.2 Zygotene

Entry into zygotene is characterised by the completion of synapsis to form tightly-coupled homologous chromosome pairs, or bivalents. Axial element associations provide a platform on which multiprotein recombination nodules, synapsis initiation complexes (SICs) (Fung, *et al.*, 2004) and proteinaceous tripartitie synaptonemal complexes can all assemble. The latter of these consists of parallel lateral elements and an intervening central element. It is the paired lateral elements of homologous chromosomes that connect with each other to establish axial associations (Rockmill, *et al.*, 1995). The synaptonemal complexes are abundant and distributed across the length of each chromosome, and mark the sites at which DSBs will be committed to reciprocal exchanges of genetic sequence (crossovers) in the forthcoming pachytene phase.

1.2.13.1.3 Pachytene

Pachytene is an important period of chromosome conformation changes. The binding of 'structural maintenance of chromosome' (SMC) proteins to synaptonemal complexes (Eijpe, *et al.*, 2000) and the action of meiotic condensins (Yu and Koshland, 2003) aid the continued compaction of chromosomes in pachytene. In addition there are events of major structural distortion within bivalents that involve the physical breakage and union of chromatin strands. For example, intra-chromosomal sister chromatid exchanges (SCEs) may be initiated between sequences of homology (e.g. DNA repeats), and crossovers between paired homologous chromosomes are also established.

Crossovers (also called chiasmata) occur at programmed double-strand breaks with their residing synaptonemal complexes. At these sites, the specific

resection of 5′ strand termini leaves complementary 3′ strand tails which are then coated by the recombination-mediating protein Rad51 to form a helical nucleoprotein filament (Sung and Robberson, 1995) also known as the presynaptic filament. This nucleoprotein complex associates with duplex DNA to form a synaptic complex and binds to the duplex when it encounters sites of sequence homology. Some of these single-stranded DNA ends go on to form a full crossover with the aid of accessory factors that help strand displacement and the formation of a D-loop, whilst the other non-crossover events are restored to intact duplex strands. In the former of these, D-loop formation is followed by the formation of two fully ligated intermediates: single-end invasions (Schwacha and Kleckner, 1995) and double Holliday junctions (Hunter and Kleckner, 2001). The resolution to mature crossovers is achieved by the end of pachytene, where the products of crossovers are observed, for example in yeast (Padmore, et al., 1991; Schwacha and Kleckner, 1995; Hunter and Kleckner, 2001) and mouse (Guillon, et al., 2005).

1.2.13.1.4 Diplotene and Diakinesis

The next stages are diplotene and diakinesis. During this period the chromosomes continue to shorten, synaptonemal complexes disassemble, and the homologues begin to separate across their length; the exception being the chiasmata which remain points of contact between the homologues throughout diplotene and diakinesis. The partitioning of bivalents and the physical linkages that remain at chiasmata may aid the separation of sister chromatids by creating tension between the chromosomes (Blat, et al., 2002).

1.2.13.2 The Remainder of Meiosis I

The final stages of meiosis I are broadly the same as what is seen in mitosis, except at metaphase I the chromosomes align in pairs in random orientations across the metaphase plate, and when pulled apart the physical exchange of genetic material between chiasmata is completed. This event instigates genetic variation and is one of the most drastic structural modifications that chromosomes will encounter in the cell cycle.

1.2.14 Chromosome Structure and Dynamics Following Mutation

The examples above describe configurational changes experienced by chromosomes during normal mitotic and meiotic cell cycle processes. However, mistakes may arise during these periods of chromosome manipulation or the cell may become exposed to DNA-damaging agents that threaten the integrity of the

genome, and such instances can potentially severely compromise the cell and the wider host organism. The next section will detail more fully how the dynamic processes of chromosome modification above can malfunction both naturally and via the actions of external genotoxic agents, and how such errors can be repaired; processes that themselves involve further chromosome structure modifications.

1.3 Mutagenesis and Repair

The dynamic nature of chromosome structure provides scope for pre-mutagenic damage to accrue both naturally and from exposure to genotoxic agents. Pre-mutagenic damage can be converted to a full mutation if it evades cellular DNA repair to become part of the template DNA for the next S-phase, and subsequently part of the nascent DNA strand following DNA synthesis for segregation into the daughter cells. In this section an overview of the types of damage encountered by a cell through its lifecycle will be presented, along with a description of the mechanisms deployed by the cell to recognise and repair these lesions.

1.3.1 DNA Damage

Any modification of the genetic material caused by chemical, physical or radiological interaction is known as DNA damage. Damage from these sources is often a consequence of the chemical properties of the DNA macromolecule, which make it stable under optimal cellular physiological conditions but reactive in abnormal environments. It also means that certain chemical compounds will react with DNA should they encounter it. Damage of this kind can be detrimental in both the primary and higher-order structure of DNA.

The source of the DNA damage may be endogenous or exogenous. Endogenous damage arises spontaneously in the cell during fluctuations in the nuclear physiological state and from reactions with by-products from metabolism and the degradation of micro-organisms. Exogenous damage, on the other hand, stems from exposure to non-native compounds or radiation doses which can chemically react with or physically disrupt the DNA macromolecule. This damage can come in a multitude of different forms.

1.3.2 Spontaneous DNA Alterations

Spontaneous DNA damage arises throughout the cell cycle during the various chromatin modifications and transactions at an estimated rate of 20,000 events per human cell per day (Lindahl, 1993). This damage arises mainly at the level of individual bases through misincorporation of nucleotides during DNA synthesis or spontaneous chemical modification, but can also affect much larger blocks of sequence through transposition events.

The mistakes encountered during DNA synthesis stem from the error-prone nature of this process. The main source of replication errors is the replisome, which can inadvertently pair uncomplementary bases together, or incorporate base

analogues such as 8-oxodGTP and 2-OHdATP which arise from ROS-induced damage to free nucleotides in the cellular nucleotide pool (Maki and Sekiguchi, 1992; Inoue, *et al.*, 1998). Errors can also arise when strands misalign at the replication fork to form single strand bulges. If the single-strand 'crease' occurs in the newly-synthesised strand then an additional length of sequence equal in size to the length held in the bulge is synthesised by the replisome to compensate for this apparent loss. This leads to a sequence insertion. If the crease emerges in the template strand, the replisome will bypass the protruding region to create a nascent sequence deletion. This 'replication slippage' is a particular problem in genomic regions rich in repetitive DNA sequences, and is discussed in more detail in section 1.4.6).

Spontaneous chemical modifications of bases result from reactions with water, the destabilisation of DNA under sub-optimal physiological conditions or through reactions with naturally-occurring DNA-reactive molecular species. This can lead to a range of lesions including base deamination, tautomeric shifts (the transient structural modification of bases into isomers or 'tautomers'), or the complete loss of bases through depurination or depyrimidination to leave apurinic / apyrimidinic (AP) sites. It has been estimated that steady-state levels of abasic sites range from 50,000 to 200,000 per cell (Nakamura and Swenberg, 1999).

A major source of cellular ROS is mitochondrial aerobic respiration. ROS such as singlet oxygen ($^1O_2$), hydrogen peroxide (H_2O_2), superoxide ($\cdot O_2^-$), and hydroxyl radicals ($\cdot OH$) originate as metabolic by-products at each step of the electron transport chain. But they may also emanate from other native sources including H_2O_2 by-products from peroxisomal fatty acid degradation, and the nitrous oxide (NO), $\cdot O_2^-$, and H_2O_2 compounds elicited by phagocytic leukocytes to eliminate bacteria- or viral-infected cells. To appreciate the significance of ROS-induced damage, cells have been estimated to produce approximately 10^{10} ROS per day, resulting in about 20,000 oxidatively-damaged DNA bases (Beckman and Ames, 1997).

In normal cells the detrimental effects of ROS accumulation are usually counterbalanced by antioxidant enzymes such as superoxide dismutase, catalase, glutathione peroxidase, and also antioxidant compounds such as vitamins A and E, ascorbate, glutathione and thioredoxin, but these will not be perfectly efficient, and so oxidative damage will inevitably arise with a variety of base lesions that include oxidised bases, abasic (AP) sites, and strand breaks. The types of oxidative DNA damage inflicted upon a cell and the mechanisms of their repair are reviewed extensively elsewhere (Evans, *et al.*, 2004).

1.3.3 Environmental Mutagens

The external environment in which an organism exists can offer an unlimited and unpredictable amount of cellular exposure to various chemical or radiological agents. Environmental agents such as UV and ionising radiations, chemicals from inhaled or digested pollutants, and even some anticancer drugs can all create additional lesions to the natural level of DNA damage caused by native sources.

The mode of action of environmental mutagens can differ, with some agents affecting the DNA directly, while others may interact with cellular constituents to generate mutagenic chemical species such as ROS which then damage the genome. Often, the genetic damage experienced by the cell from exogenous sources is structurally and chemically different to that caused by endogenous species, and as a result may not be recognised by the cell's repair machinery. This makes some exogenous damage difficult for the cell to remove.

1.3.3.1 Ionising Radiation-Induced DNA Damage

When ionising radiation traverses through a cell it carries energy and deposits it on any structure that obstructs its path. It is mutagenic towards DNA in two ways: a direct hit may deliver sufficient energy to either physically break one or both of the duplex strands or ionise that region to make it chemically reactive; or secondly it may radiolyse water to create hydroxyl radicals which themselves may directly damage the DNA or generate further ROS in downstream reactions. The reactions involved are complex and in some cases overlapping, but will begin with the abstraction of electrons from water:

$$H_2O \rightarrow H_2O\bullet + e^-$$

$$H_2O^+ + H_2O \rightarrow H_3O^+ + OH\bullet \qquad \text{[hydroxyl radical]}$$
$$OH\bullet + OH\bullet \rightarrow H_2O_2 \qquad \text{[hydrogen peroxide]}$$
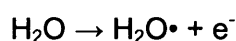
As a consequence of this, ionising radiation can promote the formation of a variety of base lesions. It can create covalent linkages between bases within the same strand (intra-strand base dimers) or between opposing complementary strands (inter-strand base dimers), and can initiate DNA-protein cross-links. Furthermore, ionising radiation can damage sugar residues in DNA to destabilise the sugar-phosphate backbone and result in single- or double-strand breaks. Of the two, single-strand breaks are the most frequently encountered (Friedberg, *et al.*, 1995).

1.3.3.2 Ultraviolet Radiation and Chemical Agents

Other environmental mutagens include atmospheric ultraviolet (UV) light and certain chemical species. UV-irradiation can lead to a number of lesions that structurally distort chromatin such as covalently linked pyrimidine dimers and other bulky lesions of cross-linked structures. Likewise, some chemicals may introduce structural irregularities, such as the alkylating agent ethylnitrosaurea (ENU) and the cross-linking agents (and also chemotherapeutic drugs) mitomycin and cisplatin. Other chemicals may instead induce mutations through interference with DNA replication. For instance, the uracil derivatives 5-bromouracil, 5-fluorouracil, and 5-iodouracil which are all thymine analogues that could be wrongly incorporated into the developing DNA strand and lead to base substitutions (Freidberg, *et al.*, 1995).

1.3.3.3 Epimutations

An increasingly important class of mutations are stochastic changes to epigenetic patterns during DNA replication. For example, DNMT1 (which maintains CpG methylation patterns through DNA replication) is estimated to copy genome-wide methylation patterns with an accuracy of 95% (Goyal, *et al.*, 2006; Vilkaitis, *et al.*, 2005). This copying inefficiency means that gene-regulatory information may be disrupted through cell divisions, leading to heritable changes in gene expression.

1.3.4 DNA Damage Response

The array of spontaneous- and mutagen-induced lesions outlined above illustrate how the dynamic nature of chromatin transactions can result in a range of structural distortions and changes to the primary sequence and higher-order chromatin organisation. These lesions necessitate a multitude of specialist cellular DNA repair pathways to identify and remove such damage as it arises, and should they fail then the sequence and structural integrity of chromatin will deteriorate with cell division events. In the next section the main cellular mechanisms of DNA repair will be detailed.

1.3.5 DNA Repair

If damage is allowed to accumulate in the genome then the primary sequence and higher order spatial configuration will become increasingly modified. These events could interfere with normal DNA transactions if genes are functionally disrupted or the wider genome becomes inaccessible for essential DNA-binding proteins. If left uncorrected, such damage could be fatal to the cell, and so it is not surprising that the cell has evolved various mechanisms to cope with all manner of

DNA adducts. These DNA damage repair responses can be broadly grouped into two categories: those that directly repair damage at the DNA level, and those that kill the cell harbouring the damage.

Repair at the molecular level can be undertaken by any one of an elaborate array of DNA repair pathways tailored to cope with specific lesion types. These pathways can act on individual bases or over larger tracts of DNA containing the damage. However, if damage is excessive or if the requisite repair pathway is either deficient or functioning sub-optimally, then the cell may be killed (necrosis), or removed by a programme of controlled cell-suicide (apoptosis), or it may be directed into an irreversible state of dormancy (G_0 senescence). In each case the objective is the same: to prevent the passage of damaged genetic material into the next generation of cells.

The nature of the damage involved and the cell cycle stage in which it occurs will determine the specific repair pathways initiated to restore genomic integrity. All these pathways will involve the manipulation of chromatin structure to some degree, and these will be described in more detail below.

1.3.6 Responding to DNA Damage at Cell Cycle Checkpoints

The checkpoints residing at each cell cycle transition utilise signal transduction pathways to monitor the genome for damage and to co-ordinate its repair. This process may involve temporary cell cycle arrest at G_1, G_2, or metaphase.

Genome surveillance is served by damage sensor proteins which detect and mark lesions as targets for DNA repair. One example is the 9-1-1 complex (a PCNA-like clamp of Rad9, Rad1, and Hus1 proteins) and its partnering clamp-loader Rad17-RFC2–5 (an RFC-like complex consisting of the Rad17 protein in combination with one of the subunits RFC2–5) (Shiomi, *et al.*, 2002). These two complexes interact together to bind to nicked, gapped, and primed DNA lesions (Bermudez, *et al.*, 2003) in a mechanism stimulated by replication protein A (RPA) (Zou, *et al.*, 2003). Another example of a damage sensor is the MRN complex of Mre11, Rad50, and Nbs1, which can assemble at DSBs (Carson, *et al.*, 2003). In each case, these sensor molecules bind to their target lesions and stimulate the action of DNA damage transducers for the next phase of the response.

The most important damage transducers are the ataxia telangiectasia-mutated (ATM) and ATM-and-Rad3-related (ATR) kinases, which instigate a cascade of reactions following their activation. The ATM kinase is activated primarily in response to double-strand breaks, and phosphorylates a series of targets that include Brca1 (Cortez, *et al.*, 1999), Nbs1 (Lim, *et al.*, 2000), Chk2 (Falck, *et al.*,

2001), and p53 (Banin, *et al.*, 1998; Canman, *et al.*, 1998). ATR, however, seems to be stimulated upon recognition of lesions that generate single-stranded DNA: for instance stalls at replication forks (as reviewed in Abraham, 2001). The complex and intermingling network of reactions elicited by both ATM and ATR will ultimately lead to the stimulation of 'effector' proteins whose action will result in characteristic repair responses. Examples of effector proteins include the tumour suppressor p53, which plays a central role in cell-cycle arrest and apoptosis after severe damage, and is thought to be essential for G_1 arrest (Harper, *et al.*, 1993). Other effectors include the cell division cycle phosphatase proteins Cdc25A, Cdc25B, and Cdc25C which ordinarily will dephosphorylate selected cyclin-dependent kinases to promote the progression of the cell through the G_1/S-phase and G_2/M-phase cell cycle checkpoints, but can be inhibited if phosphorylated by the protein kinases Chk1 and Chk2 to delay the cell cycle (Sanchez, *et al.*, 1997; Matsuoka, *et al.*, 1998).

In addition to these proteins there are a number of other 'mediator' proteins involved in the activation of the ATM/ATR checkpoint responses. These include Brca1 (Cortez, *et al.*, 1999), p53 binding protein 1 (53BP1) (Wang, *et al.*, 2002), topoisomerase binding protein 1 (TopBP1) (Yamane, *et al.*, 2002), mediator of DNA damage checkpoint (MDC1) (Goldberg, *et al.*, 2003), and Claspin (Kumagai and Dunphy, 2000). The mediators have various roles to perform in aiding the ATM/ATR transducers in their response to damage.

The activation of the various damage-sensing signal transduction pathways above directs the DNA repair and apoptotic responses characteristic of damaged cells. More details on how the cell handles such lesions at the molecular level are presented next.

1.3.7 Excision Repair Pathways

Excision repair pathways are deployed by the cell to remove isolated base lesions affecting single strands of DNA. Fundamentally they each involve steps of damage recognition, damage removal through dual incision of the phosphodiester backbone in the damaged strand, resynthesis of the deleted sequence against a complementary strand template, and ligation of the repaired strand. The result is restoration of the chromatin structure. The three main excision repair pathways are base-, nucleotide-, and mismatch-repair.

1.3.7.1 Base Excision Repair

Base excision repair (BER) pathways correct non-structurally distorting base lesions; the sort typically arising as a result of spontaneous reactions in the cell.

These include the products of base oxidation, alkylation, hydrolysis, and deamination, but may also arise from exposure to environmental agents such as ionising radiation.

The general process of BER is instigated by a set of enzymes called DNA glycosylases, with each enzyme having damage-specificity in its affinity for lesions. The role of these enzymes is to cleave the base-sugar glycosylic bonds either side of the damaged base to remove it and leave behind an apurinic / apyrimidinic (AP) site, although they may also be involved in mediating local chromatin remodelling and histone acetylation for downstream processing of the AP site (Tini, et al., 2002). If the glycosylase performs only this role then it is classed as a monofunctional glycosylase (e.g. uracil glycosylase), but other glycosylases have an additional lyase activity which cleaves the 3' side of the abasic site, and are said to be bifunctional (e.g. 8-oxoG DNA glycosylase) (Figure 1.2).

With the damaged base removed BER can proceed in either short-patch repair or long-patch repair. In short patch BER the single base is removed and replaced using DNA pol β to synthesise over the gap, and the newly incorporated base is sealed in place by a DNA ligase III-XRCC1 heterodimer that links in with DNA pol β to restore the DNA structure (Kubota, et al., 1996; Capelli, et al., 1997). In long-patch BER a larger tract of DNA of 2–10 bases that contains the damaged base is displaced for excision in a reaction that requires AP endonuclease, RFC, PCNA, DNA pol δ or ϵ, flap endonuclease 1 (FEN1), and DNA ligase I (Matsumoto, et al., 1999; Pascucci, et al., 1999). The involvement of components of the replisome suggests that BER occurs at replication foci; however there is also evidence to suggest that DNA pol β may interact with FEN1 during long-patch repair, and so could also operate outside of replication foci (Prasad, et al., 2000).

1.3.7.2 Nucleotide Excision Repair

The nucleotide excision repair (NER) pathway (Figure 1.3) has a large substrate specificity that senses and removes a range of helix-distorting yet structurally unrelated lesions. These adducts include the UV-induced cyclobutane pyrimidine dimers and other bulky chemical adducts induced by mutagenic chemicals and cytotoxic drugs. NER is thus primarily a means for dealing with damage caused by exogenous agents, which contrasts to BER with its preference for the minimally-distorting helical damage commonly associated with endogenous damage.

There are two distinct pathways of NER that can respond to damage: global genomic NER (GG-NER), and transcription-coupled NER (TC-NER). The former of

these detects and removes damage throughout the genome whether it is on transcribed or untranscribed DNA strands of active or inactive genes, whilst the latter is restricted to correcting damage to the transcribed strand of an actively transcribed gene. Both these pathways share the same set of core enzymes, but differ in the way they recognise damage. GG-NER senses structural anomalies wherever they arise, whereas TC-NER is initiated when RNA polymerase II stalls upon encountering a structural aberration in the transcribed, template strand (Selby and Sancar, 1993; reviewed by Svejstrup, 2002). Given their similarities, a description of GG-NER will be given here as a model of NER.

In the aftermath of UV irradiation, regions of genomic damage appear to undergo a series of modifications that include extensive localised histone acetylation (Yu, *et al.*, 2005) and chromatin remodelling (Ura, *et al.*, 2001; Yu, *et al.*, 2005). One example of this is chromatin reconfiguration by the ATP-dependent chromatin assembly and remodelling factor (ACF), which displaces nucleosomes to increase chromatin accessibility (Ura, *et al.*, 2001). This event allows assembly of the GG-NER machinery at the damaged regions; beginning with the binding of the protein complex XPC-H23B to the helix distortion (Sugasawa, *et al.*, 1998; Volker, *et al.*, 2001).

Once in position, XPC-HR23B recruits the transcription factor TFIIH to the site of the damage (Volker, *et al.*, 2001) and is followed by the addition of the ATP-dependent helicases XPB and XPD for the $3' \rightarrow 5'$ and $5' \rightarrow 3'$ opening of the DNA around the lesion (Riedl, *et al.*, 2003). The presence of ATP will trigger the unwinding of the helix until one of the factors, XPB or XPD, encounters a chemically modified base. This factor will stall whereas the other factor will continue unwinding to create a 2–30 base-pair opened 'bubble' structure which contains the lesion.

Following the opening of DNA, three more proteins join the complex: RPA, XPA, and XPG (Mu, *et al.*, 1995; Volker, *et al.*, 2001; Riedl, *et al.*, 2003). These proteins together constitute a pre-incision complex which lies bound to the open bubble structure. Within this complex, the XPG endonuclease makes an incision at the 3' end of the bubble (or 'flap') (O'Donovan, *et al.*, 1994), but this alone is not enough to remove the bubble, and requires the binding of its partnering 5' incision protein ERCC1-XPF to the pre-incision complex (Sijbers, *et al.*, 1996). With these two proteins bound, dual incision takes place and the XPG and ERCC1-XPF complexes then depart to leave the RPA protein at the damaged site. RPA then facilitates the transition to repair synthesis by DNA polymerase δ or ε in a reaction supported by PCNA and RFC (Shivji, *et al.*, 1995). Once complete, DNA ligase I re-establishes strand continuity by sealing the break together, and normal chromatin

structure is restored with the aid of chromatin associated factor 1 (CAF-1) (Green and Almouzni, 2003).

1.3.7.3 Mismatch Repair

During the DNA transactions of replication and recombination it is possible for base mismatches to occur. This is principally caused through errors at DNA replication (as described in section 1.3.2), but misalignments during recombination could have the same effect. The identification and correction of mismatched base pairs at replication forks is conducted initially by the 3' → 5' exonuclease proof-reading activity of replicative DNA polymerases, but this process is not 100% efficient, and some mistakes will evade detection. Any such base mismatch premuations are captured by the cell's mismatch repair (MMR) pathway before they reach the next round of replication (Figure 1.4).

The best characterised system of post-replication MMR is in bacteria. In *Escherichia coli*, mismatches in the transiently unmethylated, newly synthesised strand are detected by the protein MutS (Su and Modrich, 1986), which then recruits another protein, MutL, in an ATP-dependent manner (Acharya, *et al.*, 2003). The formation of this MutS-MutL complex stimulates incision of the unmethylated strand at a hemimethylated GATC site by the endonuclease MutH (Au, *et al.*, 1992) and the subsequent unwinding of the unmethylated DNA strand by DNA helicase II (Yamaguchi, *et al.*, 1998). The unwound strand is then degraded by exonucleases and the duplex restored with a round of gap-filling DNA synthesis and ligation.

In eukaryotes, there are a number of MutS homologues (MSH) named MSH1-6, and MutL homologues (MLH) named MLH1, PMS1, and PMS2. At present, there are no identified eukaryotic homologues for MutH. In both humans and yeast, MSH2 can form two different heterodimers: it can bind with MSH6 to yield MutSα (Drummond, *et al.*, 1995; Palombo, *et al.*, 1995), or alternatively it may associate with MSH3 to create MutSβ (Palombo, *et al.*, 1996). Human MutSα supports repair of all eight base-base mispairs as well as short misalignments of about ten nucleotides, whereas MutSβ supports the correction of shorter misalignments of less than ten nucleotides (Palombo, *et al.*, 1996; Genschel, *et al.*, 1998). In each case, the role of these heterodimers is to detect mismatch lesions in the genome.

The MutL homologues also appear to function as heterodimers in a complex called MutLα, which in humans comprises MLH1 and PMS2 (Li and Modrich, 1995), and in yeast comprises MLH1 and PMS1 (Habraken, *et al.*, 1998). MutLα is capable of supporting repair by binding to both MutSα and MutSβ complexes that have assembled on a mismatch lesion.

In addition to these complexes, the PCNA replication clamp interacts with several mismatch repair proteins to provide a physical link between repair and replication (Umar, *et al.*, 1996). Also, RFC, RPA, and the 5'→3' ExoI all support eukaryotic MMR by cleaving the DNA at positions 5' and 3' of the mismatch lesion (reviewed in Modrich, 2006). With the damage removed, DNA polymerase δ will synthesise new sequence across the gap to complete the MMR process.

1.3.8 Repair of Double-Strand Breaks

Breaks that occur in both strands at a specific locus are particularly hazardous to the cell. They can arise in a programmed manner to facilitate natural processes such as meiosis and the rearrangement of gene segments during immune cell development (called V(D)J recombination). They can also be induced by extrinsic agents such as ionising radiation and genotoxic chemicals, and intrinsic sources such as ROS and replication fork collapse.

When a DSB is formed, the chromatin in the vicinity of the lesion undergoes a series of initial configurational changes. The first event appears to be the phosphorylation of histone H2AX residues at serine 129 to form 'γ-H2AX' variants in the chromatin flanking the DSB (Rogakou, *et al.*, 1998), and histone H4 acetylation could be important too (Bird, *et al.*, 2002b). The presence of γ-H2AX mobilises chromatin remodelling factors and recruits them to the damaged site where they alter nucleosome positioning to aid the downstream processing of the broken ends (Morrison, *et al.*, 2004; van Attikum, *et al.*, 2004).

Following these initial structural modifications, the cell can initiate repair via one of two main pathways: homologous recombination repair (HRR), or non-homologous end-joining (NHEJ). HRR is an error-free process that replaces the absent DNA in the DSB with new sequence synthesised against a homologous sequence template, whereas NHEJ involves ligation of the broken ends and is thus error-prone. These two routes to DSB repair are explained more fully below (Figure 1.5).

1.3.8.1 Homologous Recombination Repair

HRR uses regions of extensive sequence homology elsewhere in the genome as templates for the resynthesis of the absent sequence. However, this reliance on homologous sequences restricts its window of operation to S- and G_2-phase of the cell cycle when a sister chromatid is available.

Mammalian HRR begins with the recognition of a DSB lesion by the damage-sensing heterotrimeric 'MRN complex' (Carson, *et al.*, 2003) consisting of the

proteins Mre11, Rad50, and Nbs1. Of these proteins, Mre11 has been shown to have both 5' → 3' (Usui, *et al.*, 1998) and 3' → 5' (Paull and Gelert, 1998) exonuclease activities, whilst Rad50 has an ATPase function (Hopfner, *et al.*, 2000), and Nbs1 is targeted by ATM for phosphorylation (Lim, *et al.*, 2000; Lee and Paull, 2005). Together, these proteins resect the DSB ends to leave two single-stranded 3' overhangs which are rapidly coated in the protein RPA. Following this, homologous recombination mediators such as Rad52 (New, *et al.*, 1998; Benson, *et al.*, 1998) and Brca2 (Sharan, *et al.*, 1997) help load the protein Rad51 onto these overhangs to displace RPA and catalyse strand exchange with the sister chromatid. There then follows a phase of strand exchange and priming of the invading 3' ends to instigate synthesis of the homologous template, and finally the resolution of the strands and their religation (Baumann and West, 1998).

1.3.8.2 Single-Strand Annealing

An alternative to HRR is the non-conservative single-strand annealing (SSA) pathway. This pathway is marked by the same initial steps as HRR, but is initiated in circumstances when a homologous donor cannot be found, and where complementary repeat units flank the DSB. If 5' resection has proceeded far enough along the strand to expose these complementary regions, then this allows the direct repeats in these 3'→5' strands to align with each other and dislodge the regions of the partnering 5'→3' strands that would otherwise have covered the gap. In yeast, this can occur with as little as 30 base pairs of homology, but is more efficient with 200–400 base pairs (Sugawara, *et al.*, 2000). The resulting flaps of dislodged 5'→3' sequence that protrude from the duplex are then removed by a FEN1-like nuclease (Wu, *et al.*, 1999), and following this the strands are sealed together by a ligation step.

1.3.8.3 Non-Homologous End-Joining

DNA double-strand breaks can arise in many different ways and embrace a diverse array of biochemical configurations at their broken ends: some of which will not be suitable for direct religation. In most cases, a pathway called non-homologous end-joining (NHEJ) will fuse the broken ends together, regardless of DNA sequence, in a manner that may be error-prone and therefore mutagenic. Given that the NHEJ pathway does not require a homologous chromosome it can operate at any phase of the cell cycle, but in G_0, G_1, and early S-phases it cannot be avoided as the cell has not replicated its DNA.

In mammals there is a core set of conserved NHEJ proteins: DNA ligase IV, XRCC4, Ku70, Ku80, DNA-PK$_{cs}$, and Artemis. Ku70 and Ku80 interact to form a DNA-binding heterodimer with ATPase activity and an affinity for DSB ends. When it attaches to DSB ends it forms a ring-like structure in preparation for ligation and to prevent further degradation (Walker, *et al.*, 2001), and then begins recruiting other proteins to that site. Initially it brings in the DNA-dependent protein kinase catalytic subunit (DNA-PK$_{cs}$) in a move that results in activation of the DNA-PK$_{cs}$ kinase function, and may also tether the broken ends to facilitate rejoining (Cary, *et al.*, 1997). Rejoining is then completed following the association of both the DNA end-joining complex XRCC4-ligase IV and the mammalian-specific 5'→3' exonuclease Artemis with the Ku70/80-DNA-PK$_{cs}$ assemblage. Here, Artemis is phosphorylated by DNA-PK$_{cs}$ to stimulate a change from its exonuclease activity to an endonucleolytic function capable of opening and removing hairpin loops encountered at DNA ends (Ma, *et al.*, 2002). This cleavage prepares the DNA ends for ligation by DNA ligase IV, with XRCC present to stabilise and activate its DNA ligase IV partner (Calsou, *et al.*, 2003). This marks the end of NHEJ.

1.3.9 Translesion Synthesis

In normal DNA synthesis, the new strands are laid down against their template by high speed, high fidelity 'replicative' DNA polymerases, such as DNA polymerases α, β, δ, and ε. In the rare event of a base mismatch occurring, the 3'→5' exonuclease proof-reading function of the DNA polymerases and cellular excision repair pathways will amend the vast majority of these errors. For the minority of errors that remain after this, and with all other avenues to DNA repair exhausted, the cell resorts to an error-prone translesion synthesis (TLS) pathway by recruiting a new set of TLS polymerases to the replication fork via PCNA in an event known as 'polymerase switching' (Hoege, *et al.*, 2002). In mammals these TLS polymerases include DNA polymerases η, ι, κ, and Rev1 from the 'Y-family' of polymerases, and DNA polymerase ζ from the 'B-family' of polymerases (Prakash, *et al.*, 2005). Enzymes such as these insert extra bases at the site of the stalled replication fork to allow the replisome to bypass the site and continue with replication. Given that this is done in the absence of a complementary strand template, it may lead to the inadvertent introduction of mutations (hence its error-prone nature).

The TLS polymerases differ from their replicative counterparts due to their modified active sites that enable them to accommodate altered bases (e.g. Ling, *et al.*, 2003). As a consequence they are slower than replicative polymerases and have

a lower fidelity. Although little is understood about the mechanisms of how these TLS polymerases operate, it seems clear that they each have their own target lesions which they can overcome to continue DNA synthesis. For example, DNA polymerase η has been shown, *in vitro*, to bypass cyclobutane dimers induced by UV-irradiation before quickly dissociating from the DNA (McCulloch, *et al.*, 2004). However, this polymerase cannot cope with the bulkier pyrimidine (6-4) pyrimidone UV-induced lesions, which instead are targeted by DNA polymerase ζ and Rev1 in yeast (Gibbs, *et al.*, 2005). Another example is DNA polymerase κ, which can synthesise across DNA containing benzo(a)pyrene-guanine adducts (Ogi, *et al.*, 2002). Should any damage evade the final TLS repair pathway, then it will be converted into a full mutation at the next round of DNA replication.

1.3.10 Damage-Induced Cell Death

Severe damage to a cell can result in its death via apoptosis or necrosis. Apoptosis is the physiological process of cell suicide invoked as a mechanism for removing severely damaged, superfluous, and unwanted cells. The process is undertaken in a controlled manner, utilising numerous genes and intracellular pathways that collectively contribute to the ordered disassembly of the cell. This gives rise to a number of characteristic features including cell shrinkage, membrane distortion, and endonucleolytic cleavage of DNA. When in *vivo*, apoptotic cells are subsequently engulfed by neighbouring phagocytes (Strasser, *et al.*, 2000).

Cell death by necrosis appears to be more of a pathological response, commonly associated with infected or severely damaged cells. Necrosis is characterised by the disruption of membranes and internal organelles, leading to the spillage of cytosolic and organellar constituents into the surrounding environment and subsequent stimulation of an immune response. The existence of an inflammatory response is thus one way to distinguish between apoptotic and necrotic cells.

1.3.11 Mutation Induction

Despite all the above mechanisms of DNA repair there is still the chance that some lesions will avoid correction and be converted into a permanent change in genetic sequence or structure following DNA replication. This marks the induction of a mutation, and the consequences of this will depend on the nature of the mutation. If it arises within a protein-coding gene or a sequence controlling gene expression then it may lead to phenotypic changes, but if it arises within non-coding regions it could go largely unnoticed. Furthermore, mutations induced in somatic tissues will

affect only the individual concerned, but should they arise within germline cells then they may be transmitted to future generations. Thus, it is important to be able to evaluate the effects of various mutagens in humans in order to assess the risk faced by these populations of acquiring potentially harmful mutations after mutagenic exposure. The next section will address this issue more thoroughly.

1.4 Assessing the Rate of Mutation Induction

There are a wide range of naturally-occurring and man-made mutagenic agents that could potentially be extremely hazardous to humans. It is therefore important that reliable estimates of mutation induction can be made for safety assessment purposes.

In this section the importance of assessing the impact of mutations induced by environmental agents will be discussed, and methods for estimating genetic mutation rates from these exposures will be introduced.

1.4.1 The Significance of Environmental Mutagens

Humans are exposed to a number of mutagenic environmental agents on a daily basis, from solar UV emissions to air pollutants, and these can have varying effects on DNA mutagenesis. Two of the most important sources of environmental mutagens are ionising radiation and genotoxic chemicals.

The global incidence of ionising radiation means exposure to its harmful effects is inescapable. Naturally occurring, terrestrial radionuclides are distributed to varying degrees throughout the environment, whilst cosmic radiations incident on the Earth's atmosphere also contribute to background levels of ionising radiation. In addition there are several sources of man-made radionuclides, such as the radioactive compounds used frequently for industrial and research purposes (in particular by the nuclear industry), and those used by the medical profession for therapeutic and diagnostic procedures. Further details can be found in a recent report by the United Nations Scientific Committee on the Effects of Atomic Radiation (UNSCEAR, 2000).

Chemical mutagens also pose a significant genetic hazard to the general population. Such chemicals may be designed for specific purposes such as pesticides, or could arise as by-products from sources such as air pollutants. These could potentially be mutagenic if inhaled or ingested via food and drink. Besides the general population, certain other groups of people are at elevated risk of chemical exposure, for instance industrial workers in the chemical industries, and cancer patients receiving chemotherapy (reviewed by Keshava and Ong, 1999). With these different mutagens being a prevalent feature of daily life, efforts have been made to assess their mutagenicity from epidemiological studies in humans, and genetic studies in animal models.

1.4.2 Epidemiological Evidence in Human Populations

To gather information on the *in vivo* genetic mutation rate in humans, epidemiological studies have been carried out on individuals exposed to mutagens occupationally, accidentally, environmentally, and medically. These studies generally look for physically identifiable abnormalities in the individuals and / or their children. For instance it is possible to track the frequency of cancer in a population following ionising radiation exposure by looking for solid tumours and leukaemia in the subjects (Kellerer, 2000), and use this as a measure of the consequences of direct exposure. If the hereditary effects are of interest, assessments of cancer risk in the children of exposed parents can be used (Gardner, *et al.*, 1990).

But the big problem with epidemiological studies is that there is little or no control on confounding factors such as the exact dose experienced by an individual, the nature of the dosage (external from the air and / or internal from contaminated food and drink) and how the lifestyle of that person may have led to environmental interactions. Together, these make epidemiological data unreliable as an assessment of the effects of different mutagens on mutation induction, and thus necessitate studies in controlled *in vivo* systems such as mouse to gain more insight.

1.4.3 The Mouse Model for Mutation Induction

The mouse has long been used as a model experimental organism for biological research given the extensive similarities that exist between mice and humans in many aspects of their biology. To this end, studies in mice have been particularly useful for evaluating rates of *in vivo* mutation induction. For example, with mice it is possible to control genetic background by using defined inbred or hybrid strains, and such homogeneity means that genetic differences can effectively be ruled out when interpreting data; something that cannot be guaranteed in epidemiological studies of human populations. In addition to this, experimental conditions can be easily controlled to ensure that all the organisms analysed are of the same age, housed within the same environment, nourished on the same dietary plan, and given identical courses of experimental treatment. This is a distinct advantage over human epidemiological studies, which will always experience variation in one or more of these factors and thus add a level of uncertainty when drawing conclusions. Moreover, the relatively rapid generation time of mice compared to humans makes it possible to conduct extensive studies that track transgenerational mutations in a relatively short space of time. For these reasons, the mouse model has been used in this thesis.

1.4.4 Traditional Approaches to Assessing Mutation Induction in Mice

The male germline has been one of the most popular systems for the study of mutation induction in mice. By dosing male mice in a controlled manner, their germline rates of mutation induction can be assessed retrospectively by monitoring the offspring for visible phenotypic abnormalities. A number of such approaches exists (as reviewed by Searle (1974)), with the most reliable being the Russell 7-locus test.

The 7-locus test is a large pedigree analysis of seven visible phenotypes such as fur and eye colour, and ear size; each associated with their own specific locus. When mutated, each of these loci produces an observable change in the appearance of the mouse, and so by crossing irradiated or control mice with homozygous recessive animals for the loci under investigation, any mutation from wild-type to a recessive or dominant allelic form could be detected. By following these phenotypes through the generations and scoring the frequency of mutant phenotype occurrence, estimates of the germline mutation rate in the parents of the analysed litters could be determined (Searle, 1974).

There are, however, a number of drawbacks of using the Russell 7-locus test for estimates of germline mutation rate. The mutation rate at protein-coding genes is low, in the range of 10^{-6} per locus per generation (Lewin, 2000), and this rarity of a mutation arising at a specific protein-coding locus makes it necessary to analyse very large numbers of mice (531,500 controls were used by Russell, *et al.* (1979)), to gain statistical significance. Also, when analysing the effects of radiation or chemical mutagens, large doses must be administered to the mice to induce mutations at these loci and make the study statistically robust. Such large doses are of a magnitude that is perhaps irrelevant to the low-levels of background radiation encountered by the general population in everyday life. To reduce the numbers of mice used and to assess lower doses of exposure, other loci characterised by higher spontaneous mutation rates would be required.

1.4.5 Repetitive DNA as Markers of Mutation Rate

Repetitive DNA sequences are lengths of sequence found in multiple copies in the genome, and classified as either tandem repeat or interspersed repetitive DNA. Tandem repeat loci are defined by a pattern of two or more nucleotides reiterated end-on-end in linear arrays, whereas interspersed repetitive DNA regions are high copy number, mobile DNA elements found scattered throughout the mammalian genome. Given their tendency to reside in non-coding regions of the genome, some repetitive DNA loci can mutate at relatively high spontaneous rates compared to

protein-coding loci, and since they are abundant in most eukaryotic genomes, estimates of mutation rate at repetitive loci could be more representative of the genome as a whole. For these reasons, repetitive loci are good candidates for the evaluation of genome mutation rates, although they are not all suitable. For instance, short and long interspersed nuclear elements (SINEs and LINEs) (such as *Alu* and L1 elements respectively) integrate into other genomic loci by retrotransposition at extremely low insertion rates in humans; it has been estimated at one germline insertion per 100 individuals (Kazazian Jr, 1999). This rarity of occurrence means interspersed repetitive loci are not ideally suited for estimating mutation rate. Telomeres too are not appropriate, as sequence differences between humans and mice prevent the reliable extrapolation of data from experimental mouse systems to humans (Wright and Shay, 2000). However, tandemly repeated sequences would make good candidates for markers of mutation induction, given the tendency of some to be unstable, and their widespread abundance in mammalian genomes.

Tandemly repetitive loci comprise three major sub-categories, defined as satellite, minisatellite, and microsatellite loci. The largest of these arrays are the satellite DNA sequences, which comprise small units of repeated DNA sequence in total array lengths of up to 5 Mb, followed by minisatellite loci (or variable number of tandem repeats (VNTRs)) which have repeat units of size 10 – 100 bp aligned in loci of up to 30 kb. Microsatellites are the smallest of these loci, with repeat units of 1 – 6 bp aligned into arrays of between 10 bp and 1 kb length.

There are also structural differences between mini- and micro-satellites. Minisatellites contain distinct repeat unit sequences organised into defined patterns (Jeffreys, *et al.*, 1990), whilst microsatellites are much more uniform in their internal structure, with uninterrupted runs of the same repeat unit sequence (Ellegren, 2004). These size and structural differences have important consequences for the susceptibility of these loci to mutation by different DNA transactions.

1.4.6 Tandem Repeat Instability

One of the key properties of tandem repeat loci that renders them vulnerable to mutation induction is their susceptibility to secondary structure formation. The primary cause of this is the sequence homogeny of repetitive loci, and the variety of abnormal DNA structures that this can generate during instances of duplex unwinding (e.g. transcription or replication). The structures form during these transient periods of strand separation because each 'released' strand becomes free to randomly fold back on itself and into biophysically-stable protruding structures.

These structures include hairpin loops, tetraplexes, triplexes, DNA unwinding elements, and sticky DNA. The requirement for sequence homogeny in the formation of these secondary structures explains why non-repetitive loci are not afflicted in the same way.

Hairpin loops form between intra-strand inverted repeats brought together by intra-strand folding to form stable alternative base-pairs. These loops are thought to be involved in instability associated with a variety of neurodegenerative disorders (Wells, 2007). Tetraplex (four-stranded DNA) structures may arise at G-rich repeat sequences such as telomeres (Neidle and Parkinson, 2003) and the Fragile X syndrome gene *FMR1* (Fojjtik and Vorlickova, 2001) from the intermingling of parallel hairpins, whereas triplex conformations can arise at long stretches of purine•pyrimidine mirror repeats such as the GAA•TTC repeat associated with Freidreich ataxia syndrome (Potaman, *et al.*, 2004). In the latter of these, a loose single-strand of this sequence will bind to its up- or down-stream duplex to introduce a third strand and whence the triplex conformation. Other secondary structures can form too, as reviewed by Wang and Vasquez (2006) and Wells (2007); each potentially leading to a number of problems during the various DNA transactions of replication, repair, and recombination.

1.4.6.1 Replication-Induced Repeat Instability

One of the most important triggering events for secondary structure formation at DNA repeats is DNA replication. Progression of the replisome through repeat arrays requires that the duplex is firstly unwound to reveal a template for synthesis, and this strand separation provides the opportunity for secondary structure formation – particularly at long homogenous repeat arrays (Kunst and Warren, 1994).

The orientation of the repeats and their proximity to replication origins has been shown to affect the susceptibility of strands to stable secondary structure formation in both trinucleotide (Kang, *et al.*, 1995) and tetranucleotide repeats (Dere, *et al.*, 2004). These reports observed that stable secondary structures arising in the nascent strand lead to expansions, whilst slipped-strand structures in the template resulted in sequence deletions. Moreover, secondary structures arose more readily when the repeats were cloned close to replication origins.

The resulting protruding structures will cause problems depending on whether they protrude inwards or outwards at the replication fork. In the model of replication pausing and slippage proposed by Mirkin (2006), secondary structures arise predominantly in the lagging strand in the transient single-stranded areas

found at the replication fork branch-point. These single-stranded "Okazaki initiation zones" may be the chief source of secondary structures at progressing replication forks.

The direction of secondary-structure protrusion from the Okazaki initiation zone could be important in determining the nature of the slippage event. If the secondary structures extend outwards and away from the progressing replisome, then the replisome will fail to read the sequence locked in the secondary structure, and so cause a deletion and hence a shortened nascent lagging strand. Furthermore, secondary structures that arise in the 5' ends of Okazaki fragments could induce reiterative lagging strand DNA synthesis, and consequently insert a stretch of sequence equal in size to the length of DNA captured by these structures (Gordenin, *et al.*, 1997).

Alternatively, any secondary structures that protrude inwards may block the ensuing replisome in its tracks as it synthesises the leading strand to induce pausing and slippage in leading strand synthesis. A possible mechanism for this is the temporary dissociation of the replisome from the template following the obstruction of its path by an inward-protruding lagging strand secondary structure. This dissociation event may release a short 3' tract of nascent leading strand, and this released sequence has the potential for secondary structure formation (Samadashwily, *et al.*, 1997). Thus when the replisome reassembles at the template to restart DNA synthesis, it will commence from a position slightly downstream of where it stalled and so reiterate DNA synthesis across this region. The result is an expansion in the nascent leading strand.

1.4.6.2 Repair-Induced Repeat Instability

The formation of secondary DNA structures can create targets for cellular DNA-excision repair pathways. In mice, MMR has been implicated in the instability of the trinucleotide CAG•CTG repeat by Manley *et al.* (1999) who reported increased stability of somatic CAG•CTG trinucleotide repeats in $MSH2^{-/-}$ knockouts, and by Kovtun and McMurray (2001) who observed that $MSH2^{-/-}$ knockouts reduce the rate of CAG•CTG length expansions in post-meiotic epididymal spermatozoa. Further evidence for the involvement of MMR was provided by Gomes-Pereira *et al.* (2004), who reported decreased levels of somatic CAG•CTG length mosaicism in $PMS2^{-/-}$ mice, to implicate components of the MMR pathway that do not directly interact with the DNA. The exact process by which MMR can increase DNA repeat instability is still not certain, but could involve a mechanism of uneven gap-repair DNA synthesis.

In addition to MMR, NER may have a role to play in the destabilisation of DNA repeat arrays. Studies in *Escherichia coli* showed that strains deficient for the NER damage recognition protein *uvrA* displayed elevated deletion rates at CAG•CTG repeat sequences (Oussatcheva, *et al.*, 2001). Together with the MMR observations, it seems that the process of damage recognition and removal common to all excision repair pathways may contribute to DNA repeat instability, and certainly does at the trinucleotide CAG•CTG.

1.4.6.3 Recombination-Induced Instability

Studies in yeast have shown that recombination processes may also take affect at slipped-strand structures. CTG•CAG tracts can induce DSBs to cause recombination-mediated repeat expansions (Freudenreich, *et al.*, 1998) which are more prevalent in meiosis compared to mitosis (Jankowski, *et al.*, 2000). The formation of secondary structures in these CTG•CAG trinucleotide repeats has been hypothesised by Wojciechowska *et al.* (2005) to induce adjacent DSB formation and result in the instigation of gross deletions.

As well as trinucleotide repeats, Kirkpatrick *et al.* (1999) showed that the pentanucleotide sequence CCGNN can act as a hot- or cold-spot of meiotic recombination depending on tract size, and when considered alongside the trinucleotide data, it would suggest that recombination proteins can interact with slipped-strand structures at DNA repeats to induce mutations. Whether this happens in mammalian cells as well remains poorly understood.

1.4.6.4 Microsatellite Mutations

The homogenous nature of microsatellite internal structure, coupled to the dynamic nature of chromatin structure through the cell cycle, makes some microsatellite loci (particularly trinucleotide repeats) particularly vulnerable to the formation of stable misaligned conformations. Thus microsatellites are often liable to mutate during replication and/or the activation of repair and recombination processes, as described above. Each of these events can lead to size expansions and contractions and inherent repeat locus instability, with estimated mutation rates of 10^{-4} to 10^{-3} per locus per generation for loci in eukaryotic genomes (Weber and Wong, 1993).

1.4.6.5 Minisatellite Mutations

Minisatellites mutate by gaining or losing repeats, and this property has been exploited to detect spontaneous germline mutations in pedigree analyses (Jeffreys,

et al., 1988a), and in PCR-based methods (Jeffreys, *et al.*, 1988b; Jeffreys, *et al.*, 1994) at mutation rates of up to 5% per gamete (Jeffreys, *et al.*, 1988a). Furthermore, minisatellite loci have been used in the study of mutation induction following exposure to ionising radiation in humans (Dubrova, *et al.*, 1996; Dubrova, *et al.*, 2002), and chemicals in herring gulls (Yauk and Quinn, 1996), which makes them useful indicators of the mutagenicity of different agents.

The predominant mechanism by which minisatellites mutate seems to be germline meiotic recombination, although detectable somatic mutations imply that somatic mutations could possibly be caused by replication slippage and / or mitotic recombination (Jeffreys and Neumann, 1997). The reasons for these minisatellite mutational mechanisms seem to lie in the interrupted order of repeat units found at minisatellite loci, which makes them relatively inert to secondary structure formation compared to microsatellites.

To elucidate the mutation mechanism, the technique of minisatellite-variant repeat PCR (MVR-PCR) (Jeffreys, *et al.*, 1991) has been used to great affect to understand the repeat unit composition of minisatellites and show how complex gene conversion processes govern their mutation (Jeffreys *et al.*, 1991; Jeffreys *et al.*, 1994). MVR-PCR cannot, however, be used at microsatellite loci due to their homogenous internal structures.

1.4.7 Expanded Simple Tandem Repeats (ESTRs)

Another class of tandemly repeated sequence is the family of expanded simple tandem repeat (ESTR) loci. These repeat loci contain repeat units of 4–9 bp arranged into uninterrupted linear arrays that can stretch to lengths of between 1 and 22 kb. They were originally classified as hypervariable mouse minisatellites (Jeffreys, *et al.*, 1987), but have since been distinguished from mini- and micro-satellites because they borrow characteristics of each of these loci without totally fulfilling the definition of either (Bois, *et al.*, 1998a). For instance, with repeat units of 4–9 base pairs and overall array lengths of up to 22 kb, ESTRs are too large for a conventional microsatellite but similar to what could be expected of a minisatellite. However, unlike minisatellites but akin to microsatellites, ESTRs contain homogenous internal structures with only one type of repeated DNA unit. Examples of ESTR loci include the locus Ms6-hm (also known as Pc-1) with its pentapeptide repeat GGGCA (Kelly, *et al.*, 1989; Kelly, *et al.*, 1991), Hm-2 with its tetranucleotide repeat unit GGCA (Gibbs, *et al.*, 1993), and the MMS10 family of repeats (Bois, *et al.*, 1998b; Bois, *et al.*, 2001).

1.4.7.1 ESTR Loci as Markers for Mutation Induction

ESTRs have been successfully used to assess spontaneous mutation rates and those induced by ionising radiation (Dubrova, *et al.*, 1993; Sadamoto, *et al.*, 1994; Fan, *et al.*, 1995; Niwa, *et al.*, 1996; Dubrova, *et al.*, 1998; Barber, *et al.*, 2000; Dubrova, *et al.*, 2000a; Dubrova, *et al.*, 2000b; Dubrova and Plumb, 2002; Yauk, *et al.*, 2002; Somers, *et al.*, 2004) and chemical exposures (Yauk and Quinn, 1996; Hedenskog, *et al.*, 1997; Barber, *et al.*, 2000; Somers, *et al.*, 2002; Vilarino-Guell, *et al.*, 2003), which makes them useful and proven tools for the study of mutagen-induced mutation frequencies.

However, there are limitations to using these loci as markers of mutation induction. For instance, given that ESTRs are non-coding loci, it is not possible to directly compare their mutation frequencies to protein-coding genes, although a recent comparison of ESTR mutation rates with those from the protein-coding hypoxanthine guanine phosphoribosil transferase (*HPRT*) locus in the same spleenocytes found similar increases in mutation rate at both these loci (Barber, *et al.*, 2006). Another problem with the use of ESTR loci is that it is still unclear as to what the mechanism of mutation is, and not knowing this presents problems when extrapolating data to other genomic loci. The purpose of this thesis is to investigate the mechanism of ESTR mutation.

1.4.7.2 Mechanism of Mutation at ESTRs

As with mini- and micro-satellite sequences, ESTRs mutate by expanding or contracting in size. Using pedigree analyses, spontaneous somatic mutation rates of 2.5% per gamete for Ms6-hm (Kelly, *et al.*, 1989) and 20% per gamete for Hm-2 (Gibbs, *et al.*, 1993) have been determined, with these mutation events occurring during the early stages of embryogenesis. These findings have also been determined by using a single-molecule PCR approach that amplifies ESTRs from individual genomes to get an estimate of the ESTR mutation rate in single cells (Yauk, *et al.*, 2002). Also, the ESTR mutation rate has been evaluated in pedigrees following exposure to ionising radiation (Dubrova, *et al.*, 1993; Sadamoto, *et al.*, 1994; Fan, *et al.*, 1995; Dubrova, *et al.*, 1998; Dubrova and Plumb, 2002; Somers, *et al.*, 2004).

The exact mechanism(s) of mutation that drive ESTR mutation remain unclear. In contrast to minisatellites, high levels of somatic instability are observed at ESTRs, inferring that meiotic recombination is not important as a mutation process. Support for this inference came from a study by Barber *et al.* (2000), which found no correlation between meiotic recombination and ESTR mutation rate. Instead, it

seems likely that ESTRs are mutating as a consequence of secondary structure formation within the structurally homogenous arrays, which could cause problems during replication, mitotic recombination, and repair. Quadruplex structures have been demonstrated across GC rich regions of the ESTR locus Ms6-hm *in vitro* (Weitzmann, *et al.*, 1998; Katahira, *et al.*, 1999; Fukuda, *et al.*, 2002), and such structures can lead to DNA polymerase stalling (Mirkin, 2006). Evidence from *in vitro* studies at the ESTR locus Ms6-hm has showed that the DNA-binding protein UP1 can reverse replication stalling and restart replication by unwinding the quadruplex structures (Fukuda, *et al.*, 2002). This provides support for the idea that replication stalling is an important feature of ESTRs, and that replication slippage could follow this stalling event and induce mutations.

1.4.7.3 Evidence from DNA Repair Deficient Mice

Further evidence that replication is the key driver of ESTR mutation comes from a series of recent papers analysing various DNA repair knockout strains. Barber *et al* (2004) measured the ESTR mutation rate in poly(ADP-ribose) polymerase (*PARP-1$^{-/-}$*) deficient mice to assess the effects of the single-strand break repair pathway, and also analysed the mutation rate in severe combined immunodeficient (*scid*) mice. The *scid* mice, with their non-sense mutation in the catalytic subunit of the DNA-protein kinase DNA-PK$_{cs}$, are unable to perform the major double-strand break repair pathway, and in each of these strains an elevated ESTR mutation rate was reported in the DNA repair-compromised mice. The same observation was made by Burr *et al.* (2007) when analysing an *MSH2* mismatch repair knockout strain, and by Burr *et al.* (2006) in a study of a TLS-deficient, DNA polymerase κ knockout strain. Taken together, these data imply that DNA repair pathways are necessary for stabilising the ESTR arrays, and so seemingly have a role in ESTR instability. But the direct cause of mutation was suggested to be replication fork stalling as a consequence of cell-cycle arrest and delayed repair in the repair-compromised strains. However, it is interesting to note that germline ESTR mutation rates do not increase in p53 knockout mice (Burr, *et al.*, 2005), although this could be the result of extra cell-killing induced by the absence of p53.

1.4.7.4 Stage Specificity

Another approach to identifying a mutation mechanism for ESTR loci is to understand the timing of mutation induction in the germline and link it to germline stage-specific DNA processing events. For example, in early diploid spermatogonia with their high mitotic indices it is expected that replication will be a key factor,

whereas in the latter stages of spermatogenesis when DNA repair ceases during nuclear condensation in elongating spermatids (Adler, 1996), this lower level of repair could be more influential. Previous work on this topic have generated controversy, with some papers showing elevated mutation rates following exposure to ionising radiation in both the pre-meiotic and post-meiotic stages of spermatogenesis, with the post-meiotic spermatids showing the highest sensitivity (Sadamoto, *et al.*, 1994; Fan, *et al.*, 1995; Niwa, *et al.*, 1996). These data lend support to the idea of an indirect post-fertilisation epigenetic mechanism (Fan, *et al.*, 1995), which contrasts to the results of Dubrova *et al.* (1998), who demonstrated a significant increase in ESTR mutation rate only in the pre-meiotic stages of spermatogenesis (spermatogonia and stem cells). Further support for this was provided by Barber *et al.* (2000), who showed that there was an increase in radiation-induced ESTR mutation rate after irradiation at all stages of spermatogenesis prior to metaphase I.

The discrepancies between these contradictory findings may be explained by the scoring of mosaics as mutants. It was reported in one of the initial studies that a high level of mosaics were observed (Sadamoto, *et al.*, 1994), and given that it is known that a high degree of somatic mosaicism takes place early in embryogenesis for Ms6-hm (Kelly, *et al.*, 1989; Kelly, *et al.*, 1991), it is possible that the mosaic bands in the offspring of irradiated males arose through somatic mutational events and do not represent germline mutations. Another discrepancy between the data is the observed elevation in maternal germline mutation rate after paternal exposure (Sadamoto, *et al.*, 1994; Fan, *et al.*, 1995), compared to reports that could find no such increase (Dubrova, *et al.*, 1993; Dubrova, *et al.*, 1998; Dubrova, *et al* 2000a; Dubrova, *et al.*, 2000b; Dubrova and Plumb, 2002). The difference in observed maternal mutation rates may also be explained by elevated somatic mutation during embryogenesis that leads to mosaicism. If it is indeed the case that mutation induction occurs in the early pre-meiotic spermatogonial stem cells, then DNA replication is once again implicated as an important driver of ESTR mutation.

1.4.7.5 Transgenerational ESTR Instability

Another insight into the ESTR mutation mechanism comes from studies into their transgenerational instability. Observations of persistently elevated germline ESTR mutation rates in all the offspring and grand-offspring of directly exposed males revealed how irradiation can cause sustained, non-Mendelian transgenerational ESTR instability through to the F_2 generation (Dubrova, *et al.*, 2000b; Barber, *et al.*, 2002), and so ruled out the possibility of specific genes in the

exposed males driving this phenomena (Barber, *et al.*, 2002). Instead, the authors suggest that the transgenerational genomic instability at ESTR loci may be due to germline-transmitted destabilising epigenetic factors, although the nature of this 'damage memory' remains undetermined.

1.5 Aims Of This Study

The aim of this thesis is to test further the hypothesis that the ESTR mutation mechanism is replication-dependent. This will be done by investigating the relationship between cell division and ESTR mutation rate.

In the first part the spontaneous ESTR mutation rates of various tissues will be analysed with age. Older mice will have experienced a higher turnover of cells in their lifetimes than younger ones, and so the ESTR mutation rate will be expected to increase with age in proliferative tissues such as the germline and bone marrow, but not in post-mitotic tissues like the brain.

Alongside this the effects of *in utero* irradiation on ESTR mutation rate will be assessed. Here, by extending the analysis into the developing embryo, adult post-mitotic tissues like the brain can be analysed when in a proliferative state, and so it would be expected that an increased mutation rate would follow in comparisons with adult post-mitotic tissues. The ionising radiation exposure will help the process of scoring mutations by inducing a higher rate compared to controls.

1.5.1 Using Single-Molecule PCR to Analyse ESTR Mutation Rate

The mutation rates will be estimated using the single-molecule (SM-) PCR technique first described by Yauk *et al.* (2002). This procedure involves diluting down bulk DNA samples to levels that contain, on average, one amplifiable DNA molecule. Using this method it is possible to analyse almost limitless amounts of molecules for mutants from individual animals, since it is analysing each genome of each individual cell for mutations. This means that the number of mice used in these single-molecule studies can be restricted further from the more traditional pedigree studies to an amount less than ten (Yauk, *et al.*, 2002). It also allows somatic mutation rates to be estimated, as pedigree studies can only analyse the germline mutation rate in the parents of the analysed progeny.

A more thorough explanation of this technique is provided in the forthcoming chapters 3 and 4, along with the results and data analysis for the experiments conducted in this thesis.
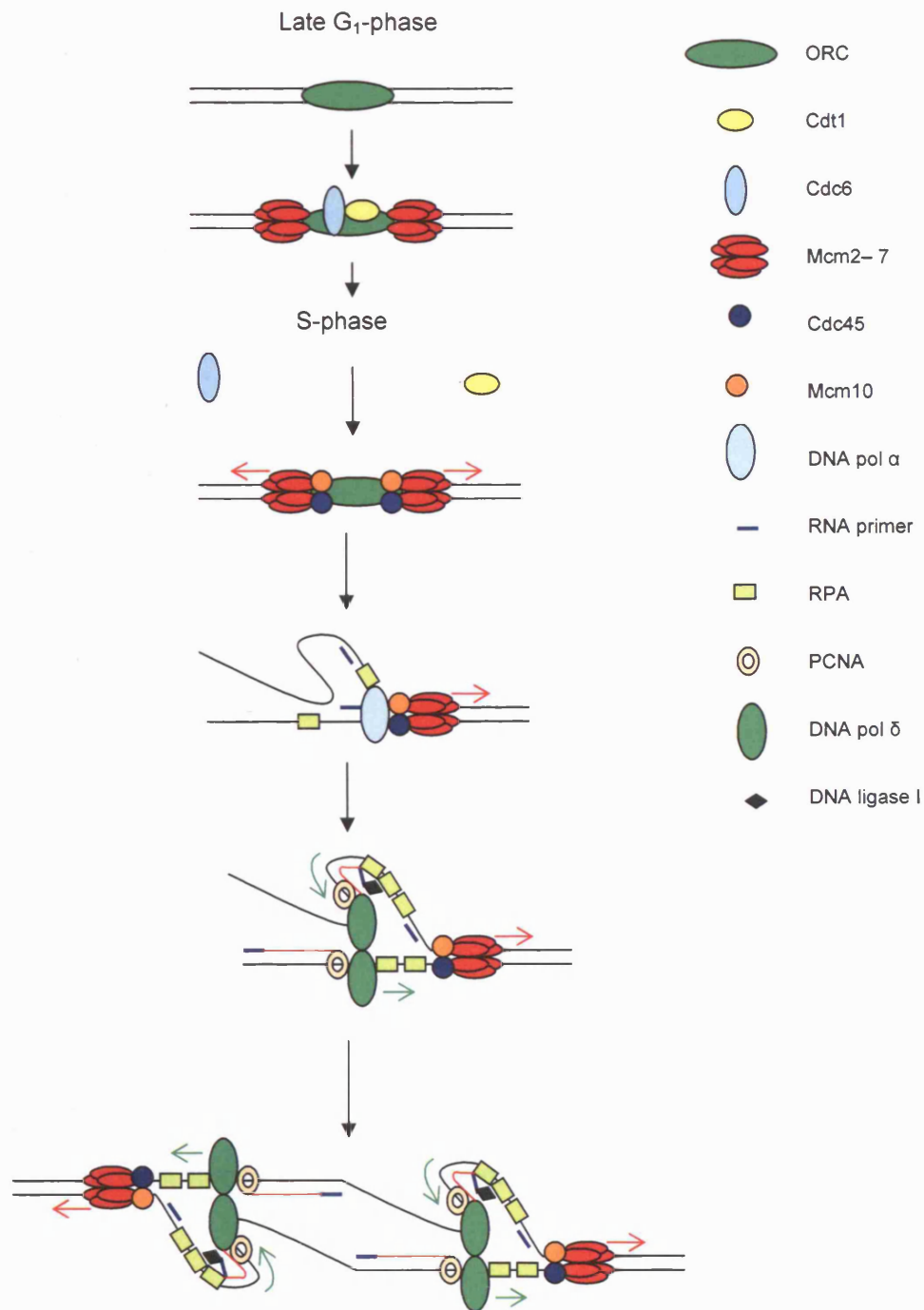
Figure 1.1

Schematic of DNA replication. See text in sections 1.2.8 and 1.2.9 for details.
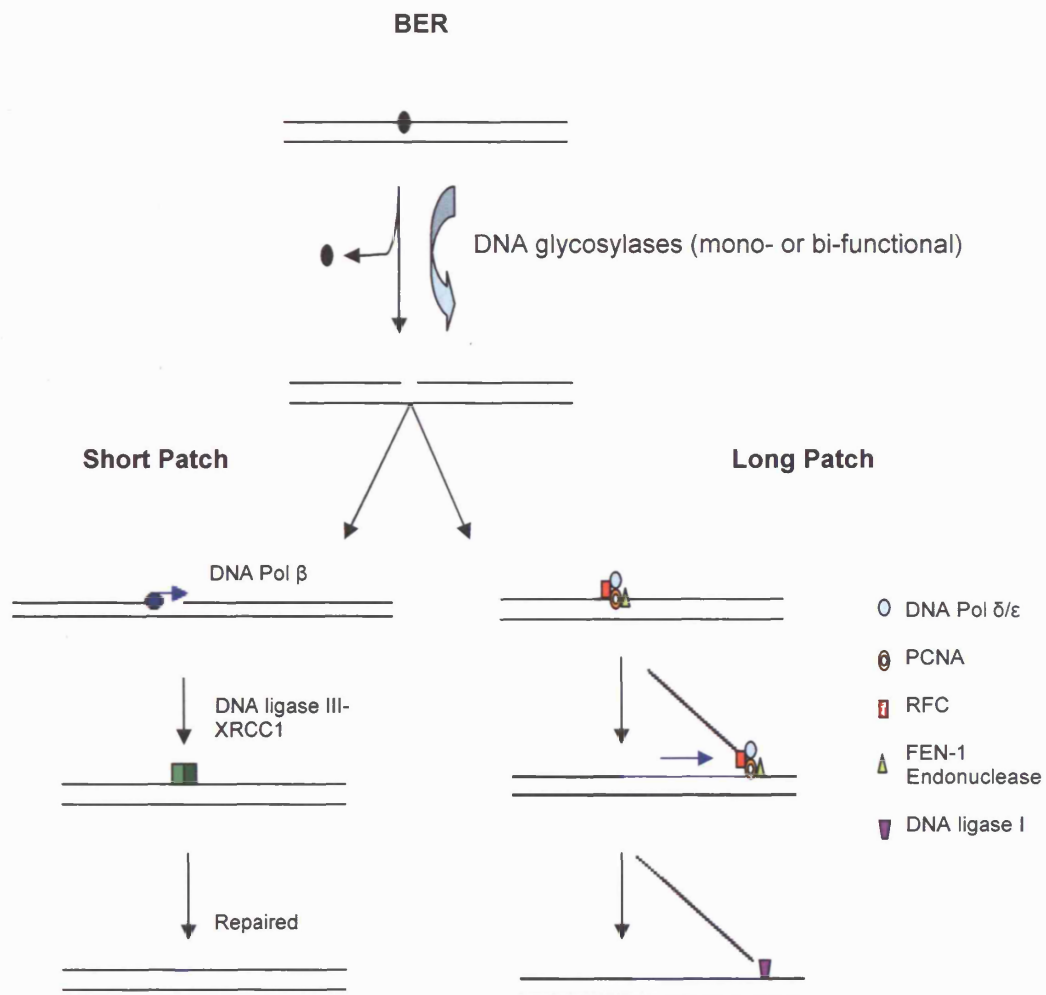
Figure 1.2

Diagram to illustrate the steps of base excision repair. See 1.3.7.1 for commentary.
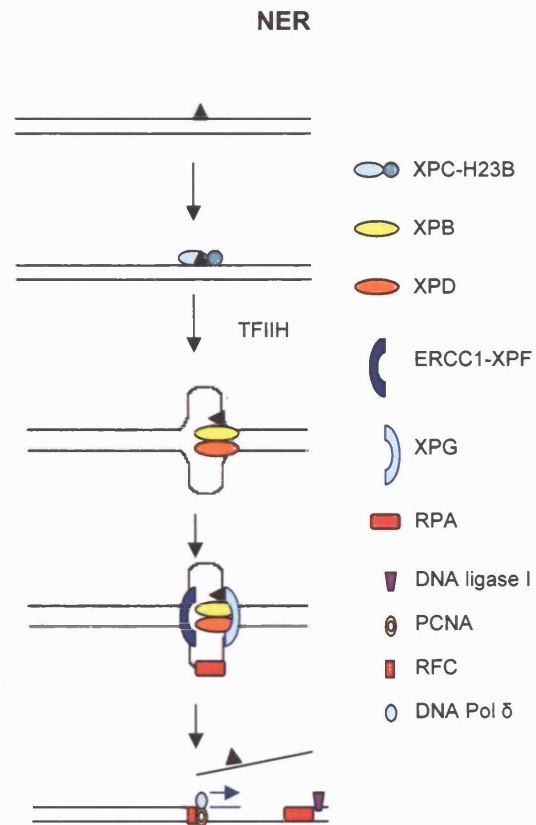
Figure 1.3

An illustration of nucleotide excision repair. See section 1.3.7.2 for information.

MMR
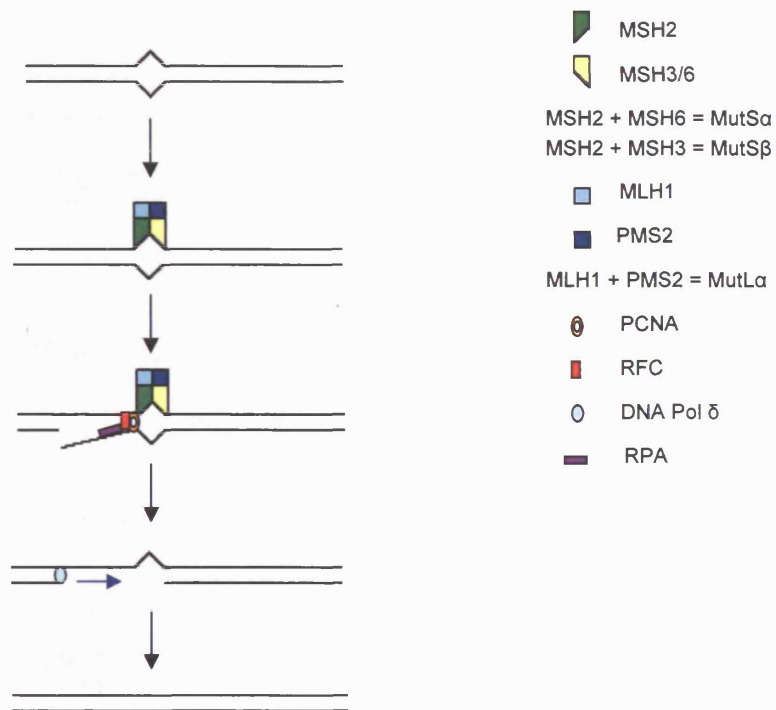
Figure 1.4

Diagram to show the events at mismatch repair. See section 1.3.7.3 for details.
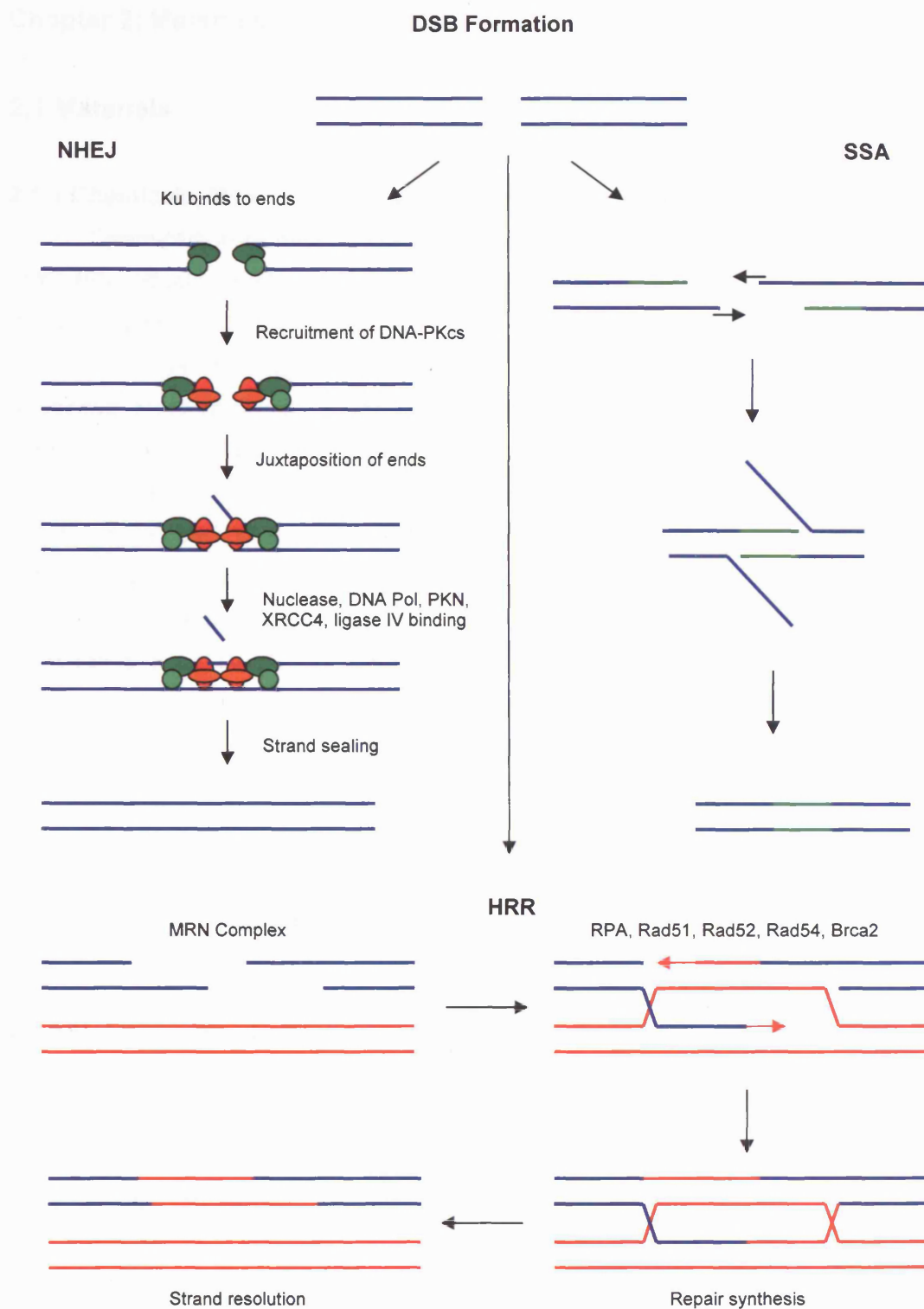
Figure 1.5

Figure to show the main pathways of DNA double-strand break repair. Commentary on these is given in section 1.3.8.

Chapter 2: Materials and Methods

2.1 Materials

2.1.1 Chemicals, Molecular Biology Reagents and Equipment

Chemicals were mainly obtained from Fisher Scientific (Loughborough, UK), FMC Bioproducts (Rochland, USA), Sigma-Aldrich Company (Poole, UK), Fisons (Loughborough, UK), and Serva (Heidelberg, Germany).

Molecular biology reagents were obtained from ABgene (Epsom, UK), Advanced Biotechnologies (Leatherland, UK), Bioline (London, UK), Boehringer Mannheim (Lewes, UK), Invitrogen UK (Paisley, UK), Life Technologies (Paisley, UK), New England Biolabs (Hitchin, UK), Pharmacia (Milton Keynes, UK), Promega (Southampton, UK), Qiagen Ltd. (Crawley, UK), and Roche Molecular Biochemicals (USA). Radiochemicals were obtained from PerkinElmer (Austria).

Most of the equipment used to perform this work was obtained from Amaxa Biosystems (Koel, Germany), Bio-Rad (Hemel Hempstead, UK), Eppendonf (USA), GE healthcare (USA), Genetic Research Instrumentation (Dunmow, UK), Hybaid (Teddington, UK), MJ Research (USA), and Perkin-Elmer/Applied Biosystems (Beaconsfield, UK).

2.1.2 Oligonucleotides

DNA oligonuleotides were synthesised by Sigma-Aldrich Company (Poole, UK).

2.1.3 Molecular Weight Markers

1 kb ladder was supplied by Invitrogen. ΦX174 DNA digested with HaeIII and λ DNA digested with $Hind$III were obtained from ABgene.

2.1.4 Standard Solutions

Southern blot solutions (depurinating, denaturing and neutralising), 20 x Sodium Chloride Sodium-Citrate (SSC) buffer and 10 x Tris-borate/EDTA (TBE) electrophoresis buffer, were made as described by Sambrook (Sambrook and Russell, 2001) and were supplied by the Media Kitchen at the Department of Genetics, University of Leicester.

2.2 Methods

2.2.1 Mice

F_1 C57BL/6 × CBA/H hybrid males and inbred BALB/c males and females were purchased from Harlan UK (Bicester, UK), and housed at the Biomedical Services Unit at the University of Leicester. All mice were marked with ear punches to permit the identification of an individual mouse, and were culled as required by dislocation of the neck under Schedule 1 of The Animals (Scientific Procedures) Act 1986 (Appropriate Methods of Humane Killing). All mice procedures were carried out under guidance issued by the Medical Research Council in 'Responsibility in the use of animals for medical research' (July 1993).

2.2.2 *In Utero* Study

Inbred BALB/c mice were mated, and successfully mated females were identified by the appearance of the vaginal plug. These females were then exposed to whole body irradiation (1 Gy X-rays delivered at 0.5 Gy/min (250 kV constant potential, HLV 1.2 mm Cu)) 12 days post-conception. This time-point was chosen as it corresponds to Theiler stage 20 (Theiler, 1989) of early organogenesis which is marked by high levels of differentiation in the primitive brain, bone marrow and testis (Kaufman and Bard, 1999).

2.2.3 Preparation of Mouse DNA

2.2.3.1 Tissue Collection

Bone marrow, brain, caudal epididymis, heart, kidney, liver, spleen, and tail samples were taken using sterilised scissors and tweezers. Bone marrow specimens were collected using a syringe to pass 500µl of phosphate-buffered solution (PBS) through each tibia and into an eppendorf tube. Tissues were initially kept on ice before being stored at −80°C.

2.2.3.2 Mouse DNA Extractions

All the DNA extractions were performed in a Class II microbiological safety cabinet (Walker Safety Cabinets Ltd, Glossop, UK) to minimise the risk of contamination by foreign DNA molecules, unless otherwise stated.

2.2.3.2.1 Somatic Tissues

Approximately half of the somatic tissue sample was finely chopped with a scalpel and suspended in 1ml of Lysis Buffer A (0.1 M NaCl, 25 mM EDTA pH 8.0,

20 mM TrisHCl pH 8.0) in a petri dish. The suspension was mixed using a pipette before being added to a 15 ml Eppendorf Phase Lock Gel™ Heavy tube containing 1 ml Lysis Buffer B (1% SDS, 12.5 mM EDTA pH 8.0, 10 mM TrisHCl pH 8.0) and 30µl Proteinase K (25 mg/ml) (Sigma-Aldrich, Poole, UK). The contents were mixed by inversion and incubated at 55°C for a minimum of 5 hours or more usually overnight, with occasional mixing.

Phenol/chloroform and chloroform washes were then used to purify genomic DNA from proteins and bone. 1 ml of phenol and 1 ml of chloroform were added to the Phase Lock Gel™ tubes and the mixture was emulsified by repeated inversion. The samples were then centrifuged at 5,000 rpm for 5 minutes in an Eppendorf Centrifuge 5804 to allow the physical separation of an aqueous layer containing the DNA from the contaminating solvent and protein phases. This step could be repeated if the DNA was not sufficiently cleaned. A final extraction was conducted by adding 1 ml of chloroform to the tube, inverting the tube, and centrifuging at 5,000 rpm for 10 minutes. This was performed to remove any residual phenol.

The final recovery of DNA was carried out by ethanol precipitation. The aqueous layer was pipetted into a 15 ml polypropylene tube containing two volumes of 100% ethanol and 1/10 volume of 3 M NaAc (pH 5.2). The solution was mixed by inversion and the DNA was transferred into a 1.5 ml eppendorf tube containing 500µl of 80% ethanol. DNA was centrifuged in a bench top microcentrifuge for 1 minute at 13,000 rpm and the ethanol subsequently removed using a pipette. The lids were then cut off the tubes so that the tubes could be covered with Nescofilm sealing film. A hole was made in the film using a needle, and the tubes were placed in a vacuum drier for 5 minutes. Finally, the DNA was dissolved in an appropriate volume (usually between 100–200 µl) of 5 mM Tris to reduce its viscosity.

2.2.3.2.2 Sperm DNA Extraction

Two caudal epidydimus tissues were finely chopped in a Petri dish using a scalpel blade until they were mushy, and 1 ml of PBS was then added and mixed in using a transfer pipette. A mesh screen (Sigma Aldrich, Poole, UK) was then folded into a cone shape and placed in an eppendorf tube so that the caudal epididymus suspension could be pipetted through the mesh to remove any large tissue chunks. A 5 µl aliquot of the collected suspension was then transferred to a counting chamber (Weber Scientific International Ltd., Middlesex, UK) and the sperm were visualised under a light microscope to confirm they were present. The sperm were then pelleted by microcentrifugation at 13,000 rpm for 2 minutes and the supernatant discarded. A further brief spin was performed to remove any residual

PBS. The pellet was then resuspended in 1 × SSC by vortex in order to lyse any remaining somatic cells. 15 µl of 10% SDS was then added to the tube, which was inverted and then centrifuged at 13,000 rpm for 2 minutes. The supernatant was removed and 960 µl of 0.2 × SSC was added, followed by thorough vortex of the solution. The specimen was then visualised under a light microscope to ensure all somatic cells had been removed. Finally, 70 µl of β-mercaptoethanol (Sigma Aldrich, Poole, UK), 100 µl of 10% SDS, and 80 µl of proteinase-K (25 mg/ml) were each added to the tubes for incubation at 37°C for 5 hours or overnight. Periodic inverting of the tubes was performed to ensure tissue sediments resting on the phase lock surface were mixed with the proteinase-K digestion buffer. If tissue was insufficiently digested, further 20–40 µl aliquots of proteinase-K were added to the tubes and left for up to an extra hour to complete the tissue digestion.

To clean up the DNA, phenol/chloroform extractions were performed as described in section 2.2.3.2.1, except here an initial 2:1 (phenol/chloroform: sample) wash was performed, followed by a 1:1 wash. DNA was precipitated by ethanol precipitation as described in section 2.2.1.

2.2.3.2.3 Ear-Punch DNA Extraction

DNA extraction from ear punch specimens was performed on the bench (not in laminar flowhood) as described for somatic tissues in section 2.2.3.2.1 except on a smaller scale. Ear punch samples were put into 2 ml Eppendorf Phase Lock Gel™ Light tubes containing 500 µl Lysis Buffer A, 500 µl Lysis Buffer B, 15 µl proteinase-K (25 mg/ml), and incubated for 1–2 hours or overnight at 55°C. 1 ml of phenol/chloroform (Phenol: Chloroform: Isoamyl alcohol in the ratio 25:24:1, equilibrated with Tris-HCl pH 8.0) was added to each sample, before being centrifuged at 13,000 rpm for 10 minutes. 1 ml of chloroform was then added for a final wash and centrifuged at 13,000 rpm for 10 minutes. The upper phase of each tube was then transferred to fresh 2 ml eppendorf tubes containing two volumes of 100% ethanol and 1/10 volume NaAc (pH 5.5), and these tubes were then inverted before being stored at –20°C for a minimum of 30 minutes to aid precipitation. The tubes were then centrifuged in a benchtop microcentrifuge at 13,000 rpm for 5 minutes, the ethanol removed, and 500 µl 80% ethanol was added. The samples were spun again at 13,000 rpm for 5 minutes and the residual 80% ethanol was discarded. The pellets were then air dried on the bench before being dissolved in 30 µl of ultra-pure water.

2.2.4 DNA Quantification

2.2.4.1 DNA Digestion

DNA was restriction-digested to aid the SM-PCR assay (section 2.2.5) using *Mse*I (restriction site: $^{5'}$TTAA$^{3'}$) (obtained from New England Biolabs, Hitchin, UK). This enzyme was selected because it will not cut into the ESTR array. For an individual digestion, 5 µg of DNA was digested in 1 × NEB Buffer 2 (supplied by New England Biolabs) and 20 U of *Mse*I, supplemented with 10 µg of bovine serum albumin (BSA). The reactions were incubated at 37°C for 2 hours.

Following digestion, DNA samples were precipitated by adding 2 volumes of 100% ethanol and 1/10 volume of NaCl (pH 5.2). They were frozen at -80°C overnight or for a minimum of 2 hours before being centrifuged in a benchtop microcentrifuge at 13,000 rpm for 20 minutes in one orientation, and then a further 20 minutes in the opposite orientation. The 100% ethanol was then removed and replaced with 50 µl of 80% ethanol, followed by a brief spin. The 80% ethanol was then discarded and the samples were vacuum dried for 5 minutes. Finally, they were dissolved in 50 µl of 5 mM Tris.

2.2.4.2 Gel Quantification of DNA

DNA was quantified on 1% agarose gels made by adding appropriate amounts of LE-agarose (SeaKem™, BioWittaker Molecular Applications, Rockland, USA) to 0.5 × TBE containing 0.5 µg/ml ethidium bromide. Next 2 µl of 5 × loading dye (5 × TAE, 12.5% Ficoll 400, 0.1% Bromophenol Blue) was added to 1 µl aliquots of restriction-digested DNA (see section 2.2.4.1) in a Class II microbiological safety cabinet, and made up to 10 µl with distilled water, and these 10 µl samples were quantified by running them alongside molecular weight markers of varying concentration. The molecular weight markers used were either ΦX174 DNA digested with *Hae*III or λ DNA digested with *Hind*III (each obtained from ABgene, Epsom, UK). The concentrations used were 500, 100, 50, 25, 10 and 5 ng/µl. DNA concentrations were estimated by electrophoresing the DNA products through the gel at 150V for 5 minutes so that the samples had migrated only a short distance out of their wells, and then visualising the intensity of the bands using a Gene Genius Bio Imaging System (Syngene, Cambridge, UK) and looking for the molecular weight marker concentration that matched most closely to a given DNA sample.

2.2.4.3 Spectrophotometer Quantification

An alternative approach to DNA quantification was to use a UV-spectrophotometer (Eppendorf BioPhotometer). DNA samples for the

spectrophotometer were prepared in a Class II microbiological safety cabinet by adding 2 μl of a given sample to 98 μl of ultrapure water. The spectrophotometer was zeroed using 100 μl of ultra-pure water, and the dilution factor was set to 2 in 98. 100 μl of a given DNA sample was added to the cuvette, and the absorbance readings at 260 nm were noted. Between samples, the cuvette was rinsed with distilled water and then dried on the bench. Care was taken to ensure no bubbles were present in the cuvette to distort the light reading, and that the cuvette was placed in the spectrophotometer in the same orientation each time. If DNA concentration was too low to be detected or if extremely variable results were delivered for each sample, then lower dilution factors were used.

The UV-spectrophotometer was also used to measure DNA purity. DNA absorbs UV light at 260 nm, whilst proteins absorb UV light at 280 nm, so absorbance measurements at 280 nm were taken for comparison to the 260 nm readings. 260/280 ratios were calculated, and compared to the expected ratio of 1.8 for a pure DNA sample. Protein contamination would result in a ratio <1.8.

2.2.5 Determination of Single-Molecule DNA Concentration

All DNA manipulation for SM-PCR was conducted in a Class II microbiological safety cabinet in order to minimise the risk of contamination with foreign DNA.

2.2.5.1 SM-PCR Optimisation

Before SM-PCR can be conducted, the single-molecule concentration must be established. Initial PCRs were performed on each specimen using the Expand High Fidelity PCR System from Roche (Mannheim, Germany) to optimise the DNA concentrations that achieve the single-molecule level. This concentration is derived from the Poisson distribution to determine the average number of template molecules per reaction for a given percentage of positive reactions from a 96-well PCR plate. From this distribution a value of 60% positive reactions from a 96-well plate corresponds to an average of one molecule per reaction.

To perform the SM-PCR optimisation, stock DNA samples (10 ng/μl) were diluted using a dilution buffer (5 mM Tris-HCl (pH 7.5) in the presence of 5 μg/ml carrier salmon sperm DNA (Sigma)) to various concentrations (pg/μl) of 100, 50, 20, 10, 5, and 2.5, ready for PCR amplification of the ESTR locus Ms6-hm. Ten microlitre PCRs were performed using 1/10 volume of diluted DNA in 1 × PCR buffer (from High Fidelity Kit), 2mM dNTPs, 4 μM of Ms6-hm forward primer (Hm1.1F) (^{5}AGAGTTTCTAGTTGCTGTGA^3), 4 μM of Ms6-hm reverse primer (Hm1.1R)

(^{5}GAGAGTCAGTTCTAAGGCAT^3), 1 M betaine (Sigma-Aldrich, Poole, UK), 1 U/µl enzyme mix (from High Fidelity Kit), and made up to 10 µl by adding sterile, UV-irradiated ultra-pure water. Eight replicates of each PCR assay at each concentration from two samples were set up in parallel in thin-walled 96-well PCR tube strips.

The PCR conditions used are presented in Tables 2.1 and 2.2, for the F_1 C57BL/6 × CBA/H hybrid mice and inbred BALB/c mice respectively. These required different elongation times due to the different sized Ms6-hm alleles in these strains (C57BL/6: 5 kb; CBA/H: 3.5 kb; BALB/c: 3 kb). All PCRs were performed using a DNA Engine Tetrad™2 Thermal Cycler (MJ Research, USA).

Table 2.1: PCR conditions used for F_1 C57BL/6 × CBA/H hybrid mice.

Temperature	Time	Cycles
96°C	3 mins	× 1
96°C	20 sec	
58°C	30 sec	× 34
68°C	8 mins	
68°C	10 mins	× 1
15°C	For ever	

Table 2.2: PCR conditions used for BALB/c inbred mice.

Temperature	Time	Cycles
96°C	3 mins	× 1
96°C	20 sec	
58°C	30 sec	× 34
68°C	3 mins	
68°C	10 mins	× 1
15°C	For ever	

Following completion of the PCRs, 5 µl of 5 × loading dye (5 × TAE, 12.5% Ficoll 400, 0.1% Bromophenol Blue) was added to each tube, and 5 µl of each of these samples was electrophoresed at 150–200 V for 2 hours or 20 V overnight in a

1% LE-agarose (SeaKem™, BioWittaker Molecular Applications, Rockland, USA). The gel was made by initially resuspending the agarose in 0.5 × TBE containing 0.5 µg/ml ethidium bromide, heating in a microwave until boiling, and then allowing to set in a gel casting tray on the bench. The samples were run against 200 ng of a 1 kb ladder (Invitrogen UK, Paisley, UK) for determination of PCR product size.

2.2.6 Genomic Profiling of Ear-Punch Genomic DNA

To validate the strain of mouse, ear-punch genomic DNA samples, collected as described in section 2.2.3.2.3, were profiled for the presence of the correct alleles. This was particularly important for the age study, as mice were due to be kept for up to two years.

Purified DNA samples were quantified using the spectrophotometer method described in section 2.2.4.3. Using these concentrations, DNA samples were diluted to 10 µg/ml. The genomic DNA was then digested to completion in a 20 µl reaction comprising 5 µg DNA, 2 µl NEB buffer 2 (New England Biolabs, Hitchin, UK) and 20 U/µl *Mse*I enzyme (New England Biolabs, Hitchin, UK) at 37°C overnight. The reaction was stopped through the addition of 5 µl loading dye (5 × TAE, 12.5% Ficoll 400, 0.1% Bromophenol Blue).

A 0.8% LE-agarose gel (SeaKem™, BioWittaker Molecular Applications, Rockland, USA) was prepared by suspending the agarose in 1 × TBE buffer containing 0.5 µg/ml ethidium bromide. The digested DNA samples were then electrophoresed through the gel alongside a visible and a sub-visible marker: 2 µg of λ *Hind*III (ABgene, Epsom, UK) and 200 ng of 1 kb ladder (Invitrogen UK, Paisley, UK) respectively. The λ *Hind*III ladder could be visualised using a UV wand (Chromato-vue UVM-57, UVP Life Sciences, Cambridge, UK), and electrophoresis was stopped once the 2.027 kb fragment reached the bottom of the gel. The sub-visible 1 kb ladder was loaded for probing during the forthcoming hybridisation step.

2.2.7 Southern Blotting
2.2.7.1 Southern Blotting of PCR Products

Following electrophoresis, the agarose was cut to the minimum size that held all samples and inverted in distilled water. The water was poured off, and the gel was depurinated in 0.25 M HCl for 2 × 5 minutes (depurinated DNA is more readily cleaved by NaOH), then the gel was alkali-denatured in 0.5 M NaOH, 1 M NaCl for 2 × 10 minutes, and finally the gel was neutralised in 0.5 M Tris-HCl (pH 7.5), 3 M NaCl for 2 × 10 minutes. In each case, the second wash was performed in fresh blotting solution. DNA was transferred to MAGNA nylon membrane (MSI, Osmonics

Laboratory Products) (pre-soaked in 2 × SSC) by the capillary transfer method using 20 × SSC as the transfer buffer. The membrane was rinsed in 2 × SSC, dried at 80°C for 15 minutes, and the DNA covalently linked to the membrane by exposure to 7 × 10^4 J/cm^2 of UV light in the RPN 2500 ultraviolet crosslinker (Amersham Biosciences, Little Chalfont, UK).

2.2.7.2 Southern Blotting of Genomic DNA

Southern blotting of genomic DNA samples was performed as described in section 2.2.7.1, with slight modification. Here, 2 × 10 minute washes in depurinating solution were performed followed by 2 × 20 minutes in denaturing solution, and finally 2 × 10 minutes in neutralising solution.

2.2.8 DNA Hybridisation

2.2.8.1 Preparation of Probes

Stocks of double-stranded probe DNA (5 ng/µl) were generated by PCR amplification of the Ms6-hm ESTR locus by R. C. Barber and K. L-A. Burr. Ms6-hm probes were produced by PCR amplification of synthetic primers containing the appropriated repeat unit. The PCRs were performed in 20 µl reactions with 2 µl of 11.1x PCR buffer (45 mM Tris-HCl pH 8.8, 11 mM ammonium sulphate, 4.5 mM MgCl$_2$, 0.045% 2-mercaptoethanol, 4.4 µM EDTA pH 8.0, 1 mM dATP, 1 mM dCTP, 1 mM dGTP, 1 mM dTTP, 110 µg/ml BSA) (Jeffreys, et al., 1990), 1 µM of forward primer (HMA) (^{5}GGGCAGGGCAGGGCAGGGCA$^{3'}$), 1 µM reverse primer (HMB) (^{5}CCCTGCCCTGCCCTGCCCTG$^{3'}$), and 2.5 U/µl Taq polymerase (ABgene). No DNA input was necessary as the repeat specific primers act as the templates. Amplification was performed in thin-walled 96 well-plates (ABgene), with 20 × [(96°C for 20 sec) (70°C for 20 sec)], then 40 × [(96°C for 30 sec) (70°C for 1 min 30 sec)]. These Ms6-hm PCR probe products were then purified using a QIAquick PCR Purification Kit (Qiagen), following the manufacturer's instructions.

2.2.8.2 Radiolabelling of Probes

To radioactively label the probe, the random primed labelling reaction (Feinberg and Vogelstein, 1983; Feinberg and Vogelstein, 1984) was used, in which α-^{32}P-dCTP (1000 Ci/mmol, NEN, Belgium) is incorporated into newly synthesised DNA using randomly generated hexamers and the Escherichia coli DNA polymerase Klenow fragment. The labelling reactions were performed in a 30 µl volume containing 20 ng of double stranded probe DNA and 2 ng of 1 kb ladder added to

water, and incubated at 37°C for 1–18 hours. The probe was recovered from unincorporated deoxyribonucleotides by ethanol precipitation using 100 µg high molecular weight salmon sperm DNA (Sigma-Aldrich, Poole, UK) as a carrier. Probes were re-dissolved in 600 µl of distilled water, and were boiled for 3 minutes prior to use.

2.2.8.3 Hybridisation

Membranes were pre-hybridised for at least 15 minutes at 65°C in 7% SDS, 0.5 M Na_2PO_4 pH 7.2 and 1 mM EDTA. Hybridisation was carried out at 65°C for 5 hours or overnight in Maxi 14, or Mini 10 hybridisation ovens (ThermoHybaid, Ashford, UK).

2.2.8.4 Post-Hybridisation Washing

After hybridisation the membrane was washed at 65°C once in phosphate wash solution (40 mM $NaHPO_4$, 0.5% SDS), for 10 minutes each, until the wash solution recovered after washing was less than 5 counts/second.

2.2.8.5 Autoradiography

Filters were wrapped in Saran Wrap and placed in autoradiographic cassettes (Genetic Research Instrumentation, Braintree, UK). The pattern of hybridisation was visualised by autoradiography using Fuji RX100 X-ray film (FujiFilm, USA) at −80°C with an intensifying screen for overnight or up to one week depending on the strength of the signal.

2.2.8.6 Stripping Filters for Re-Hybridisation

Nylon filters required for hybridisation with a different probe were stripped by immersing in boiling 0.1% SDS, and shaken for 15 minutes, and repeated if necessary until the counts detected were less than 5/second.

2.2.9 Mutation Detection
2.2.9.1 Single-Molecule PCR

Following the steps of single-molecule optimisation (section 2.2.5), Southern blotting of PCR products (section 2.2.7.1), and DNA hybridisation (section 2.2.8), the concentration at which 50% of PCRs are a positive result was identified and recorded as the single-molecule concentration. In some cases an average between two concentrations was taken if, for example, one concentration had six positive PCRs and the next concentration down had two. PCR was then performed at this

single-molecule concentration into 96-well plates using the PCR buffer composition and PCR conditions as described in section 2.2.5. The SM-PCR-amplified products were then run on an agarose gel, Southern blotted, and hybridised with radioactive probe as detailed in sections 2.2.5, 2.2.7, and 2.2.8. Each well containing a positive reaction was then labelled at the corresponding position on the 96-well plate.

2.2.9.2 Resolution of ESTR Mutants

Forty-centimetre long, 1% agarose gels containing 0.5 µg/ml ethidium bromide were prepared and 200 ng of 200 bp ladder (Promega) was loaded into each of the end lanes and also into the middle lane of the samples as a sub-visible marker to be visualised later upon radioactive probe hybridisation. In addition, 1 µg of 1 Kb ladder (Invitrogen) was loaded into the middle lane (along with the 200 bp ladder) as a visible marker for tracking the distance migrated by the ladder DNA fragments. 5 µl of each of the positive SM-PCRs was then loaded into the remaining wells. The gels were run at 200V for about 16 hours until the 3 kb ladder marker had migrated up to approximately 5 cm from the end of the gel (for the F_1 C57BL/6 × CBA/H hybrid mice with lower CBA/H ESTR allele size of 3.5 kb), or when the 2 kb ladder marker had reached the end of the gel (for inbred BALB/c mice with ESTR allele size of 3 kb). At this point, the gels were nicked with a scalpel blade at the 8 kb ladder marker migration length (for the F_1 C57BL/6 × CBA/H hybrid mice with upper C57/BL6 ESTR allele size of 5 kb), or at the 6kb ladder marker migration length (for the inbred BALB/c mice). The top half of the gel was cut and discarded, and the bottom half containing the ESTR PCR products retained for Southern blotting as described in section 2.2.7, except here the 200 bp ladder was probed. The nylon transfer membranes were then hybridised with Ms6-hm radioactive probes and visualised by X-ray autoradiography as described in section 2.2.8.

2.2.9.3 Scoring and Sizing of SM-PCR ESTR Mutants

Parental ESTR alleles were identified on X-ray autoradiographs from the long-gel experiments by virtue of their band sizes (C57BL/6: 5 kb; CBA/H: 3.5 kb; BALB/c: 3 kb). Mutants were scored by eye as any band which deviated by a minimum of 1 mm up or down from either of the parental alleles (1 mm corresponds to approximately 10 base-pairs (2 repeat units) for the BALB/c Ms6-hm allele). The 1 mm cut-off was employed to avoid ambiguity when classifying potential tiny mutants. The size of the parental and mutant alleles was estimated using the method of Southern (1979) with 200 bp ladder markers (Promega, UK) and by entering the

measured distances migrated (mm) by each of the 200 bp ladder markers and the ESTR alleles into the software prgram CALIBRATE (© Yuri Dubrova).

All samples were scored blindly to ensure personal bias did not affect the estimations.

2.2.10 Statistics

All the results of SM-PCR estimation and optimisation were tabulated and recorded using Microsoft Excel 2003. The software used for analysing the SM-PCR data was written in BASIC by Professor Yuri Dubrova. The calculation of mutation frequency and estimation of the mutation spectrum was achieved using the STATISTICA software packages (StatSoft, Inc., 2001. STATISTICA, version 6. www.statsoft.com), SYSTAT (SYSTAT, version 10, SPSS, 2000). The frequencies of ESTR mutation, 95% confidence intervals and standard errors were estimated using a modified approach of Zheng *et al.* (2000).

Chapter 3: Results I

Analysis of Age-Related Changes in Spontaneous Mutation Frequency at Mouse Expanded Simple Tandem Repeats (ESTRs)

3.1 Introduction

3.1.1 General Introduction

There is growing evidence to suggest that the mechanism of mutation at mouse expanded simple tandem repeats (ESTRs) could be associated with DNA replication (Dubrova, *et al.*, 1998; Barber, *et al.*, 2000; Barber, *et al.*, 2002; Dubrova, *et al.*, 2002; Barber, *et al.*, 2004; Burr, *et al.*, 2005; Burr, *et al.*, 2006). To reinforce this argument, it would be interesting to see if the ESTR mutation frequency is correlated to the cell division proficiency of a tissue. If a correlation is found, this will provide more evidence to implicate DNA replication as a key driver of ESTR mutation. However, other contributing genetic processes associated with cell division such as sister chromatid exchanges and epigenetic factors could not be entirely ruled out.

One approach to test this hypothesis is to conduct analyses comparing the mutation frequency of various tissues with differing mitotic indices in mice of different ages. The rationale is that proliferative tissues in older mice will have experienced an appreciably higher amount of cell divisions than the post-mitotic tissues of those same mice, and consequently had more opportunities for mutation induction. Therefore, if the hypothesis is valid, it would be expected that the mutation frequency will:

i)   be significantly higher in tissues with a high mitotic index than in age-matched non-dividing tissues;

ii)   be significantly higher in the proliferative tissues of old mice compared to the same tissues of younger mice, and

iii)   show no significant increase in the post-mitotic tissues of young and old mice.

With this in mind, three tissues were selected for study: brain, bone marrow and sperm. Here, the brain is the non-dividing post-mitotic tissue, while the bone marrow, with its varied population of cells with differing mitotic indices, will have an

overall intermediate cell turnover, and the sperm cells will be the products of the proliferative male germline.

In this chapter the results generated from this investigation into age-related ESTR mutation frequencies will be detailed, beginning with a general overview of ageing and its effects on DNA repeat loci, and ending with a description of the results and experimental procedure undertook to collect this data.

3.1.2 Ageing

Ageing is a natural process of gradual deterioration in an organism's fitness over time; it is a symptom of a weakened stress response, an increased homeostatic imbalance, and an elevated susceptibility to disease. The factors underpinning this deterioration are multifaceted and complex, and are found from the molecular level right up to the whole organism level. For example, organs may be affected by the endocrine system, the immune system, and brain retardation, whilst cells can experience damage to their membranes and organelles. At the molecular level there may be an accumulation of DNA mutations and protein modifications (Dufour and Larsson, 2004).

The biological basis of ageing at the molecular level resides in the optimal functioning of molecules within the cell. As an organism grows older its cells and macromolecules become ever more damaged from the persistent attack of endogenous and exogenous reactive species. For example, free radicals can damage proteins, lipids, and DNA, and sugar residues may bind to proteins (glycosylation). Moreover, DNA can be subjected to spontaneous errors in its replication, and proteins may acquire further spontaneous errors during post-transcriptional processing, translation, and post-translational modifications.

For the purpose of this thesis it is the damage to DNA that is of principal interest, and so will be the focus of attention for age-related effects.

3.1.3 Genetic Basis of Ageing

At the DNA level, ageing organisms experience changes including increased heterochromatinisation, a reduced DNA repair capacity, changes in gene expression, telomere length shortening, and epigenetic modifications. As a consequence, there are a number of diseases associated with ageing, including hereditary neurodegenerative disorders caused by unstable DNA repeats. In this section, an overview of these age-related genetic factors will be given.

3.1.3.1 Genes and Longevity

At the genetic level the detrimental effects of ageing are the result of the interplay between differentially regulated genes and stochastic damage. A number of genes have been identified as being important in this process (reviewed in Warner, 2005), and these tend to appear in one of four different categories: anti-stress genes (e.g. anti-heat shock and anti-oxidative stress), energy metabolism (e.g. insulin/IGF-1 signalling, caloric intake, and mitochondrial function), mutation prevention (e.g. DNA repair and restoration), and the protection of hormone homeostasis.

One of the best studied genes to be associated with ageing is the yeast transcription repressor *SIR2*. The importance of this gene was demonstrated by Kaeberlein *et al.* (1999), who observed that while yeast *SIR2* mutants show a decreased life-span, an additional copy of the gene actually increases longevity. Given the involvement of *SIR2* in NHEJ (Tsukamoto, *et al.*, 1997) and in the prevention of homologous recombination at yeast ribosomal DNA loci (Kaeberlein, *et al.*, 1999), this gene could provide a potential mechanistic link between ageing and chromatin modification.

Other factors could also be important in the ageing process. In one study an observed reduction in the ability of ageing fibroblasts to remove DNA lesions was attributed to a general decrease in DNA repair efficiency with the cause being the down-regulation of repair genes (Weirich-Schwaiger, *et al.*, 1994). Other papers report the involvement of cell proliferation regulators such as CDK-1, IGF-1, MAPK, P16, and P13K (Wang, *et al.*, 2001; de Magalhaes, 2005), and taken together this evidence suggests that longevity is governed by numerous genes working together in networks. These networks could drive the regulation, control, defence and restoration of processes such as homeostasis and metabolism, and any breakdown of this system could lead to an age-related deterioration in fitness.

3.1.3.2 Telomere Shortening

Telomeres are specialised chromatin structures found at the extremities of chromosomes, and provide protection for chromosome ends against recombination and degradation. In vertebrates, telomeres are composed of tandem repeats of the TTAGGG sequence, and undergo characteristic age-related length changes in normal somatic and germline cells.

In somatic cells there is a tendency for these repeats to be lost at each cell division, and this results in a progressive shortening of telomere length over time. The underlying mechanism is incomplete telomere replication by conventional DNA

polymerases, and a low or absent activity of a telomere-length maintenance reverse-transcriptase enzyme called telomerase (Hayley, et al., 1990).

The enzyme telomerase targets TTAGGG repeats and catalyses telomere elongation in cells in which it is expressed (Blackburn, 2001; Collins and Mitchell, 2002). Such telomerase-proficient cells include germ cells and some cancer cells, and in these cells the telomeres are effectively buffered against this end-replication problem and cell viability is increased (Collins and Mitchell, 2002). However, the generally telomerase-deficient somatic cells experience a gradual erosion of their telomeres with age, which will eventually result in them becoming critically short and eliciting a DNA damage response. This action may ultimately result in cell-cycle arrest and apoptosis.

3.1.3.3 DNA Repeat Loci

The dynamics of DNA repeat loci are also subject to age-related changes. In the main there seem to be some critical factors that have a significant bearing on how any given DNA repeat locus will behave, including: repeat motif size and sequence, total array size, the parental origin of the locus, cis- and trans-acting factors, tissue type, and possibly the immediate genomic environment in which the locus resides. For most DNA repeats it seems that replication slippage is the primary mechanism of mutation (Ellegren, 2004), although trinucleotides are emerging as a possible exception to this rule.

3.1.3.3.1 Trinucleotide Repeats

Trinucleotide repeats are known to play an important role in a number of hereditary diseases with age-related effects. For example, expansions of simple trinucleotide repeats have been shown to result in diseases such as Fragile X syndrome (Kremer, et al., 1991) (with $(CGG)_n$ expansions in the FMR1 gene), Huntington's disease (Huntington's Disease Collaborative Research Group, 1993) (with $(CAG)_n$ expansions in the Huntington gene), spinobulbar muscular atrophy (La Spada, et al., 1992) (with $(CAG)_n$ expansions), myotonic dystrophy (Harley, et al., 1992) (with $(CTG)_n$ expansions), and Friedrich's ataxia (Campuzano, et al., 1996) (with $(GAA)_n$ expansions), to name but a few. In all cases, the repeats are stably inherited until their lengths exceed a threshold of approximately 100 – 200 bp. Beyond this size, the repeats may experience intergenerational expansion.

To describe how these repeat arrays mutate there is a growing body of evidence to suggest that replication slippage is not a key player. Despite the susceptibility of trinucleotides to secondary slipped-structure formation (Kang, et al.,

1995; Pearson, *et al.*, 2002) which can lead to replication slippage, a number of publications suggest that other DNA transactions have stronger affects on trinucleotide repeat instability. For example CTG repeats appear not to mutate in accordance with cell division (Lia, *et al.*, 1998; Fortune, *et al.*, 2000), nor do CAG repeats (Lorenzetti, *et al.*, 2000; Gomes-Pereira, *et al.*, 2001) or GAA repeats (Clark, *et al.*, 2007). Instead, *cis*-acting factors could be responsible, or maybe the MMR system as hypothesised by Gomes-Pereira *et al.* (2004).

3.1.3.3.2 Other Microsatellite Repeats

If replication slippage is the primary mechanism of mutation at most other microsatellites then it would follow that the higher the turnover of cells in a tissue, the higher the rate of mutation. For example a study by Brinkmann *et al.* (1998) surveyed the mutation rates of a panel of human microsatellites of varying size repeat motif composition and found a significant age-related increase in mutation rate between a cohort of 'young' men (mean age 28.7 ± 7.6 years) and a group of 'old' men (mean age 32.5 ± 7.8 years). Furthermore, they reported how the mutation rate per locus per gamete per generation increased in a near exponential manner with the mean size of uninterrupted repeats, but the rate was reduced when interruptions were present. However, a study into mutation rates at human Y-chromosomal microsatellites found no significant increase in mutation rate per locus per gamete with age (Dupuy *et al.*, 2004), and another study by Brohede *et al.* (2004) went further to seemingly contradict the prevailing view of replication-slippage-mediated microsatellite mutation by reporting an age-related decrease in mutation rate per locus per gamete at the hypermutable human microsatellite locus *D21S1245*. This locus, with its complex and interrupted structure of repeated GAAA motifs, presented a higher mean mutation rate in men aged 18-23 years than in a group aged 48-56 years, although the authors viewed their own data with caution. In addition to this, the tetrameric repeats $(CCTG)_n \cdot (CAGG)_n$ (Liquori, *et al.*, 2001), the pentameric repeats $(AATCT)_n \cdot (AGATT)_n$ (Matsuura, *et al.*, 2000), and the dodecameric repeats $(C_4GC_4GCG)_n \cdot (CGCG_4CG_4)_n$ (Lalioti, *et al.*, 1997) have all been shown to be able to expand and cause human disease with age. This illustrates the importance of some non-trinucleotide repeats in the context of human disease.

3.1.3.4 Epigenetics and Ageing

It is becoming increasingly clear that advancing age can also lead to epigenetic changes. As cells age their methylation patterns change with a general

global incidence of hypomethylation (Wilson and Jones, 1983; Richardson, 2002) that is reflective of decreased methylation at CpG dinucleotides dispersed throughout repetitive sequences and some transcriptionally-active genes (Fraga, *et al.*, 2005). In addition, there is localised gene-specific hypermethylation at some gene promoter CpG islands (Issa, 2000), with Toyota *et al.* (1999) observing age-related promoter hypermethylation of ER (estrogen receptor), IGF2 (insulin-like growth factor 2), MYOD (Myogenic Differentiation Antigen), N33, and CSPG2 (chondroitin sulphate proteoglycan 2 (versican)) in normal colon mucosa. The spread of transcriptionally-repressive facultative heterochromatin with age could also be the consequence of epigenetic manipulation involving the recruitment of proteins to form foci in senescent cells (Narita, *et al.*, 2003). However, there is still much to be learned about epigenetic processes in ageing organisms.

3.2 Experimental Design

3.2.1 Objectives of this Study

The purpose of this study is to investigate the age-related spontaneous ESTR mutation frequencies in different tissues to provide further evidence of the relationship between mutation frequency and the number of DNA replication events. This work will build on previous ESTR spontaneous mutation frequency estimates in young C57BL/6 × CBA/H F_1 hybrid male mice by analysing other cohorts of varying but older ages. The estimates in these hybrid males at the CBA/H allele were 3% in brain and 13% in sperm at an age of 8–12 weeks (Yauk, et al., 2002).

3.2.2 Using Single-Molecule PCR to Assay ESTR Mutation Frequency

Previous papers from our laboratory detailed a pedigree approach to analysing ESTR mutation induction in the male germline and detected mutation frequencies of, for example, 6% (Dubrova, et al., 1998) and 7% (Barber, et al., 2002) in CBA/H mice aged 8–12 weeks, and 5% (Burr, et al., 2007) in BALB/c strain mice. In these studies tail samples were taken from the offspring of treated and control animals, their DNA restriction-digested, and then digested DNA was ran on an agarose gel to resolve allelic size differences. By Southern blotting these gels and radiolabelling the retrieved nylon membranes, size changes at ESTR loci indicative of mutation induction could be visualised by X-ray autoradiography and scored in relation to the wild-type progenitor-sized alleles. This scheme provided valuable information on parental germline ESTR mutation frequencies, and at the expense of greatly reduced sample sizes (59 controls were used by Burr et al. (2007)) compared to traditional phenotype-driven analyses such as the Russell 7-locus test (531,500 controls were used by Russell et al. (1979)). The reason for this is the hypermutability of ESTRs compared to the relatively stable protein-coding genes used in the Russell 7-locus test, and consequently fewer animals are required before a mutation will be observed. However, in recent years our laboratory has been increasingly using the single-molecule (SM-) PCR method of ESTR mutation frequency estimation as first developed by Yauk et al. (2002).

The reason for this is the enhanced sensitivity of the SM-PCR approach over the conventional pedigree method. SM-PCR is able to target an individual genome derived from a single cell, and consequently detect mutations arising independently in different cells of the same tissue. This contrasts with the pedigree analysis which uses whole or partial tissue DNA samples in a single assay and is thus equivalent to many millions of cells at once. As a consequence, numerous mutation events can

be detected in individual mice using SM-PCR, and so samples as small as three mice are sufficient to achieve a robust statistical analysis (cohorts of five mice were used by Yauk *et al.* (2002)). Another advantage is that whilst the pedigree approach is retrospective in its estimation approach (meaning it is limited to investigations of parental germline mutation induction), the SM-PCR method is able to assess mutation induction directly from the animal of interest in both germline and somatic tissues.

Given the higher degree of sensitivity of the SM-PCR technique and its ability to assess mutation frequencies directly from the target mice, it is this method that will be used in this investigation to estimate age-related spontaneous mutation frequencies. The locus to be used will be Ms6-hm, given that this locus was previously used to great success by Yauk *et al.* (2002) in the original description of the methodology for SM-PCR at ESTR loci.

3.2.3 Single-Molecule PCR

The SM-PCR method for assaying mutation induction is based on the same principle of analysing radiolabelled Southern blots for ESTR allele size differences as seen with the pedigree approach, but it differs in the way in which the DNA to be analysed is prepared.

The crucial difference between SM-PCR and conventional PCR protocols is the input concentration of DNA. Bulk DNA stocks are diluted down to a level at which the average PCR will only receive one DNA molecule as a template. Theoretically, the quantity of DNA for input into SM-PCRs in mice is approximately 1.5 pg based on a mouse genome size of 2.5 Gbp (Mouse Genome Sequencing Consortium, 2002). However, in reality the amount of DNA required for SM-PCR can vary depending on the accuracy of initial DNA concentration estimates and on the quality of that DNA (poor quality DNA may not be amplifiable or will amplify at lower efficiencies). Therefore it is necessary to optimise the DNA concentration to be added to the SM-PCR buffer for each tissue from each animal from each age group.

Optimisation PCRs are carried out by using various DNA concentrations from serial dilutions of the stock DNA. The resulting PCR products can be separated on an agarose electrophoresis gel, Southern blotted and radioactively probed for detection by X-ray autoradiography. This way, the number of positive PCRs from each serial dilution can be determined, and the concentration at which 60% of reactions yielded a band can be recorded as the single-molecule concentration. Then, a larger batch of PCRs (96-well plate) can be conducted using a buffer containing this single-molecule DNA concentration, and these bands can then be

visualised by the same process as before. Each of the 96 wells that holds a PCR product is labelled as such ready for the final stage of mutant detection.

The stage of mutant detection involves preparing a long, 40 cm 1% agarose gel, and loading the contents of each of the positive reaction wells from the previous round of SM-PCR onto the gel. By applying an electric field these fragments will separate by gel electrophoresis over this greater gel distance to ensure a high level of fragment length resolution. Once visualised, the parental alleles can be identified, and deviating either side of these progenitor bands will be size-variant alleles. These alleles are scored as mutants, and this provides the basis for the estimation of ESTR mutation frequency. As a general rule, the size difference must be a minimum band migration distance of 1 mm more or less than the parental alleles to be classed as a mutant (Dubrova, 2005).

3.2.4 Mice

The mice used in this study were F_1 heterozygous C57BL/6 × CBA/H hybrid males, with their individual Ms6-hm allele sizes of 5 kb for C57BL/6, and 3.5 kb for CBA/H. This strain has previously been used by Yauk et al. (2002) because of the improved allele resolution that can be achieved from hybrid mice with significant size differences between the parental alleles. The explanation for this improved resolution stems from the fact that each PCR in the SM-PCR method has on average a single DNA template, and so some reactions will have no template whilst others will have two or maybe more templates. By using C57BL/6 × CBA/H hybrid mice it is easier to distinguish between paternally- and maternally-derived alleles because of the 1.5 kb size difference, whereas in inbred homozygous mice the two parental alleles will be almost identical in size, and consequently may cast doubt on whether a given band should be classified as parental in origin or as a small mutation.

When selecting the ages of the mice to be used it was important to get a broad range of ages. The ages of the mice used in this investigation were chosen as 12, 26, 48 and 96 weeks, as these were deemed representative of young, middle-aged, and old mice.

Given that mice of almost two years of age would be analysed, it was necessary to verify the genotype of each mouse at the beginning of the study to ensure that the correct strain had been received from the suppliers. This way, the possibility of arriving at the end of the study with mice of an unrequested genotype could be avoided. Thus, all the hybrid mice were genetically screened from ear-punch tissue taken during the marking process, and any mice of an unrequested

genotype were identified and removed. The remaining mice were then portioned into age cohorts.

3.2.5 Tissues Analysed

This investigation was founded on the hypothesis that DNA replication provides the main impetus for ESTR mutation induction, and so to test this assumption it is necessary to analyse tissues with varying rates of cell division and therefore DNA replication events. With this in mind the post-mitotic brain was used as a non-dividing tissue which, theoretically, should not experience an elevated mutation frequency with age, and the bone marrow was selected as a somatic tissue with an overall intermediate rate of cell division. In addition to this, the male germline will be studied owing to its high mitotic index, but also because of its unique DNA processing involving germline-specific meiotic recombination. In both the bone marrow and in sperm it is predicted that the mutation frequency will increase with age as the high cell turnover will provide numerous opportunities for replication errors to cause ESTR mutation should this be the principle mechanism of mutation.

3.2.5.1 Brain

The nervous system comprises two classes of cells: neurons and glial cells. Neurons are the cells responsible for synaptic transmissions and must remain active throughout the life-span of an organism. They cannot divide, and make up <10% of the cells in the whole brain (Brooks, 2002). The glial cells can be divided into three cell types: astrocytes, oligodendrocytes, and microglial cells. Astrocytes are responsible for controlling the extracellular neuronal environment, oligodendrocytes form myelin for insulation of neuronal axons, and microglial cells are activated in response to infection and inflammation (Brooks, 2002).

The process by which nerve cells are generated during brain and central nervous system formation is called neurogenesis, and this is driven by a small population of multipotent neural stem cells (NSC). The NSCs may divide in one of two ways: proliferative or differentiative cell division. In proliferative cell division an NSC divides into two identical NSCs to double their number, whereas in differentiative cell division the NSC divides to create one NSC and a functionally-distinct neural progenitor cell that will subsequently go on to initiate a range of specific new neural cell lineages. These differentiated neural cells will give rise to one of three types: neurons, astrocytes, or oligodendrocytes (Gage, 2000) (Figure 3.1).

Prenatal neurogenesis is a mitotically-proficient event, but cell division is mostly redundant in most areas of the adult postnatal brain. However, by using the uracil analogue bromodeoxyuridine (BrdU), several studies have measured the number of dividing S-phase cells to highlight areas of the adult mammalian brain that undergo cell division. For instance, Kuhn *et al.* (1996) showed that a population of continuously dividing progenitor cells resides in the subgranular zone of the dentate gyrus of the hippocampus in rodents, and another study calculated that approximately 10,000 or more new neurons are added each day to the adult dentate gyrus in rats (Cameron and McKay, 2001). This finding has been extended to humans too, when Eriksson *et al.* (1998) illustrated the existence of hippocampal neurogenesis in post-mortem human brain specimens. That said, the mitotic activity of the brain overall is incredibly low, and thus makes it a suitable tissue for the analysis of mutation-induction in, effectively, replication-deficient cells.

3.2.5.2 Bone Marrow

The adult bone marrow (or haemopoietic) system is characterised by a hierarchical organisation of differentiating multipotent, pluripotent, and unipotent cellular intermediates. These stem cells will ultimately result in the formation of functionally distinct mature myeloid or lymphoid (including the B- and T-cells of the immune system) blood cell types (Figure 3.2).

The relatively rare haemopoietic multipotent mast cells that head this hierarchy are called haemopoietic stem cells (HSC). These stem cells may either differentiate into a pluripotent lympho-myeloid progenitor stem cell-type, or they may regenerate HSCs in a process called self-renewal. However, this process is heavily biased in favour of differentiation, given that HSCs account for only 0.02% of the total mix of bone marrow cells, and so only this small fraction needs to be replenished (Greaves, 1996).

Moving down to the hierarchy of differentiated cells and after the myeloid-lympho divergence, the stem cells become increasingly narrow in the types of cell they may generate. Myeloid progenitor stem cells can differentiate into cell lineages that eventually lead to terminally differentiated red blood cells (erythrocytes) or platelets (megakaryocytes) to name but a few. Lymphoid progenitor pluripotent stem cells can diverge into lineages that culminate in the production of fully functional and terminally differentiated B- and T-lymphocytes.

This pattern of cellular differentiation has been established by the use of morphological features, cell-surface antigens, and cell-specific enzymes, as well as through cell line differentiation studies (Greaves, 1996). Given that heamopoiesis is

a dynamic process $(1 \times 10^{10}$ red blood cells per hour) the self-renewal and differentiation processes have to be highly regulated (Cheshier, *et al.*, 1999).

3.2.5.3 Sperm

The process by which mature sperm are produced from their early, stem cell progenitors, is called spermatogenesis. It comprises a sequential set of events called spermatocytogenesis, spermatidogenesis, and spermiogenesis, and occurs within the seminiferous tubules of the testes and epididymis where specialised somatic Sertoli cells lining the basal membrane help provide an environment for spermatogenesis to thrive in.

The best characterised system of spermatogenesis is in rodents. Rodent spermatocytogenesis begins in individual spermatogonial stem cells called A-single (A_s) spermatogonia with a series of proliferative mitotic divisions. These mitotic divisions can serve either as a self-renewing source of new A_s spermatogonia, or alternatively they may form a pair of spermatogonia (called A_{pr} spermatogonia) that do not complete cytokinesis and stay connected by an intercellular bridge. The A_{pr} spermatogonia will then divide further to create long chains of four, eight, and sixteen A-type spermatogonia called A-aligned (A_{al}) spermatogonia, before differentiating into so-called A_1 spermatogonia. From here there are further differentiative divisions as the A_1 spermatogonia cells form A_2, A_3, A_4, In (intermediate) and B-type spermatagonia. The B-type spermatogonia then divide into primary spermatocytes to complete spermatocytogenesis (see Aponte, *et al.*, 2005 for a more extensive review of spermatogenesis) (Figure 3.3).

The primary spermatocytes then commence with spermatidogenesis by duplicating their genomes and undergoing meiosis I to produce two diploid secondary spermatocytes. This is promptly followed by entry into meiosis II and another cell division to produce haploid round spermatids with intermediate types Sa, Sb, Sc, Sd_1, and Sd_2 spermatids.

Once spermatidogenesis is complete, the round spermatids move into spermiogenesis and go through a series of morphological changes within Sertoli cells to become non-motile spermatozoa. These non-motile spermatozoa are then released from their hosting Sertoli cells so that they may be shed into the lumen of the seminiferous tubule for transport out of the testis in a process called spermiation. From here, the spermatids are carried into the epididymis where they continue their maturation into fully mobile spermatozoa.

3.2.6 Singleton, Mosaic, and Unique Mutations

In any breeding scheme the progeny mice will inherit a paternal and a maternal ESTR size-variant, and these non-mutant, wild-type alleles will be found in all tissues of the offspring. However, should any of these paternal or maternal alleles mutate to a different size in a given tissue, this new allele of unique, non-parental size will be detected on an agarose gel by the methods described above. Such isolated size-variant alleles are called singleton mutations, and will have arisen as an independent mutation event. In the event of two or more ESTR mutant alleles of equal size being detected on an agarose gel, it becomes uncertain whether these alleles arised independently of each other or if they arose as derivatives of a common mutation event. These clusters of two or more same-sized mutant alleles are called mosaic mutations (Favor and Neuhäuser-Klaus, 1994).

Unfortunately it is not possible to verify whether mosaic mutations are derived from a common mutation event or as independent mutation events. At minisatellite loci, with their heterogenous internal sequence structures, the technique of minisatellite variant repeat (MVR)-PCR can be used to identify the component sequence sub-units by using primers specific for different internal sequences (Jeffreys, et al., 1991). This method allows the order of sequence subunits to be determined, and thus reveal important information on how these minisatellites mutated and where they originate from (Jeffreys et al., 1991). However, this approach cannot be used at ESTRs, as their homogenous internal structure prohibits the use of multiple internal primers. With this in mind, ESTR mutants are classified as singleton or mosaic during the final analysis of data.

Another problem of analysing mosaic mutations at ESTR loci comes from the inherent hypermutability of ESTRs. Their high spontaneous mutation frequencies mean that mutant alleles readily arise, and so it is highly likely that two or more mutants of the same size will be generated. To account for this, mosaic mutations in this analysis were defined more stringently as having five or more same sized alleles in a given sample, and were assumed to arise from a single mutation event; possibly during early embryogenesis (Kelly, et al., 1989; 1991; Gibbs, et al., 1993). With the mutants thus classified as singleton or mosaic, a third category named 'unique' mutations was created to encompass each singleton mutation and each cluster of mosaic alleles. In this scheme, for example, five mosaic alleles of the same size would thus be counted as one unique mutation, as would a solitary singleton mutation.

3.3 ESTR Spontaneous Mutation Frequency Analysis

The results of the age-related study on ESTR mutation frequency at the locus Ms6-hm in F_1 heterozygous C57BL/6 × CBA/H hybrid males are presented in Figure 3.4 and discussed below.

3.3.1 Brain ESTR spontaneous mutation frequency does not change significantly with age

SM-PCR analysis of DNA extracted from whole brain tissues was performed to determine the ESTR spontaneous mutation frequency caused by this largely post-mitotic tissue. If the mechanism of mutation is replication-dependent, then the frequency would be expected to increase with age.

The graph in Figure 3.4 illustrates clearly how the spontaneous frequency of total ESTR mutations remains stable across age groups, and Figures 3.10 and 3.11 illustrate two representative autoradiographs to show how mutants are identified. This is supported by the pairwise comparisons of singleton, mosaic, and unique mutation frequencies between the 12 week old mice and the other age cohorts in Tables 3.1 and 3.2, and the correspondingly insignificant statistical differences. In each of these pairings, there was no significant increase in mutation frequency with age.

3.3.2 Bone marrow ESTR spontaneous mutation frequency does not increase significantly with age

The bone marrow from each mouse was collected by passing phosphate-buffered solution (PBS) through each of their tibia and collecting the bone marrow suspension in an Eppendorf tube. Thus all cells from the heterogenous bone marrow cell population were captured for analysis, some of which will be actively dividing such as early haemopoietic stem cells, whilst others will be terminally differentiated, such as macrophages and neutrophils. This meant that overall the rate of cell division from this population of cells will be intermediate between the brain and a highly proliferative system.

By inspecting Figure 3.4 it can be seen that the mutation frequency at the ESTR locus Ms6-hm shows a general slight increase with age, but Tables 3.1 and 3.2 reveal that the statistical significance of this increase is marginally insignificant

for each comparison. However, there is a statistically significant increase between age 12 and 96 weeks when the mosaic mutations are considered (Table 3.1).

.

3.3.3 Sperm ESTR spontaneous mutation frequency increases significantly with age

In this study, mature, epididymal sperm cells were analysed. This way a homgenous population of mature sperm could be obtained, given that only the mature sperm products of spermatogenesis are stored in the caudal epididymis, ready for ejaculation. To ensure the purity of the homogenised caudal epididymi samples, the homogenate was washed with a small volume of 10% sodium dodecyl-sulphate (SDS) which differentially lyses the somatic Sertoli cells but not the sperm. The reason for this is the relatively high osmotic potential of the somatic cells compared to sperm. Confirmation that the homogenate was somatic-cell-free was delivered by eye using a light microscope. DNA was then extracted from this remaining pool of purely sperm cells, and SM-PCR performed.

Figure 3.4 depicts how the ESTR mutation frequency in sperm rises dramatically with age in a highly statistically significant manner. Looking at the frequency curve reveals that, as with bone marrow, there is an upward trend in mutation frequency with age, although in sperm it is much more pronounced. Statistical analysis by the t-test in Tables 3.1 and 3.2, show no significant increase in unique mutations between ages 12 and 26 weeks, but a significant elevation between 12 and 48, and 12 and 96 weeks. It is the same for singleton and mosaics, although the mosaics are also significantly higher between 12 and 26 weeks. This showed that in a homogenous population of cells from a proliferating system such as spermatogenesis, the ESTR mutation frequency significantly increases with age.

Another analysis of sperm data is presented in Figure 3.5. If the mutation mechanism is directly attributed to DNA-replication-associated events, then it might be expected that the ESTR mutation frequency increases linearly with the number of cell divisions, and therefore age. Looking at the total mutation frequency of singletons and mosaics, it shows how the there is a sharp increase between 12 and 48 weeks of age, but the curve then plateaus as the mice reach 96 weeks old. This data, however, scores each mosaic mutant, but if it were assumed that each cluster of mosaic mutants in a sample originated from a single mutation event, then each cluster of unique size in fact represents one unique mutation, and not, for example, five mosaics. When the frequency of unique ESTR mutations is analysed in Figure 3.5, it can be seen that the increase is linear with age.

3.3.4 Ages 12 and 26 weeks were classified as 'young' mice, and ages 48 and 96 weeks classified as 'old' mice based on similar mutation frequencies

Table 3.2 and Figure 3.5 show that for unique mutations in sperm, there is a general upward linear trend in ESTR mutation frequency with age, but the biggest increase comes in the comparison of the 48 weeks old group to both the 12 and 26 weeks old cohorts. This allowed the data to be pooled together into two cohorts: 'young' mice (ages 12 and 26 weeks), and 'old' mice (ages 48 and 96 weeks). By doing this, the number of mice per cohort was doubled and this made for a more robust analysis.

3.3.5 Analysis of the mutation spectra for brain, bone marrow, and sperm shows no age-related effect but possible tissue-specific differences

By analysing the ESTR mutation spectrum data for the distribution of repeat gains and losses (*i.e.* the number of repeats gained or lost and their sizes), it is possible to shed more light on the potential mechanism of mutation. The rationale here is that if there is a common mechanism of mutation at work then the spectra can be expected to be the same or not significantly different, whereas if there is a significant difference between the spectra of different cohorts it is conceivable that each of these has its own distinct principle mutational mechanism. The questions to be answered are: do the age and tissue-type affect the mutation spectrum at the ESTR locus Ms6-hm?

Figures 3.6, 3.7, and 3.8 show the mutation spectra analyses for both young and old mice in the brain, bone marrow, and sperm tissues respectively. By applying the Kolmogorov-Smirnov two-sample test to the data, it was shown that the spectra do not significantly differ across all age cohorts for each tissue. This means there is no significant change in the mutation spectra of each tissue category that can be attributed to age. However, this does not resolve the issue of whether tissue-type has a bearing on the mutation spectra.

Since the mutation spectra for each tissue did not change significantly with age, these data could be pooled together on the basis of tissue, with each spectrum encompassing all ages (Figure 3.6). By comparing these three tissue spectra by analysis of variance (ANOVA), the effects of age, tissue and any interacting effects could be assessed, and the resulting *P*-values were again insignificant.

The implications of these results will be discussed below.

3.4 Discussion

This study aimed to analyse the effects of age on the spontaneous mutation frequency at the mouse ESTR locus Ms6-hm in different tissues. The objective was to provide further information on the biological mechanisms that promote ESTR mutation, with the hypothesis being that DNA replication slippage is chiefly responsible. If this assertion was correct, then the mutation frequency would be expected to significantly increase with age in actively dividing tissues such as sperm and bone marrow, and remain stable in non-dividing tissues such as the brain. Thus, these three different tissues were investigated in untreated male F_1 C57BL/6 × CBA/H hybrid mice of ages 12, 26, 48, and 96 weeks. The SM-PCR method of Yauk et al. (2002) was used to detect size-varying mutants for the purpose of estimating mutation frequency.

The data reported here generally agree with the hypothesis of replication-induced ESTR mutation induction. Analysis of the mitotically-inactive brain showed no evidence of a significant increase in total mutation frequency with age, and further support came from the sperm tissue with its high cell turnover and corresponding statistically significant ESTR mutation frequency increase between young (ages 12 and 26 weeks) and old (ages 48 and 96 weeks) mice. The elevated mutation frequencies in sperm can be attributed to an increase in both the number of singleton and mosaic mutations with age, and when these total mutation data are interpreted as unique mutations (i.e. one singleton mutation equals one unique mutation, and one cluster of same-sized mosaic mutants also equals one unique mutation) there emerges a linear age-related increase. This suggests the involvement of DNA replication in the generation of ESTR mutations at each independent cell division event. It should also be noted that the origin of these mutations is likely to be the rapidly dividing spermatogonial stem cells. This is because spermatogonial stem cells persist in the germline throughout the lifetime of the mouse; continually and actively dividing to produce new sperm to replace any unused epididymal sperm. Thus, the observed age-related ESTR mutation frequency increases in the mature epididymal sperm are likely to be reflective of replication-related mutation accumulation in actively replicating spermatogonial stem cells, rather than events during spermatogenesis. This theory would be supported by studies which showed the spermatogonial stage of mutation induction to be the pre-meiotic spermatogonial stem cells (Dubrova, et al., 1998; Barber et al., 2000), although other work has pointed to post-meiotic stages to be the time of ESTR mutation induction (Sadamoto et al., 1994; Fan et al., 1995; Niwa et al., 1996).

One possible exception to this theory is the bone marrow tissue. The bone marrow ESTR mutation frequency increased with age but was marginally statistically insignificant. Given that whole bone marrow samples (like the ones analysed here) comprise an assortment of cell lineages and cell types of differing proliferative status, the overall rate of cell division will lie intermediate between that of the brain and sperm, and it might be expected that this rate of division would be high enough to translate into a statistically significant increase in ESTR mutation frequency. The data in this study, however, suggest that perhaps it is the non-dividing cells which dominate the analysis and dilute the effects of the dividing bone marrow cells. Thus the lack of a significant increase in ESTR mutation frequency in bone marrow does not necessarily contradict the hypothesis of a replication-mediated mutation mechanism. It is thus concluded that ESTR mutation induction is linked to cell division, and DNA replication is a likely driver of this process due to its active presence in the dividing cell.

DNA replication has been implicated as an important driver of microsatellite instability (reviewed in Ellegren, 2004), and given the structural sequence similarities between microsatellites and ESTRs, it is reasonable to propose from these observations that DNA replication is important in the mutation process at the ESTR locus Ms6-hm. However, it is still feasible that other mechanisms not directly associated with DNA replication could play a role (however small) in ESTR mutation induction. For example, the brain with its mitotic inactivity still has mutation frequencies of between 7 and 10% across the ages analysed in this study (Tables 3.1 and 3.2), although one explanation consistent with the involvement of DNA replication is that the mutant ESTR loci identified in the brain samples from each age group arose during embryonic neurogenesis when neural cell division was prolific. Once the mature brain was formed and cell division ceased, these mutants remained in their host nerve cells. This explanation is plausible, as all normal mice should theoretically experience the same amount of pre- and early post-natal neuronal cell divisions to generate the mature brain. Alternatively, in light of evidence that specific regions of the mammalian brain can remain weakly mitotically active into adulthood (Kuhn, *et al.*, 1996; Cameron and McKay 2001), it could be possible that mutations observed in this study from whole brain extracts were the effect of low-level DNA replication activity in the adult mouse brain. However, the latter scenario seems unlikely to have a pronounced effect, given the steady mutation frequency across all age groups – including those aged 12 weeks.

To check if the same mutation mechanism operates at ESTRs in all tissue types it is possible to compare the mutation spectra of repeats gained and lost to

look for commonalities. The ANOVA results showed that age, tissue, and possible interaction effects appear to have no bearing on the mutation spectra of Ms6-hm. This is despite an observed subtle difference in the spectrum directionality in bone marrow compared to the brain and sperm. When all age data are pooled together, the bone marrow mutation spectrum is slightly skewed in favour of gains (55:45 gains:losses), compared to the brain (50:50), and the sperm (44:56) (Table 3.3). Based on the ANOVA results, however, it seems that these differences are not significant and so it can be concluded that the same main mutation mechanism is in operation in all tissues at all ages.

Further clues for a common mutational mechanism come from a closer inspection of the most common size changes in all of the spectra, regardless of direction. This reveals that the majority of repeat gains and losses in all three tissues are short expansions and contractions that lie in the range of +/- 4–10 repeats, and very few of the mutants fall outside this window with size differences of >10 repeats. Jeffreys *et al.* (1988a) suggested that small size changes of 4–10 repeats are likely to be attributed to replication slippage whilst larger changes of up to 200 repeats could be caused by recombination pathways. If this logic is applied to these data, then it would be consistent with the hypothesis that replication events are the main cause of ESTR mutation. The bigger repeat expansions and contractions in this data set could possibly be held accountable to relatively rare recombination events, although a study by Barber *et al.* (2000), which monitored the crossover frequency of a panel of microsatellite markers in mice with various ESTR mutation rates, found no correlation between crossover frequency and ESTR mutation rate, and concluded that meiotic recombination was not a key instigator of ESTR mutation induction. Overall, from these data in this chapter, it would seem that replication-slippage is the main driver of mutation induction at the ESTR locus Ms6-hm.

The possible bias to repeat gains in the bone marrow when compared to the brain and sperm may reflect a greater tendency in this tissue for the nascent strand to fold into slipped-DNA structures. In sperm, with their possible bias for repeat losses, the folding could mainly be occurring in the template strand. Mirkin (2006) suggested that the main cause for these replication-slippage events is erroneous lagging-strand DNA synthesis due to its discontinuous nature and the subsequent greater opportunity for secondary structure formation when compared to leading strand synthesis, and may offer a potential mechanistic template to describe the process of ESTR replication-slippage. To explain a possible tissue-specific difference in mutational dynamics, perhaps *cis*-acting tissue-specific factors exert an influence on the replisome to bias the directionality of ESTR mutation induction?

However, as stated above from the ANOVA data, these slight biases may not be important and so it remains unclear and speculative to suggest any directional bias.

The conclusion drawn so far is that DNA replication-slippage is the primary mutation mechanism at ESTRs, and this is well supported by previous studies on ESTR mutation induction. Barber *et al.* (2000) could find no link between meiotic recombination and ESTR mutation induction, whilst various DNA-repair deficiencies were concluded to be significant in inducing mutations at ESTR arrays (Barber, *et al.*, 2004; Burr, *et al.*, 2006; Burr, *et al.*, 2007), but in each case these studies proposed the involvement of DNA replication-pausing during slippage as the key contributing factor to ESTR mutation induction.

The replication-slippage model is also in-keeping with the prevailing view of how most microsatellite loci mutate (Ellegren, 2004). This could be expected to be the case, given the similarities in internal structure between ESTRs and microsatellites. Both of these tandem repeat loci are characterised by highly homogenous sequence structures that contain numerous uninterrupted repetitions of the same repeat motif, and are thus likely to present similar problems to DNA polymerases during replication. That said, ESTRs are typically more unstable than microsatellites, with observations in this study pointing to spontaneous mutation frequencies on a magnitude scale of 10^{-2} in young mice, and 10^{-1} in sperm samples from old mice. This is higher than most microsatellites, whose spontaneous mutation frequencies typically lie in the range of 10^{-4} to 10^{-3} (for example Brinkmann, *et al.*, (1998); Dupuy, *et al.*, (2004)). These higher mutation frequencies are likely to reflect the much larger allele size of ESTRs (between 3 and 15 kb) coupled to their homogenous and uninterrupted sequence structure, which is known to be a cause of repeat instability (Kunst and Warren, 1994). Together, these factors would provide more opportunity for secondary-structure formation across the array and subsequently more frequent replication-slippage. This proposal is supported by Brinkmann *et al.* (1998) who found that the microsatellite mutation rate increased almost exponentially in line with the mean size of uninterrupted repeats.

In conclusion, the data presented in this chapter indicate that replication slippage is the underlying mutational mechanism at the ESTR locus Ms6-hm. This is based primarily on the observation of age-related increases in Ms6-hm spontaneous mutation frequency in the mitotically-proficient tissues of bone marrow and sperm, but not in the post-mitotic brain. Furthermore, the mutation spectra do not differ significantly with age or tissue, which lends support to the idea that the replication-slippage model can be applied to all the tissues studied and across the range of ages.

As a model of spontaneous ESTR instability, the initiating event would be duplex unwinding during DNA replication, which would leave the array susceptible to intra-strand folding and the creation of short tetraplex structures (Weitzmann, *et al.*, 1998; Katahira, *et al.*, 1999; Fukuda, *et al.*, 2002). Our data suggest that these structures will mainly entrap short tracts of 4–10 repeats, as indicative of replication slippage (Jeffreys, *et al.*, 1988a). Following this, the ESTR tetraplexes could protrude out from the leading strand and interfere with fork progression in the lagging strand to cause replication-pausing, or alternatively they may establish themselves in the lagging template strand and effectively remove a short tract of sequence from the template during DNA synthesis by DNA polymerases. These events would trigger expansions and contractions respectively. This conclusion would complement previous work that proposed replication fork pausing to be the cause of ESTR mutation induction (Dubrova, *et al.*, 1998; Barber, *et al.*, 2000; Barber, *et al.*, 2002; Dubrova, *et al.*, 2002; Barber, *et al.*, 2004; Burr, *et al.*, 2005; Burr, *et al.*, 2006), and thus add to the evidence implicating DNA replication as the main cause of ESTR mutations.

Table 3.1

Table to show the age-related changes in ESTR mutation frequencies in mouse tissues. Presented is the total frequency of singleton and mosaic mutations at the ESTR locus Ms6-hm and their summed total, in brain, bone marrow, and sperm tissues taken from F_1 C57BL/6 × CBA/H hybrid male mice of ages 12, 26, 48, and 96 weeks. Also shown are the ratios of the mutation frequencies for each age relative to that of the 12 week old cohort, and the associated *P-value* from Student's *t*-test analysis comparing the frequencies in these ratios.

Tissue, Age (weeks)	No. Molecules	No. mutants[a]	Total Number of Mutations				Singletons			Mosaics		
			Frequency ± s.e.[b]	Ratio[c]	t^d	Prob[d]	Frequency ± s.e.[b]	t^d	Prob[d]	Frequency ± s.e.[b]	t^d	Prob[d]
Brain												
12	326	28 (18)	0.0859±0.0171	-	-	-	0.0552±0.0134	-	-	0.0307±0.0099	-	-
26	447	31 (19)	0.0694±0.0131	0.81	0.77	0.4425	0.0425±0.0101	0.76	0.4496	0.0268±0.0079	0.30	0.7624
48	367	36 (22)	0.0981±0.0173	1.14	0.50	0.6154	0.0627±0.0135	0.39	0.6962	0.0354±0.0100	0.34	0.7361
96	484	38 (23)	0.0785±0.0136	0.91	0.34	0.7356	0.0475±0.0103	0.45	0.6502	0.0310±0.0082	0.02	0.9804
Bone marrow												
12	394	39 (29)	0.0990±0.0169	-	-	-	0.0736±0.0144	-	-	0.0254±0.0082	-	-
26	642	60 (29)	0.0935±0.0131	0.94	0.26	0.7962	0.0452±0.00087	1.69	0.0911	0.0483±0.0091	1.88	0.0606
48	426	68 (44)	0.1596±0.0212	1.61	2.24	0.0256	0.1033±0.0165	1.36	0.1758	0.0563±0.0119	2.15	0.0322
96	546	82 (35)	0.1502±0.0186	1.52	2.03	0.0422	0.0641±0.0114	0.52	0.6049	0.0861±0.0135	3.86	0.0001
Sperm												
12	426	49 (30)	0.1150±0.0177	-	-	-	0.0704±0.0135	-	-	0.0446±0.0105	-	-
26	552	84 (36)	0.1522±0.0187	1.32	1.44	0.1494	0.0652±0.0115	0.29	0.7684	0.0870±0.0135	2.47	0.0135
48	401	125 (56)	0.3117±0.0328	2.71	5.27	$<10^{-6}$	0.1397±0.0202	2.85	0.0045	0.1721±0.0228	5.07	$<10^{-6}$
96	397	118 (60)	0.2972±0.0325	2.58	4.92	10^{-6}	0.1511±0.0215	3.19	0.0015	0.1461±0.0210	4.31	2×10^{-5}

[a] Number of singleton mutations is given in brackets.

[b] ± standard error.

[c] Ratio to the 12-week group.

[d] Student's test and probability for difference from the 12-week group.

Table 3.2

Table to show the age-related changes in ESTR mutation frequencies in mouse tissues. Presented is the total frequency of singleton and mosaic mutations at the ESTR locus Ms6-hm and their summed total, in brain, bone marrow, and sperm tissues taken from F_1 C57BL/6 × CBA/H hybrid male mice of ages 12, 26, 48, and 96 weeks. Also shown are the ratios of the mutation frequencies for each age relative to that of the 12 week old cohort, and the associated *P-value* from Student's *t*-test analysis comparing the frequencies in these ratios.

Tissue, age (weeks)	No molecules	No mutants[a]	Total number of mutations				Unique mutations			
			Frequency ± s.e.[b]	Ratio[c]	t[d]	Prob[d]	Frequency ± s.e.[b]	Ratio[c]	t[d]	Prob[d]
Brain										
12	326	28 (20)	0.0859 ± 0.0171	-	-	-	0.0613 ± 0.0142	-	-	-
26	447	31 (20)	0.0694 ± 0.0131	0.81	0.77	0.4425	0.0447 ± 0.0104	0.73	0.94	0.3455
48	367	36 (25)	0.0981 ± 0.0173	1.14	0.50	0.6154	0.0681 ± 0.0142	1.11	0.34	0.7360
96	484	38 (25)	0.0785 ± 0.0136	0.91	0.34	0.7356	0.0517 ± 0.0108	0.84	0.54	0.5875
Bone marrow										
12	394	39 (30)	0.0990 ± 0.0169	-	-	-	0.0761 ± 0.0146			
26	642	60 (32)	0.0935 ± 0.0131	0.94	0.26	0.7962	0.0498 ± 0.0092	0.65	1.52	0.1288
48	426	68 (46)	0.1596 ± 0.0212	1.61	2.24	0.0256	0.1080 ± 0.0169	1.42	1.42	0.1555
96	546	82 (39)	0.1502 ± 0.0186	1.52	2.03	0.0422	0.0714 ± 0.0121	0.94	0.25	0.8042
Sperm										
12	426	49 (32)	0.1150 ± 0.0177	-	-	-	0.0751 ± 0.0139	-	-	-
26	552	84 (41)	0.1522 ± 0.0187	1.32	1.44	0.1494	0.0743 ± 0.0123	0.99	0.05	0.9640
48	401	125 (59)	0.3117 ± 0.0328	2.71	5.27	$<10^{-6}$	0.1471 ± 0.0208	1.96	2.87	0.0042
96	397	118 (65)	0.2972 ± 0.0325	2.58	4.92	10^{-6}	0.1637 ± 0.0225	2.18	3.35	0.0008

[a] Number of unique mutations is given in brackets.

[b] ± standard error.

[c] Ratio to the 12-week group.

[d] Student's test and probability for difference from the 12-week group.

Table 3.3

Mutation spectra analysis of spontaneous unique mutation repeat unit gains and losses at the mouse ESTR locus Ms6-hm in brain, bone marrow, and sperm of F_1 C57BL/6 × CBA/H hybrid male mice aged 12–26 weeks (Young) and 48–96 weeks (Old).
Chi-squared analysis compares the frequency of gains and losses between age groups or tissues.

Tissue, age (weeks)	Gains	Losses	x^2	df	P
Brain					
12–26	22 (55.0)	18 (45.0)			
48–96	22 (44.0)	28 (56.0)	1.06	1	0.3032
Bone marrow					
12–26	37 (59.7)	25 (40.3)			
48–96	44 (51.8)	41 (48.2)	0.90	1	0.3427
Sperm					
12–26	37 (50.7)	36 (49.3)			
48–96	50 (40.3)	74 (59.7)	1.98	1	0.1594
All ages					
Brain	44 (48.9)	46 (51.1)			
Bone marrow	81 (55.1)	66 (44.9)			
Sperm	87 (44.2)	110 (55.85)	4.02	2	0.1282
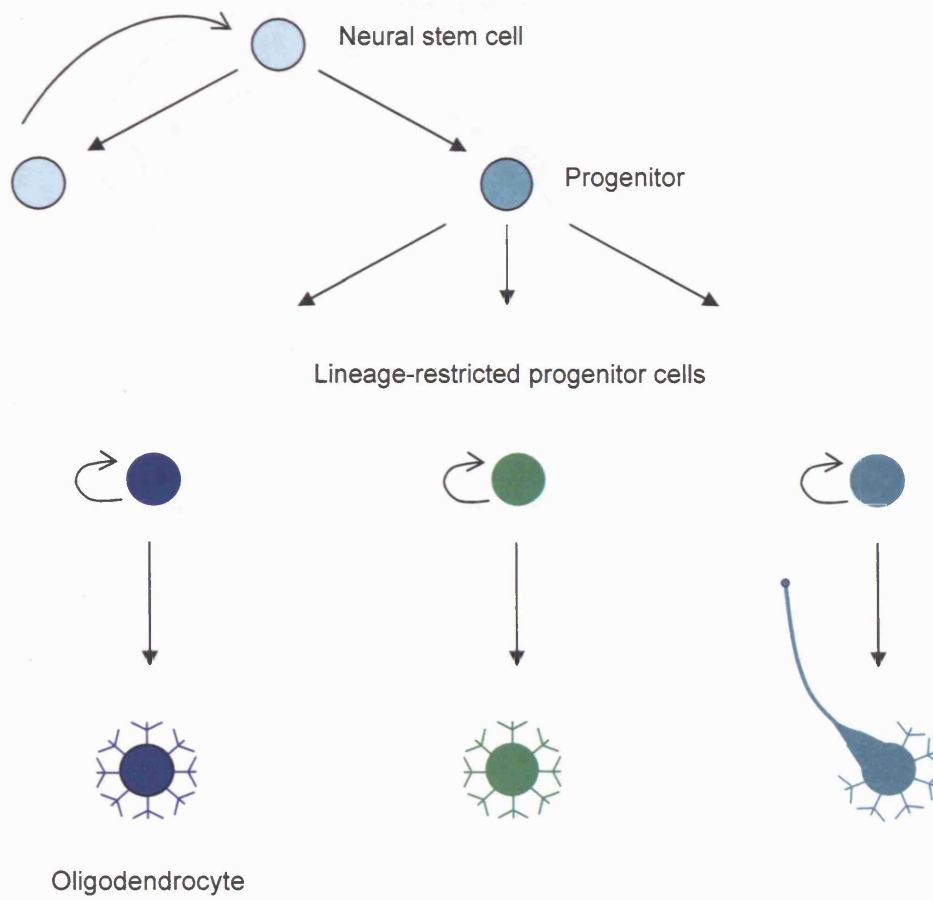
Figure 3.1
Diagram to illustrate neurogenesis. This figure accompanies the text in section 3.2.5.1.
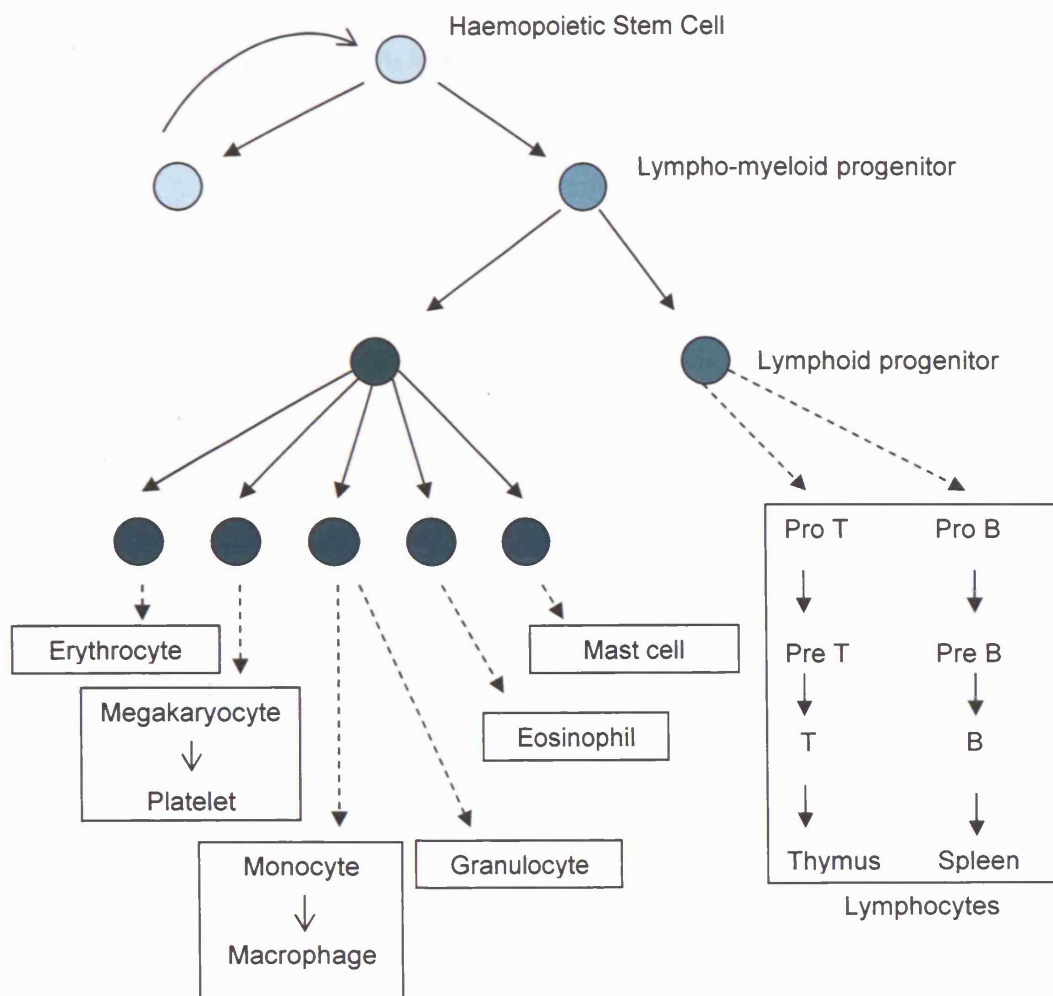
Figure 3.2
Schematic of haemopoesis. Details in section 3.2.4.2.
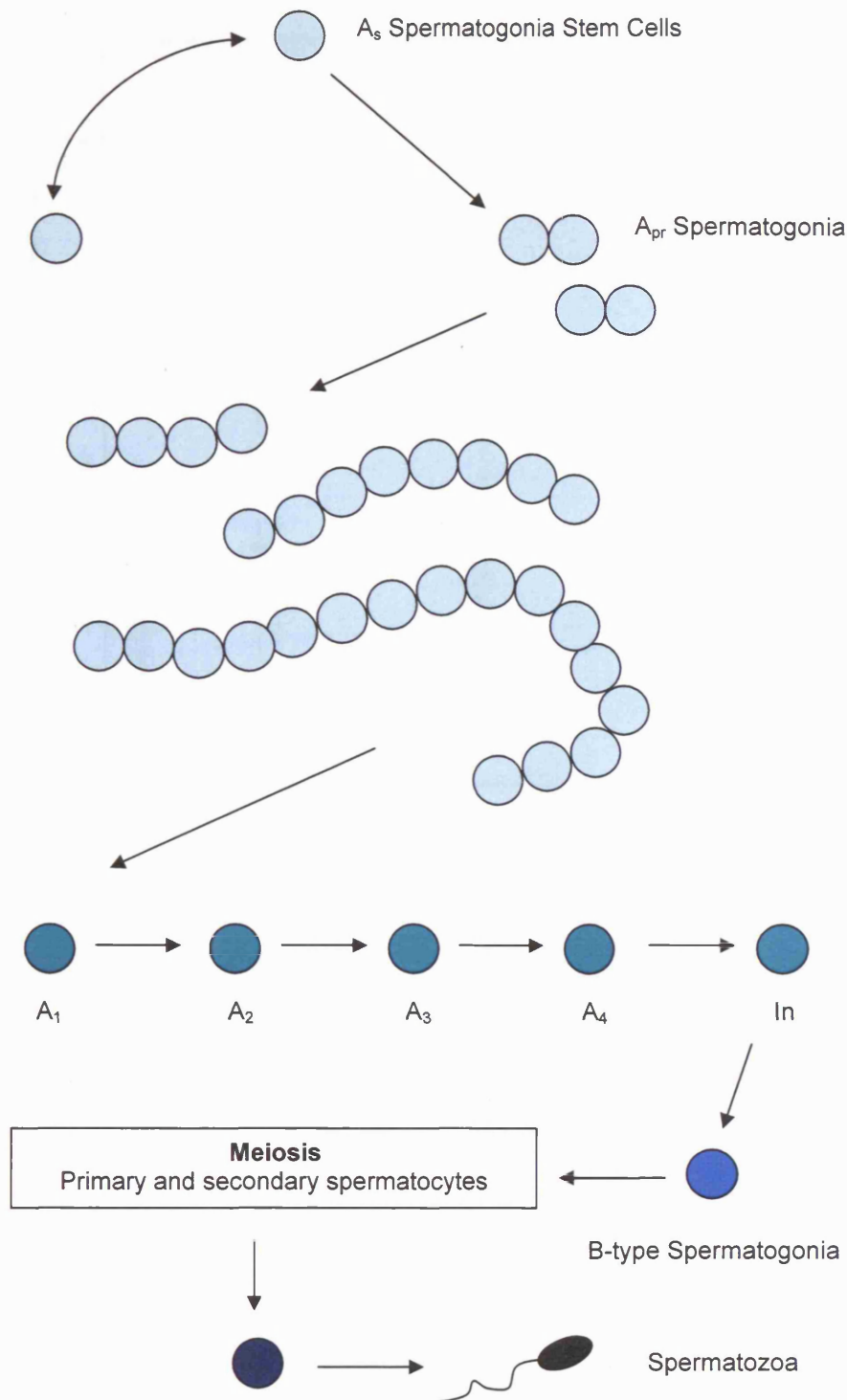
Figure 3.3
Diagram of spermatogenesis. Accompanying text in section 3.2.4.3.
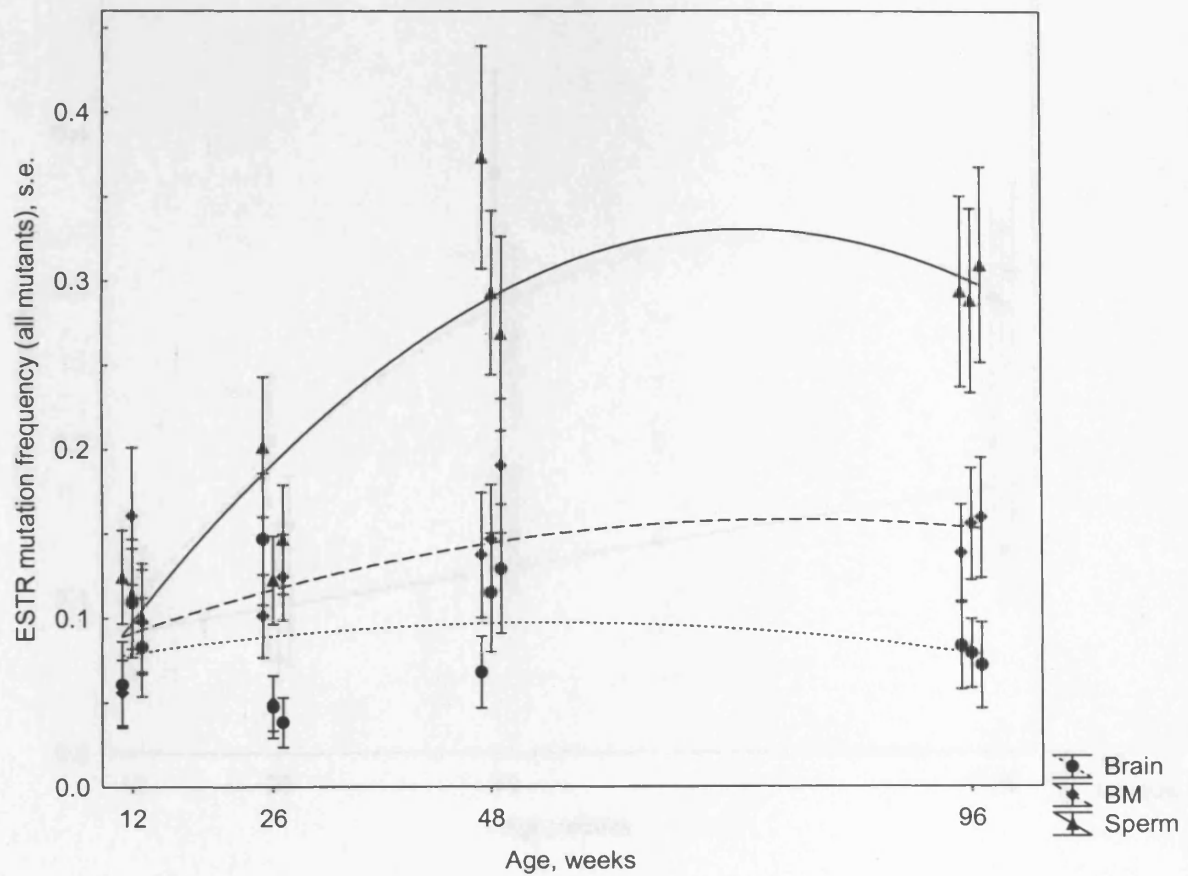
Figure 3.4
Spontaneous mutation frequencies at the ESTR locus Ms6-hm in F_1 C57BL/6 ×
CBA/H hybrid male mice. This graph compares the total mutation frequencies of
brain, bone marrow, and sperm tissues in mice of ages 12, 26, 48, and 96 weeks.
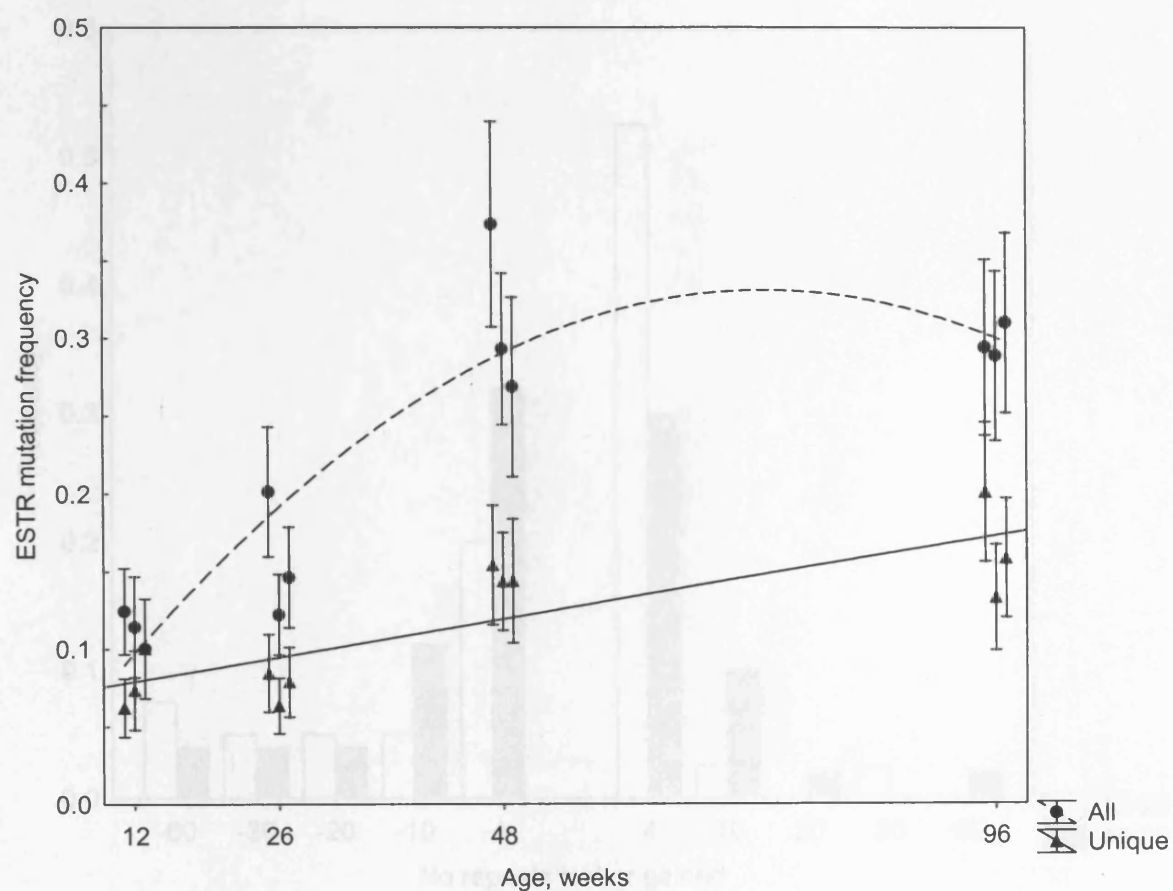
Figure 3.5
Age-related spontaneous mutation frequencies at the ESTR locus Ms6-hm in F_1 C57BL/6 × CBA/H hybrid male mice. This graph compares the mutation frequencies of total and unique mutations in the sperm tissues in mice of ages 12, 26, 48, and 96 weeks.
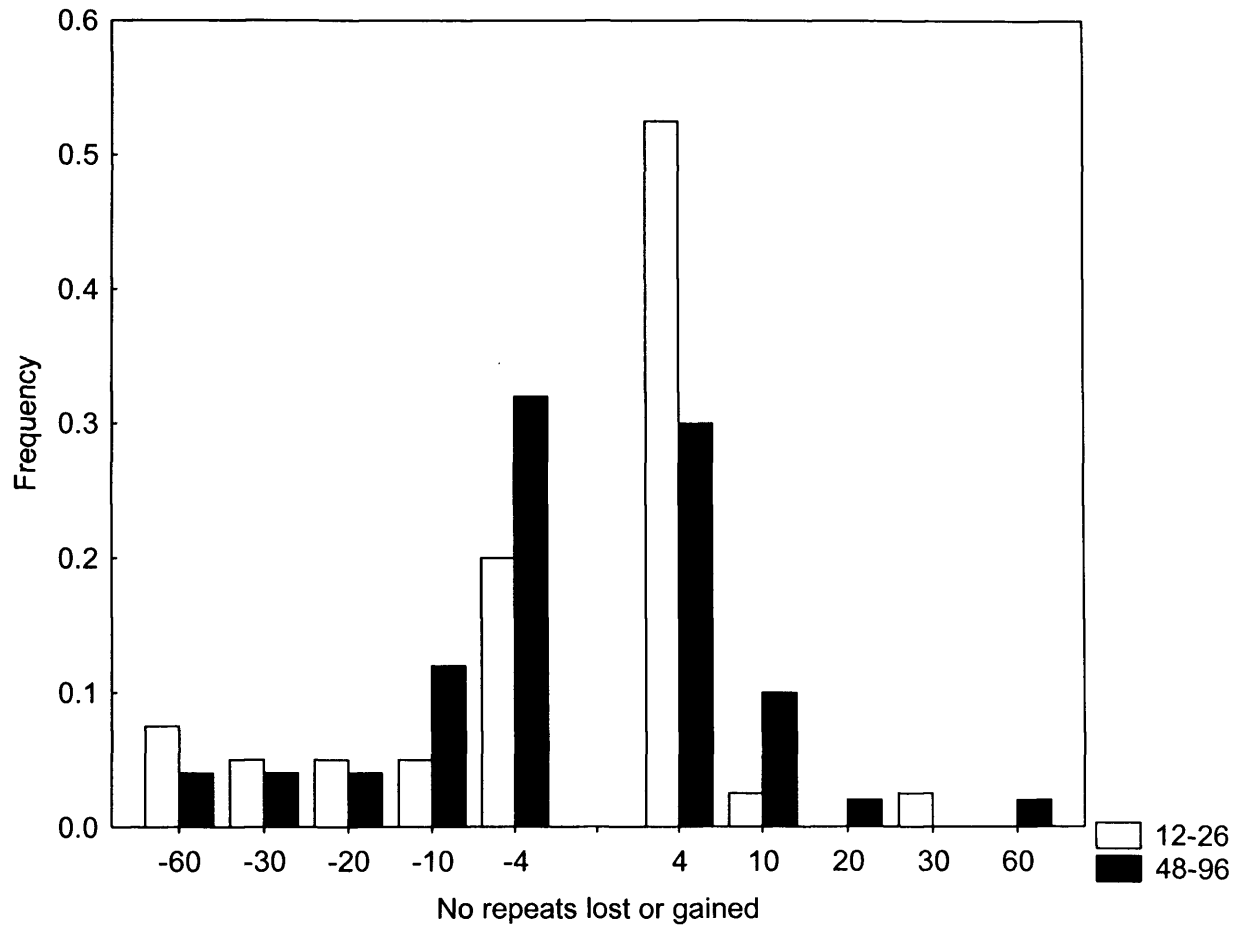
Figure 3.6
Graph to show the spectrum of unique spontaneous mutations at the ESTR locus Ms6-hm in brain from F_1 C57BL/6 × CBA/H hybrid male mice. Here, all data from ages 12, 26, 48, and 96 weeks old mice was pooled together to give an overall mutation frequency, and all mosaic mutants were treated as a single mutational event. The number of repeats lost or gained are binned as ± 4–9 repeats (± 4), ± 10–19 repeats (± 10), ± 20–29 repeats (± 20), ± 30–59 repeats (± 30), and ± 60+ repeats (± 60).
Kolmogorov-Smirnov two-sample test, P=0.7689.
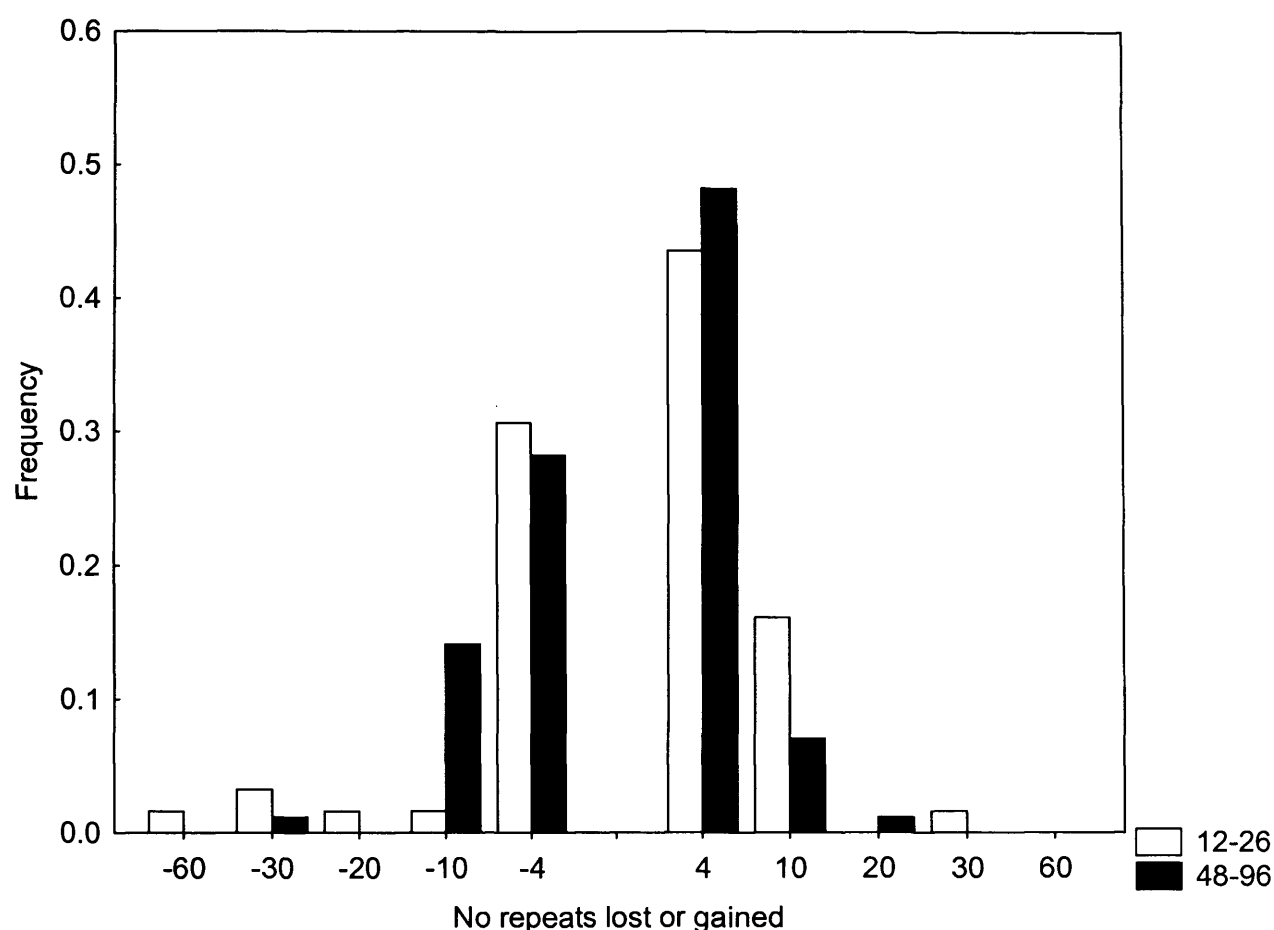
Figure 3.7
Graph to show the spectrum of unique spontaneous mutations at the ESTR locus Ms6-hm in bone marrow from F_1 C57BL/6 × CBA/H hybrid male mice. Here, all data from ages 12, 26, 48, and 96 weeks old mice was pooled together to give an overall mutation frequency, and all mosaic mutants were treated as a single mutational event. The number of repeats lost or gained are binned as ± 4–9 repeats (± 4), ± 10–19 repeats (± 10), ± 20–29 repeats (± 20), ± 30–59 repeats (± 30), and ± 60+ repeats (± 60).
Kolmogorov-Smirnov two-sample test, P=0.9098.
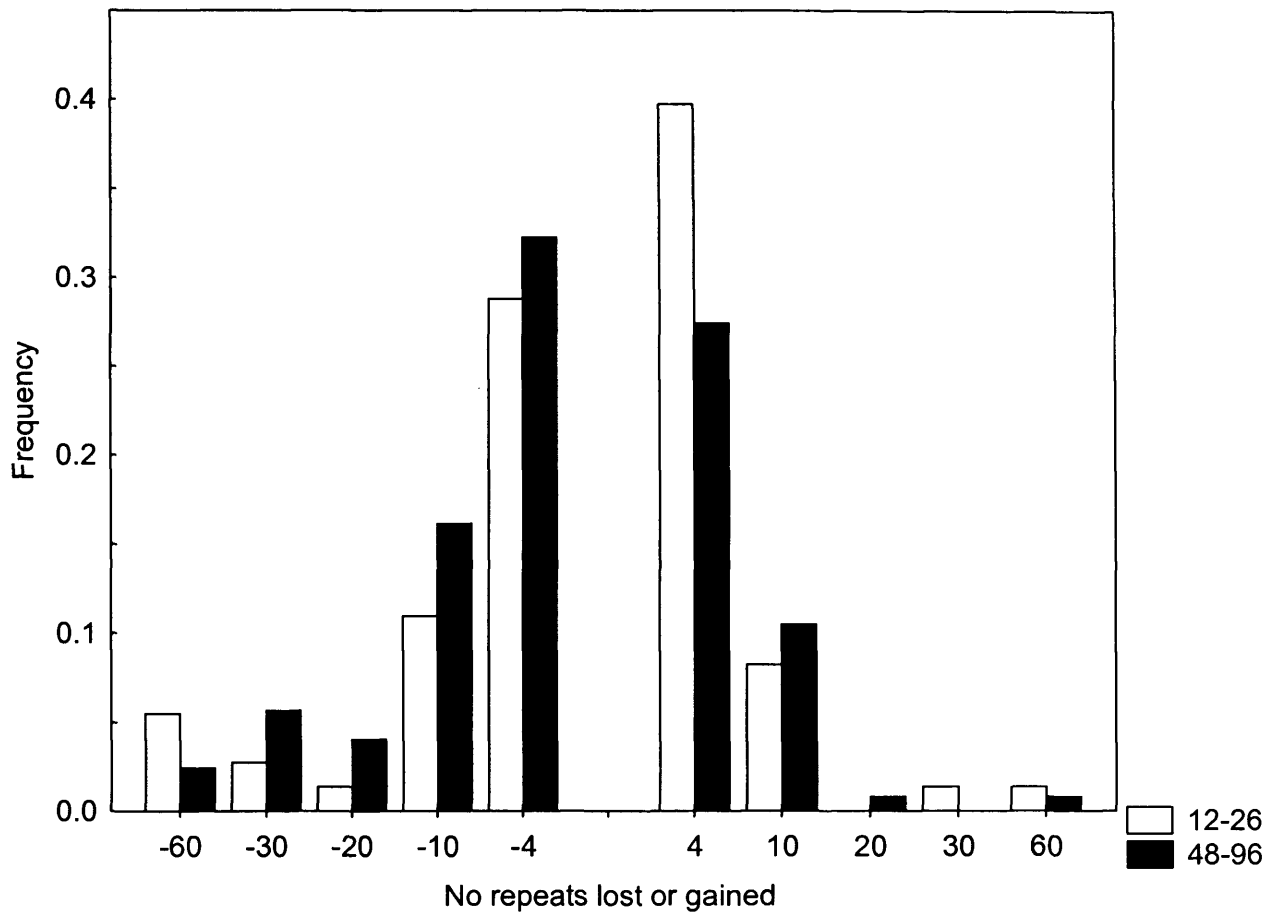
Figure 3.8
Graph to show the spectrum of unique spontaneous mutations at the ESTR locus Ms6-hm in sperm from F_1 C57BL/6 × CBA/H hybrid male mice. Here, all data from ages 12, 26, 48, and 96 weeks old mice was pooled together to give an overall mutation frequency, and all mosaic mutants were treated as a single mutational event. The number of repeats lost or gained are binned as ± 4–9 repeats (± 4), ± 10–19 repeats (± 10), ± 20–29 repeats (± 20), ± 30–59 repeats (± 30), and ± 60+ repeats (± 60).
Kolmogorov-Smirnov two-sample test, P=0.2187.
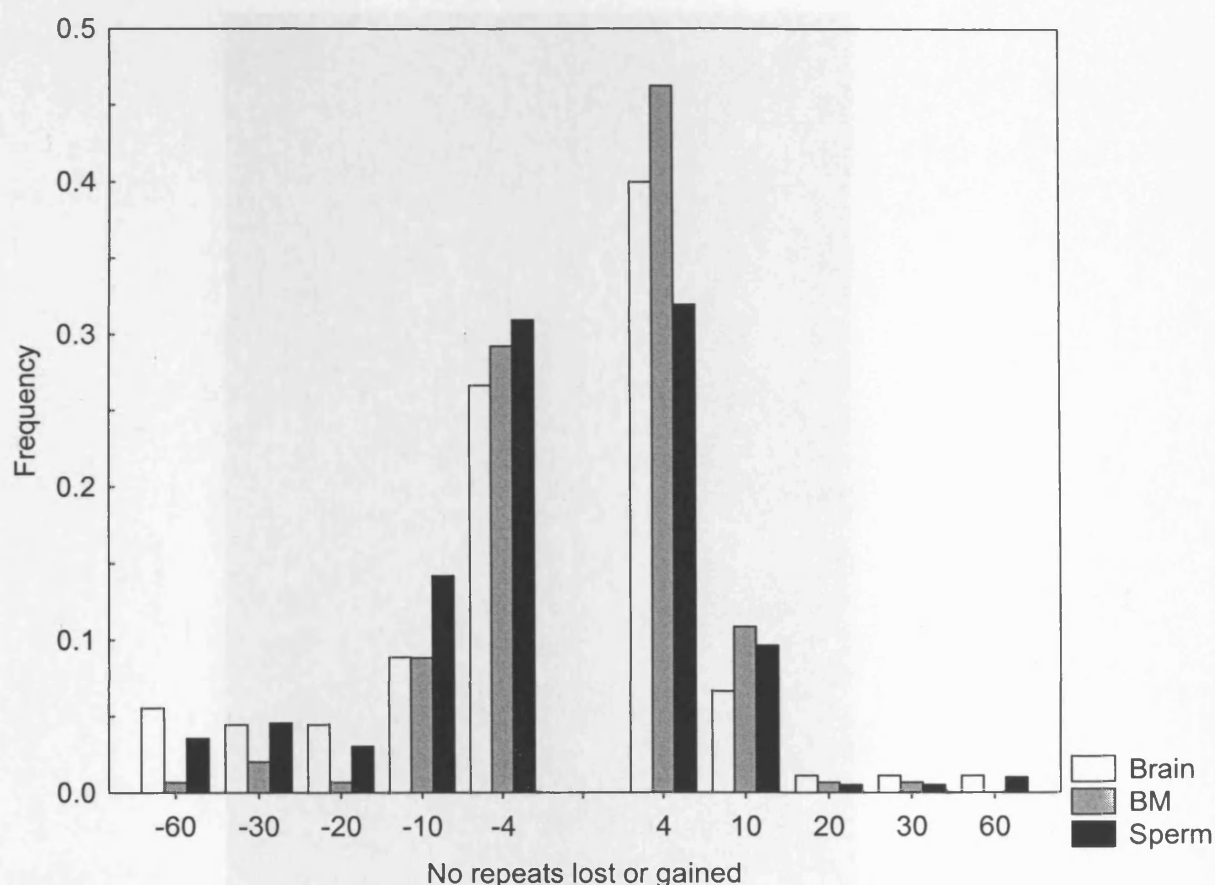
Figure 3.9
Graph comparing the spectrum of spontaneous mutations at the ESTR locus Ms6-hm from brain, bone marrow, and sperm tissues from F_1 C57BL/6 × CBA/H hybrid male mice. Each tissue mutation spectrum encompasses all the age data from young and old mice. The number of repeats lost or gained are binned as ± 4–9 repeats (± 4), ± 10–19 repeats (± 10), ± 20–29 repeats (± 20), ± 30–59 repeats (± 30), and ± 60+ repeats (± 60).
Analysis of variance for the effects of age (F=0.01; df=1, 428; P=0.9528), tissue (F=1.99; df=2, 428; P=0.1382) and their interaction (F=0.31; df=2, 428; P=0.7372).
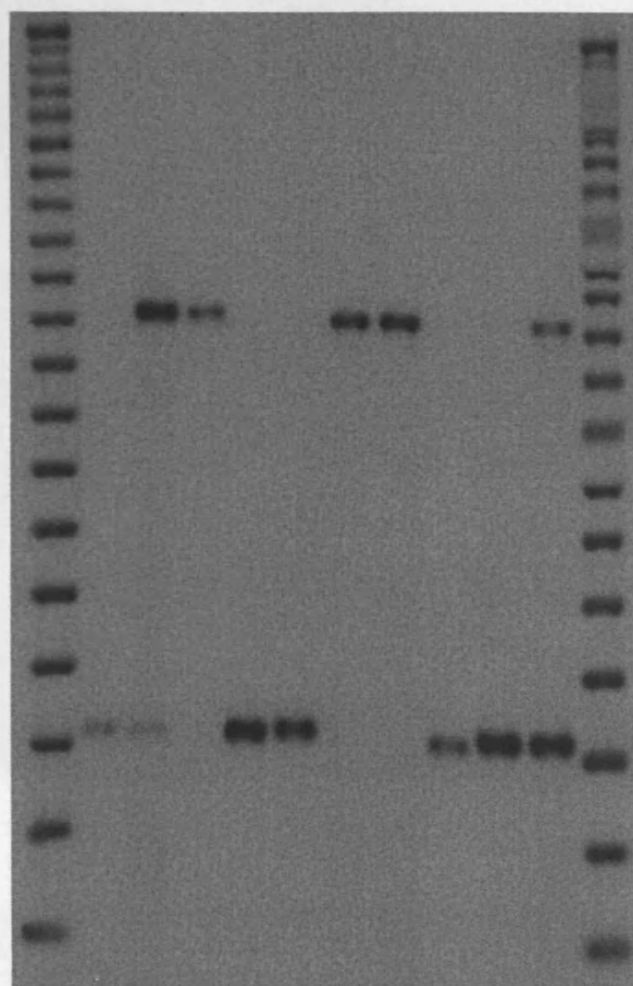
Figure 3.10
Picture of an X-ray autoradiograph of an SM-PCR Southern blot probed for the ESTR locus Ms6-hm from an F_1 hybrid C57BL/6 × CBA/H male mouse with no mutants.
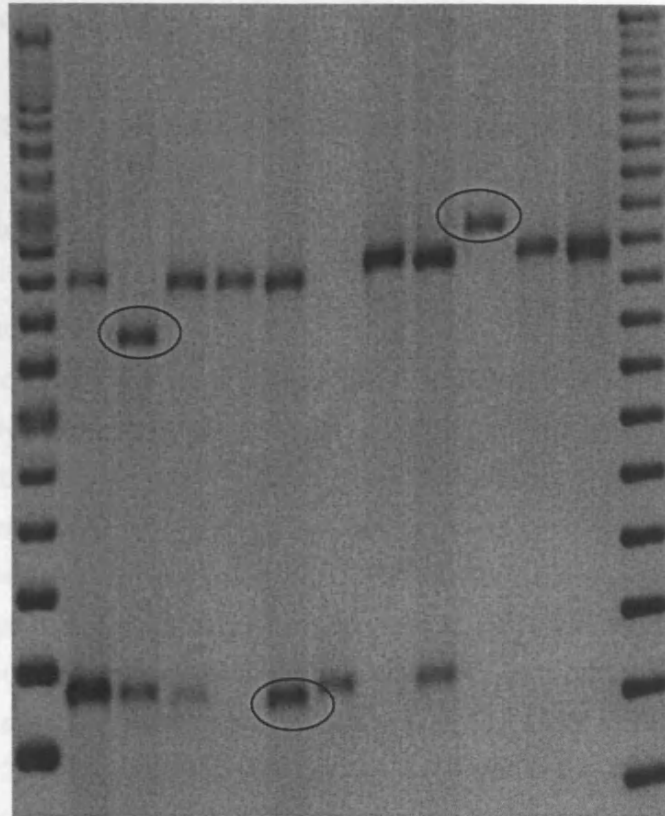
Figure 3.11
Picture of an X-ray autoradiograph of an SM-PCR Southern blot probed for the ESTR locus Ms6-hm from an F_1 hybrid C57BL/6 × CBA/H male mouse with no mutants. Mutant bands were scored as those which deviated a distance of 1 mm or more from the parental alleles and are circled. This distance of 1mm is equivalent to approximately 20 base-pairs (or 4 repeat Ms6-hm repeat units) for CBA/H alleles mice.

Chapter 4: Results II

Analysis of ESTR Mutation Frequency in Irradiated Male Mice

4.1 Introduction

4.1.1 General Introduction

The mechanism by which mouse ESTR loci mutate is widely believed to be mediated by DNA replication (Dubrova, *et al.*, 1998; Barber, *et al.*, 2000; Barber, *et al.*, 2002; Dubrova, *et al.*, 2002; Barber, *et al.*, 2004; Burr, *et al.*, 2005; Burr, *et al.*, 2006; Burr, *et al.*, 2007), and so the frequency of mutation would be expected to rise in line with increased rates of cell division. Furthermore, ever since Dubrova *et al.* (1993) first reported that ionising radiation can induce elevated ESTR mutation frequencies, subsequent studies have not only confirmed this observation (Sadamoto, *et al.*, 1994; Fan, *et al.*, 1995; Niwa, *et al.*, 1996; Dubrova, *et al.*, 1998; Barber, *et al.*, 2000; Dubrova, *et al.*, 2000a; Dubrova, *et al.*, 2000b; Dubrova and Plumb, 2002; Yauk, *et al.*, 2002; Somers, *et al.*, 2004), but some have also shown that the underlying mechanism of radiation-induced ESTR mutation is likely to be the same as that for spontaneously-arising ESTR mutations (Dubrova, *et al.*, 1998; Barber, *et al.*, 2000; Barber, *et al.*, 2002; Dubrova, *et al.*, 2002; Barber, *et al.*, 2004; Burr, *et al.*, 2005; Burr, *et al.*, 2006; Burr, *et al.*, 2007). Thus it can be hypothesised that ESTR loci mutate via a DNA replication-mediated process that somehow becomes destabilised following exposure to ionising radiation. This aberrant replication-associated process will induce mutations at a higher frequency than normal.

In this chapter the effects of exposure to ionising radiation on ESTR mutation frequency will be analysed in two different contexts. In the first instance the mitotically-proficient process of embryogenesis will be irradiated in order to assess the frequency of mutations in the brain, bone marrow, and sperm tissues. This system was selected for study because mitosis will be highly active in all tissues during the prenatal development phase, and so it would be expected that irradiation will cause a universal increase in ESTR mutation frequency across the embryo in all the tissues analysed. This includes the brain, which in adult mice is mitotically-inactive.

In the second experiment the ESTR mutation frequencies will be analysed and compared between two treated groups of adult male mice: a group of one-week

post-irradiation mice, and a group of eight-week post-irradiation. These exact cohorts have previously been used to investigate the effects of spermatogenesis stage-specific irradiation on ESTR mutation induction (Dubrova, *et al.*, 1998; Barber, *et al.*, 2000), but in this chapter the analysis of sperm will be extended with an additional cohort of *in utero*-irradiated animals. Doing this will offer a comparison of both the developing and mature germline, with their respective high rates of cell division. Under this scheme, it would be expected that both the spermatogonial-irradiated (eight-weeks post-irradiation) and *in utero*-irradiated mice will display elevated frequencies of germline ESTR mutation induction, due to their inherently prolific rates of mitosis.

Further to this, the somatic tissues bone marrow and brain will be assessed for ESTR mutation frequencies in the one- and eight-week post-irradiation mice to provide insight into the delayed effects of irradiation on ESTR mutation frequency in tissues of differing proliferative status. Under this scheme it would be predicted that the bone marrow ESTR mutation frequency would be higher than that in the brain, and especially in the eight-week post-irradiation group. The frequency would not be anticipated to be as high as that seen in eight-week post-irradiation sperm, as this tissue is marked by a much higher rate of mitosis.

The results from both of these studies will be presented here, following a brief introduction and overview of the experimental procedures.

4.1.2 Post-Irradiation Cellular Responses

One aspect of this chapter is to assess the effects of different post-irradiation time periods on ESTR mutation frequency. A number of immediate and long-term biological responses will be initiated by the cell following irradiation, in order to alleviate the harmful effects this may have. These responses will also be relevant when considering the effects of prenatal irradiation.

4.1.2.1 Cellular and Genomic Damage Caused by Ionising Radiation

When an organism is exposed to ionising radiation, linear tracks of radiation energy will follow random paths through each cell, depositing their energy at any random, interrupting cellular component that they encounter. This can inflict damage at the point of contact, with a level of severity dependent upon the nature and dosage of the ionising radiation. For example, at equal doses, high-LET (Linear Energy Transfer) radiations are more damaging to the cell than low-LET forms, given that they concentrate their energy content over a relatively small area. Low-

LET radiations, on the other hand, deposit their energy more uniformly over a larger area, and this causes less severe but more sporadic and widespread cellular injury.

At its most fundamental level, ionising radiation-induced damage is inflicted upon the cell and its constituent molecules, and can broadly be defined as DNA or non-DNA damage. At the DNA level lesions may arise in the form of single- and double-strand breaks, sugar and base modifications, oxidative base damage, inter-strand cross-links, DNA-protein cross-links, and localised sites of clustered, multiple damage. The non-DNA damage comprises lesions in any of the other potential cellular targets, and includes lipid peroxidation due to ROS. Beyond the level of the cell these damaged cells can ultimately affect the tissue and whole organism environment too through a range of extracellular responses. This makes the correction of such damage a vital job of any normal cell.

In the next section the processes by which the cell tolerates and repairs ionising radiation-induced damage will be briefly discussed.

4.1.2.2 Tolerance and Repair of Radiation-Induced Damage

When DNA is exposed to ionising radiation the effects may be tolerated or repaired. Less severe forms of damage, such as individual base lesions, may be repaired by one of the excision repair pathways of mismatch repair (MMR), base-excision repair (BER), or nucleotide excision repair (NER), but should any base adducts avoid correction here, they may simply be bypassed by translesion synthesis (TLS), which allows normal DNA replication and gene expression to proceed unhindered in such circumstances. TLS is thus an effective means of tolerating low-impact damage (see section 1.3.9). However, when dealing with more severe damage forms such as physical strand breakage or the generation of highly complex clustered lesions in a given DNA strand, processes of genetic re-synthesis are required to replace or re-ligate these damaged sites.

Recent work suggests that ionising-radiation induced DSBs are detected by the ATM kinase, which is activated at the site of a DNA break by auto-phosphorylation (Bakkenist and Kastan, 2003), and this can initiate a cascade of downstream events that involves a variety of factors including p53 (Canman, *et al.*, 1998) and Chk2 (Matsuoka, *et al.*, 1998) at the G_1 checkpoint, Nbs1 (Lim, *et al.*, 2000) and Brca1 (Cortez, *et al.*, 1999; Xu, *et al.*, 2001) at the S-phase checkpoint, and Brca1 (Xu, *et al.*, 2001) and Rad17 (Bao, *et al*, 2001) at the G_2/M-phase checkpoint. Repair is principally achieved by either non-homologous end-joining in G_1 and early S-phase cells, or homologous recombination repair in late S- and G_2-

phase cells. More details of these repair pathways are in section 1.2.5 of the Introduction.

The response to non-DNA damage in cellular macromolecules is varied, but involves the stimulation of a range of cellular signal transduction pathways. Damage inflicted upon cellular membranes is relayed inwards and can result in activation of protein kinase C (PKC) and mitogen-activated protein kinase (MAPK) (Liu, *et al.*, 1996), the ceramide pathway (Kolesnick and Fuks, 2003), or other signal transduction pathways. All these responses are important in the control of the cell cycle, DNA repair and cell death, and in situations of excessive DNA or cellular damage, these pathways may force the cell into apoptosis in a p53-regulated fashion (Clarke, *et al.*, 1993; Lowe, *et al.*, 1993).

4.1.2.3 Non-Targeted and Delayed Responses

In addition to the direct damage caused by the physical interaction between DNA and ionising radiation, it has emerged in recent years that non-DNA-targeted irradiation can also induce mutations. This was first demonstrated by Wu *et al.* (1999) who found cytoplasmic irradiation to be mutagenic to DNA *in vitro*. This could have consequences for the long-term effects of irradiation, including genomic instability and bystander effects.

4.1.3 Genomic Instability

Genomic instability refers to the situation where one or more of the processes responsible for maintaining genomic integrity are disrupted to cause successive and increasingly uncontrolled genetic alterations with each subsequent cell division. This state of elevated susceptibility to mutation induction is known as the "mutator phenotype", and this may ultimately lead to the onset of cancer (Loeb, *et al.*, 2003).

The direct cause of this instability is DNA damage. For example, delayed *de novo* chromosomal aberrations (Kadhim, *et al.*, 1992), and mutation induction (Chang and Little, 1992) have all been reported as characteristics of instability, with the source of this delayed response being attributed to DNA strand breaks (Mothersill, *et al.*, 1998). However, instability could also be a consequence of epigenetic alterations in methylation, acetylation, and phosphorylation patterns (Hake, *et al.*, 2004) and persistent oxidative stress (Clutton, *et al.*, 1996).

4.1.4 Bystander Effects

It is now clear that cells which sustain a direct 'hit' of ionising radiation can trigger symptoms of damage in neighbouring cells which themselves did not receive a dose of ionising radiation (Belyakov, *et al.*, 2001), and that these damaging effects can be induced by non-nuclear, cytoplasmic irradiation (Wu, *et al.*, 1999). The extracellular responses can be mediated by secreted signals (Lehnert and Goodwin, 1997) or by cell-to-cell gap junction cross-talk (Azzam, *et al.*, 1998), and are collectively known as bystander effects. One effect of this appears to be the activation of inflammatory-type responses, as described by macrophage activation in haemopoietic tissues exposed to ionising radiation (Lorimore, *et al.*, 2001). The existence of these bystander effects implies that epigenetic and/or extracellular DNA damage signals may be relayed between cells to cause unexposed cells to behave in the same manner as irradiated cells, and thus translate cellular damage into more widespread tissue damage.

4.1.5 The Effects of Prenatal Irradiation on the Developing Embryo

The second aspect of this chapter is the examination of the effects of *in utero* irradiation on ESTR mutation frequency. This will help to gain insight into the hypothesised link between ESTR mutation and DNA replication. However, performing this study will also provide a possible means for assessing the genetic risks of prenatal irradiation; a topic of interest to expectant mothers and the medical profession.

Pregnant women may be exposed to ionising radiation in a number of different contexts. They may receive doses from medical examination techniques such as computer tomography and interventional radiology, from occupational exposures encountered at work, or from widely diffused environmental radioactive contamination from accidents such as the 1986 Chenobyl disaster. But to evaluate the effects of prenatal irradiation in humans, researchers have had to rely mainly on epidemiological studies which assess mutagenicity by, for example, tracking the transmission of inherited diseases and cancer risks (Parker, *et al.*, 1999). Such studies are hindered by a number of confounding factors, and the only way to overcome this is to conduct controlled laboratory-based experiments in animal models such as the mouse, and extrapolate these data to humans. Thus ESTR loci could potentially become useful markers for the genetic effects of *in utero* irradiation. In the following section a commentary on what is currently known about the risks to the developing embryo and foetus from prenatal ionising radiation exposure will be given.

4.1.6 Embryogenesis and *In Utero* Irradiation

Embryogenesis is the process by which the embryo develops from the fertilised egg. The process is characterised by a high level of cellular proliferation, differentiation and migration as the embryo grows and transforms from a ball-shaped mass of cells and into a recognisable organism with primitive limbs and organ structures. Due to this high level of cellular activity, the mammalian embryo and then foetus are extremely vulnerable to damage from ionising radiation exposure (ICRP, 2003), although the nature and severity of these prenatal radiation-induced biological effects will depend on the developmental stage during which the exposure occurs. To describe these effects it is possible to divide prenatal development into three main periods: the pre-implantation phase, major organogenesis, and a foetal stage.

4.1.6.1 Pre-implantation Phase

The pre-implantation phase begins with fertilisation of an ovum by a sperm cell and the subsequent fusion of the male and female pronuclei to form a zygote. There then follows a succession of mitotic divisions called cleavages in which the cells do not grow between divisions. This means that after several cleavages the cells have shrunk in size but remain in close contact as a multicellular, ball-shaped entity known as the blastocyst which is not significantly larger than the original zygote. The blastocyst then implants into the uterus to complete the pre-implantation period, which in total lasts for 5 days in mice, 7 days in rats, and 8 days in humans (Kaufman and Bard, 1999: pp.4–14; ICRP, 2003: pp.11–20).

To assess the risk of radiation exposure during the pre-implantation period animal models must be used as it is not possible to know the time of conception in humans. Studies in mice have shown the risk of lethality in the developing organism from radiation exposure is highest during the pre-implantation period, as cells may be killed from excessive cytogenetic damage. As a case-in-point, irradiation of pregnant mice with X-ray doses as low as 100 mGy and up to 250 mGy during the first day post-conception has been shown to be sufficient to cause significant lethality in several studies (Pampfer and Streffer, 1988; Müller and Streffer, 1990; Gu, *et al.*, 1997). However, not all irradiation at the pre-implantation stage is lethal, but it may still be harmful to the embryo, with structural and numerical genetic anomalies reported to accumulate in irradiated mouse embryos in studies such as that by Pampfer and Streffer (1989).

4.1.6.2 Organogenesis and Foetogenesis

Following implantation of the blastocyst in the uterus the embryo goes through phases of cellular rearrangement and differentiation called gastrulation and neurulation, during which time the basic body plan and nervous system is established. After this the embryo moves into organogenesis, when primitive organ structures are formed as the embryo begins to take shape as a recognisable organism. In humans it occurs between weeks 3–7 post-conception, and in mice 8–14 days post-conception (Kaufman and Bard, 1999; ICRP, 2003). Following this the embryo enters the foetogenesis phase to create the final foetus and complete the process of prenatal development.

The effects of irradiation during these phases can be lethal, but generally the embryo is less susceptible to death from irradiation than during the pre-implantation phase. But it is still possible for irradiation to cause harm to the embryo at this stage, as any cell killing during the cellular proliferation, differentiation, and migration events of organogenesis may disrupt these processes and result in organ malformations.

The severity of the malformations depends on the timing of irradiation during organogenesis. The effects can be classified in general terms as deterministic or stochastic effects. Deterministic effects include organ malformations and mental retardation, and are associated with early organogenesis irradiation. An example of this is the reduction in head size and brain weight seen in mice following prenatal irradiation 11.5 days post-conception with doses of ≥ 0.15 Gy (Uma Devi, *et al.*, 1994). Stochastic effects include leukaemia, solid tumours, and genetic anomalies, and are caused by irradiation during late organogenesis and foetogenesis. Studies by Nitta, *et al* (1992) and Uma Devi and Hossain (2000a) found a high susceptibility to solid cancers after foetal gamma irradiation with a dosage of 1 Gy, whilst Uma Devi and Hossain (2000b) reported structural aberrations such as chromatid breaks and fragments in both foetal and adult haemopoietic cells following 1 Gy irradiation. This was attributed to the induction of genomic instability.

4.2 Experimental Design

4.2.1 Objectives of this Study

The objective of this investigation was to test the hypothesised model of replication-mediated ESTR mutation induction in the mitotically-proficient process of prenatal development, and in post-irradiation tissues of varying proliferative status. This was achieved by assessing the mutation frequencies in brain, bone marrow and sperm tissues from BALB/c inbred mice and drawing comparisons between the two experimental systems.

4.2.2 Measuring ESTR Mutation Frequency

In both the experiments reported in this chapter, the ESTR mutation frequency will be evaluated using the same SM-PCR approach as described in section 3.2 of this thesis and originally by Yauk *et al.* (2002). Mutants will be classified in the same manner: as singletons, mosaics, and uniques (section 3.2.6). However, in this case inbred BALB/c mice with an Ms6-hm allele size of 3 kb were used as the test strain. As in the previous age study, the three tissues analysed were brain, bone marrow, and sperm; selected because of their varying proliferative states (section 3.2.5).

4.2.3 Prenatal Irradiation Scheme

To analyse prenatal irradiation, pregnant females were administered with whole-body X-irradiation at a dose of 1 Gy, twelve days into their pregnancy. This time-point coincided with the late organogenesis phase of mouse embryogenesis when a primitive central nervous system, haemopoietic system, and germline would all have been successfully differentiated and established (Kaufman and Bard, 1999). This means that the responses to the radiation dosage could be viewed as prenatal tissue-specific responses, and not a common response derived from damage to a single immature stem cell lying upstream of the final differentiated tissue cell lines. Moreover, irradiation during this phase is less likely to result in abortion of the embryo than in other stages, such as the pre-implantation phase (ICRP, 2003: pp. 11–20).

To conduct this experiment, mice were mated and the successfully mated females were identified by the characteristic appearance of the post-fertilisation vaginal plug. These mice were then placed into separate cages for maternal irradiation twelve days after this recorded time.

4.2.4 Scheme for Study of Post-Irradiation Effects

To study the post-irradiation effects of ionising radiation on ESTR mutation frequencies, adult male mice were whole-body irradiated with 1 Gy of X-rays when aged seven weeks, and then culled either one week later when aged eight weeks to form the "one-week post-irradiation" group, or alternatively they were sacrificed eight weeks later when aged fifteen weeks to form the "eight-week post-irradiation" cohort.

The time-periods of one- and eight-weeks post-irradiation were chosen deliberately to mimic the studies of Dubrova *et al.* (1998) and Barber *et al.* (2000), who were testing the spermatogenesis stage-specific timing of ESTR mutation induction in CBA/H and C57BL/6J × CBA/Ca mice respectively. Both these studies achieved this by using knowledge of the duration of mouse spermatogenesis and its constituent time-limited developmental stages (Adler, 1996) to irradiate precise stages of spermatogenesis, and then compare the radiation-induced ESTR mutation frequencies of these various stages. The known series of spermatogenesis developmental stages and their associated time intervals instructed that sperm taken from mice eight weeks post-irradiation would have been dosed during the early spermatogonial stem-cell stage when spermatogonia were actively dividing to self-renew and differentiate, and from there progressed through the remaining seven weeks of spermatogenesis for collection as mature sperm. With the one-week post-irradiation group, the sperm would have been irradiated in the latter stages of spermatogenesis when mature spermatozoa had formed and cell division had ceased, and collected one week later prior to ejaculation. Both these papers found that sperm mutation frequencies were higher in the eight-week post-irradiation cohort, and the authors therefore concluded that ESTR mutation induction was induced strongly in the actively dividing spermatogonial stem cell stage. However, this claim remains disputed by other studies suggesting that ESTR mutation induction arises later in spermatogenesis during the post-meiotic phase (Sadamoto, *et al.*, 1994; Fan, *et al.*, 1995; Niwa, *et al.*, 1996).

For the purpose of this chapter, this same experimental design was employed but with a new test strain: inbred BALB/c mice. Furthermore, whilst the focus of Dubrova *et al.* (1998) and Barber *et al.* (2000) was solely on spermatogenesis, this chapter extended the analysis of ESTR mutation induction to the somatic tissues bone marrow and brain in one- and eight-week post-irradiation cohorts. The theory was that the proliferating bone marrow tissue should show an increase in ESTR mutation frequency eight weeks post-irradiation, as this time period may give the speculated radiation-induced, replication-mediated process of

ESTR mutation induction sufficient cell divisions to generate an overall increase in ESTR mutation frequency. In post-mitotic adult brain, there should be no corresponding increase in ESTR mutation frequency.

4.3 ESTR Mutation Frequency Analysis

For this analysis there were three groups of irradiated mice: *in utero-*irradiated, one-week post-irradiation and eight-week post-irradiation. Of these groups, the *in utero*-irradiated and one-week post-irradiation were aged eight weeks, whilst the eight-week post-irradiation cohort was aged fifteen weeks. This required two age-matched controls of eight and fifteen weeks to be analysed alongside these exposed groups.

Analysis of the control groups showed no significant differences between the age groups for each tissue (Table 4.1), and because of this the two age data sets were merged together to give a combined control cohort against which all the irradiated samples could be compared. These data are presented in Table 4.2, and Figure 4.1.

4.3.1 *In utero*-irradiation induces an elevated mutation frequency in brain, bone marrow, and sperm

Whole brain and bone marrow tissues and mature epididymal sperm cells from *in utero*-irradiated male BALB/c mice were analysed for ESTR mutations at the locus Ms6-hm using the SM-PCR approach. The results in Table 4.2 and Figure 4.1 show that this treatment causes a highly statistically significant increase in the frequency of unique ESTR mutation induction in each tissue, and Figures 4.7 and 4.8 illustrate BALB/c mutants at the Ms6-hm locus as seen on X-ray autoradiographs. This is of particular interest in the brain tissue, which undergoes rapid mitosis during prenatal development, but then switches to a mitotically inactive state in the adult mouse. This observation hints that a radiation-induced, DNA replication-mediated mechanism could be important in ESTR mutation induction.

4.3.2 Spermatogonia-irradiated sperm cells show a significant increase in ESTR mutation frequency, but spermatozoa-irradiated sperm does not

The data in Table 4.2 and Figure 4.1 indicate that sperm taken eight weeks post-irradiation showed a statistically significant increase in the frequency of unique ESTR mutations, whereas sperm taken one week post-irradiation did not show a statistically significant elevation. This suggests that there are significant increases in the frequency of ESTR mutation induction in the rapidly dividing spermatogonia stem cells, but no such increase in mature spermatozoa when cell division has ceased. This observation is supported by Dubrova *et al.* (1998) and Barber *et al.*

(2000) who studied CBA/H mice and C57BL/6J × CBA/Ca mice respectively, and suggests that replication is prominent in driving up the ESTR mutation frequency.

4.3.3 Bone marrow and brain from the one- and eight-weeks post-irradiation groups do not show statistically-significant differences in ESTR mutation frequency

The data presented in Table 4.2 and Figure 4.1 illustrates how in bone marrow there is an observable increase in ESTR mutation frequency from 4.6% in controls to 6.3% in eight-week post-irradiation mice, but this difference is not statistically significant based on the t-test. In brain there is neither an observable nor statistically significant change in ESTR mutation frequency between control and exposed groups (3.4% and 3.5% respectively). When eight-weeks post-irradiation and *in utero*-irradiated samples were compared within each tissue cohort for bone marrow and brain, there were respective significant and highly significant differences. This analysis shows that two irradiated systems with differing proliferative states experience increases in ESTR mutation frequency dependent on cell turnover.

4.3.4 Sperm from both eight weeks post-irradiation and *in utero*-irradiated mice is statistically significantly higher than controls

Comparing the sperm ESTR mutation frequencies from the proliferating spermatogonial-irradiated (eight-week post-irradiation) and *in utero*-irradiated cohorts revealed that both these systems have significantly higher ESTR mutation frequencies than the control animals. Although these samples are from the same tissue they would have experienced irradiation at different time-points which were both characterised by high rates of mitosis, to highlight the importance of DNA replication in ESTR mutation induction.

4.3.5 Mutation spectra between all control and exposed groups are not statistically significantly different

One way of checking this data for evidence of common or differing mechanisms of mutation is to assess the distribution of gains and losses of repeat units for each ESTR mutant identified. If the mutation spectrum is the same between cohorts then it can be inferred that a common mechanism is operating, but should there be differences in the spectra then there it is possible that the different treatments are eliciting different mechanisms of ESTR mutation. Here the unique

mutations identified in this study are classified into gains and losses of their various sizes in order to assess the size spectrum of mutations.

The size of each mutant can be estimated based on the distance that each allele migrates on an agarose electrophoresis gel. By marking the distance migrated (mm) by the two parental alleles, mutants can be measured +/- these values relative to the nearest parental allele. Using the software package CALIBRATE (© Yuri Dubrova), the distances migrated by ladder markers and the ESTR alleles were translated into gains or losses of Ms6-hm pentanucleotide repeat units. Table 3 presents these findings as the percentage gains and losses of all the unique mutations, and shows chi-squared calculations between these gains and losses to test for significant differences. The Table is firstly divided into tissue-specific analyses for sperm, bone marrow and brain to determine how each different treatment takes affect in each different tissue, but in each case there is no significant change regardless of tissue or treatment. To confirm this, data were pooled together in two ways: firstly an analysis of the combined tissue data for each treatment to determine if any particular treatment exerts a tissue non-specific effect on mutation spectra, and secondly an analysis of how tissue-type may be influential on the mutation spectra regardless of the treatment administered by pooling the treatment data for each tissue. Again, it was found by chi-squared analysis that there were no significant differences and thus reinforced the point that the spectra of ESTR mutations is not influenced by tissue-type or treatment, and so is likely to be arising via a common mutation mechanism in each case. The spectra are represented as graphs for each separate analysis in Figures 4.2–4.6. Given that there are no significant differences between the incidence of gains and losses, the data for each repeat unit size change, whether a loss or a gain, was pooled into categories of the respective size changes.

4.4 Discussion

This study aimed to establish if the mechanism of ESTR mutation induction following ionising radiation exposure was a DNA replication-associated event. It addressed this issue by firstly investigating the frequency of radiation-induced ESTR mutations in the actively dividing system of prenatal development, and secondly by investigating the post-irradiation effects of ionising radiation exposure on ESTR mutation frequency in proliferating and non-proliferating tissues.

An integral part of this experiment was the use of ionising radiation to induce ESTR mutations. It is now well established that ionising radiation exposure results in ESTR mutation induction (Dubrova, *et al.*, 1993; Sadamoto, *et al.*, 1994; Fan, *et al.*, 1995; Niwa, *et al.*, 1996; Dubrova, *et al.*, 1998; Barber, *et al.*, 2000; Dubrova, *et al.*, 2000a; Dubrova, *et al.*, 2000b; Dubrova and Plumb, 2002; Yauk, *et al.*, 2002; Somers, *et al.*, 2004) and that the mechanism of mutation is the same for spontaneous and radiation-induced mutations (Dubrova, *et al.*, 1998; Barber, *et al.*, 2000; Barber, *et al.*, 2002; Dubrova, *et al.*, 2002; Barber, *et al.*, 2004; Burr, *et al.*, 2005; Burr, *et al.*, 2006; Burr, *et al.*, 2007). These conclusions, together with other papers that demonstrate a link between DNA replication and ESTR mutation induction (Dubrova, *et al.*, 1998; Barber, *et al.*, 2000; Barber, *et al.*, 2002; Dubrova, *et al.*, 2002; Barber, *et al.*, 2004; Burr, *et al.*, 2005; Burr, *et al.*, 2006; Burr, *et al.*, 2007), suggest that ESTR loci may mutate via replication-mediated events that somehow become disrupted or destabilised following ionising radiation exposure to induce higher frequencies of mutation. Thus it would be expected that irradiated, proliferating tissues would have an elevated ESTR mutation frequency relative to controls, whilst no increase would be observed in irradiated, non-dividing tissues. These predictions led to the formulation of this study.

The first part of this chapter aimed to evaluate the effects of ionising radiation on the ESTR mutation frequency during prenatal development. This system was selected for study given that all developing tissues experience a near uniform high rate of mitosis (regardless of their adult proliferative states) as the embryo grows and its tissues differentiate. Consequently, embryogenesis provides a unique opportunity to study an actively dividing brain, and permit comparison to its adult form when mitosis has ceased to operate at any significant level. When this comparison was made with the results in this chapter, the results showed that *in utero*-irradiated brain had a highly statistically-significant increase in ESTR mutation frequency compared to the control tissues (Table 4.2), which suggested that a DNA replication-associated event had become affected by ionising radiation exposure

and acted to drive this upward turn in mutation induction. The other tissues, bone marrow and sperm, likewise displayed statistically significant levels of ESTR mutation induction in the *in utero*-irradiated cohort to lend more support to this chapter's hypothesised mechanism of ESTR mutation induction. Interestingly, the *in utero*-irradiated ESTR mutation frequencies for brain, bone marrow, and sperm were almost identical, standing at 9.9%, 9.6%, and 9.5% respectively, which would be in-keeping with the involvement of DNA replication given the uniformly high rate of mitosis in all tissues during prenatal development. Also, it might be expected that the adult brain would provide a good indicator of the spontaneous *in utero* ESTR mutation frequency as this tissue switches from a state of rapid mitosis to a mitotically-inactive state soon after birth. In this chapter, the control ESTR mutation frequency for brain stood at 3.4%.

Further arguments for an ionising radiation-induced, DNA replication-associated ESTR mutational event were provided by the data retrieved from the one- and eight-week post-irradiation cohorts of mice. Analysis of spermatogonia-irradiated (eight week post-irradiation) and spermatozoa-irradiated (one-week post-irradiation) sperm showed that higher levels of ESTR mutation induction were induced by irradiation during the actively dividing phase of spermatogonial stem cell renewal and differentiation, but not in the non-dividing spermatozoa. This observation is in agreement with the findings of Dubrova *et al.* (1998) and Barber *et al.* (2000), although contrasts with the conclusions of other studies that point to a post-meiotic stage of germline ESTR mutation induction (Sadamoto, *et al.*, 1994; Fan, *et al.*, 1995; Niwa, *et al.*, 1996). However, a comparison of sperm data from the spermatogonial-irradiated and *in utero*-irradiated cohorts of mice in this chapter revealed a strong similarity in their ESTR mutation frequencies (recorded at 8.3% and 9.5% respectively), and so again would reinforce the argument for a strong role played by DNA replication in determining the frequency of ESTR mutation.

When attention is turned to the somatic tissues it can be seen that in the brain the ESTR mutation frequencies were fairly stable across the control, one-, and eight-week post-irradiation cohorts, standing at 3.4%, 2.8%, and 3.5% respectively. Unsurprisingly, these frequencies were not significantly different from *t*-test comparisons. In the bone marrow an ESTR mutation frequency of 6.3% was recorded in the eight-week post-irradiation cohort, compared to 4.6% in the control and 3.6% in the one-week post-irradiation group. Although this was an observable increase it was not a statistically significant difference, which is perhaps not surprising given that bone marrow contains a mixed population of cells with an overall rate of cell division intermediate to the brain and sperm, and the period of

eight weeks post-irradiation was probably not large enough for statistically significant increases to be witnessed. Of more interest though was the intra-tissue comparison of the eight-week post-irradiation brain and bone marrow samples with their *in utero*-irradiated counterparts. This comparison aligns two separate irradiated systems: the actively dividing *in utero* system and the eight-week post-irradiation cohorts of non-dividing brain and dividing bone marrow. This yielded a significant increase in bone marrow and a highly significant increase in brain, to suggest that when cells tissues are irradiated with equal doses, the tissue that has experienced the highest number of cell divisions will have the highest ESTR mutation frequency. On this basis, the theorised model of replication-induced ESTR mutation would still be valid.

The above results all seemingly pointed towards a model of ESTR mutation induction whereby events during DNA replication induce size-changing mutations in a manner that becomes aggravated by an ionising radiation-induced signal to cause increased levels of ESTR mutation. To check if the same mechanism is occurring in both spontaneous and radiation-induced cohorts, the mutation spectra were compared to check if the distribution of repeats lost or gained differed between the two cohorts. Previous papers have concluded that there is no difference in mutation spectra between control and ionising radiation exposed groups, and thus the mechanism of ESTR mutation is likely to be the same (Dubrova, *et al.*, 1998; Barber, *et al.*, 2000; Barber, *et al.*, 2002; Dubrova, *et al.*, 2002; Barber, *et al.*, 2004; Burr, *et al.*, 2005; Burr, *et al.*, 2006; Burr, *et al.*, 2007). Mutation spectra for all the possible factors were presented in Table 4.3 and Figures 4.2–4.6. Each analysis failed to provide a significant difference caused by either the tissue involved or the treatment administered. Thus even when the ESTR mutation frequency increased in the irradiated cohorts compared to controls, the distribution of repeats gained and lost did not alter significantly, and so was indicative of a common mechanism of mutation that becomes somehow up-regulated during irradiation. Following the conclusions made earlier, this shared process of ESTR mutation induction would appear to be associated with DNA replication, and supported by the observations of previous studies that infer the involvement of DNA replication slippage (Dubrova, *et al.*, 1998; Barber, *et al.*, 2000; Barber, *et al.*, 2002; Dubrova, *et al.*, 2002; Barber, *et al.*, 2004; Burr, *et al.*, 2005; Burr, *et al.*, 2006; Burr, *et al.*, 2007).

If a model of replication-slippage is assumed, then it is possible to use the spectra data to look for any potential biases towards gains or losses to gain insight into possible mutation directionality tendencies. However, the mutation spectra in this chapter did not reveal any obvious bias towards gains or losses amongst the

different treatments and tissues, and so did not support a directional bias caused by any of these parameters. That said, the *in utero*-irradiated tissues each reported a roughly 60:40 bias towards repeat gains, which could be indicative of an inclination for slipped-strand structures to form in the nascent strand during replication of the ESTR locus Ms6-hm in prenatal development.

In summary, the data from *in utero*-irradiated and post-irradiation tissues have strengthened the argument for a replication-based mechanism of ESTR mutation. This mechanism appears to be common to both unexposed and ionising radiation-exposed groups from their similar mutation spectra data, but the increased frequency of ESTR mutations in irradiated cohorts suggests that this mechanism becomes somehow up-regulated by an unknown ionising radiation-induced signal. Possible models of this mechanism will be given in the Conclusion chapter of this thesis.

Table 4.1 Table to show the frequency of unique mutations at the ESTR locus Ms6-hm in control brain, bone marrow, and sperm tissues taken from inbred BALB/c male mice of ages 8 and 15 weeks. Also shown are the associated Student's t-test analyses and P-values.

| Tissue | 8-week-old | | 15-week-old | | $t^{\dagger}$ | $P^{\dagger}$ |
	Number of mutations*	Frequency ± s.e.	Number of mutations*	Frequency ± s.e.		
Brain	12 (392)	0.0306 ± 0.0090	17 (459)	0.0370 ± 0.0093	0.50	0.6196
BM	24 (642)	0.0374 ± 0.0079	22 (352)	0.0625 ± 0.0139	1.57	0.1165
Sperm	19 (497)	0.0382 ± 0.0090	16 (461)	0.0347 ± 0.0089	0.28	0.7814

* Total number of amplifiable molecules is given in brackets.
$\dagger$ Student's test and probability for difference.

Table 4.2 Table to show the frequency of unique mutations at the ESTR locus Ms6-hm in control and irradiated groups in brain, bone marrow, and sperm tissues taken from inbred BALB/c male mice of ages 8 and 15 weeks. The control data from both 8 and 15 weeks was merged into an overall control group. Also shown are the ratios of each treated group to the controls. Also shown are the Student's t-test analyses and their associated P-values.

Tissue, group	No mutations*	Frequency ± s.e.	Ratio†	$t^{\ddagger}$	$P^{\ddagger}$
Brain					
Control	29 (851)	0.0341 ± 0.0065	-	-	-
1 week PIR	12 (436)	0.0275 ± 0.0081	0.81	0.63	0.5282
8 weeks PIR	14 (398)	0.0352 ± 0.0096	1.03	0.09	0.9246
In utero IR	37 (373)	0.0992 ± 0.0173	2.91	3.52	0.0004
			In utero IR:8 weeks PIR	3.23	0.0013
Bone Marrow					
Control	46 (994)	0.0463 ± 0.0071	-	-	-
1 week PIR	13 (362)	0.0359 ± 0.0102	0.78	0.83	0.4040
8 weeks PIR	30 (480)	0.0625 ± 0.0119	1.35	1.17	0.2429
In utero IR	40 (418)	0.0957 ± 0.0161	2.07	2.81	0.0051
			In utero IR:8 weeks PIR	1.66	0.0973
Sperm					
Control	35 (958)	0.0365 ± 0.0064	-	-	-
1 week PIR	16 (420)	0.0381 ± 0.0098	1.04	0.13	0.8936
8 weeks PIR	36 (435)	0.0828 ± 0.0146	2.27	2.90	0.0038
In utero IR	47 (493)	0.0953 ± 0.0149	2.61	3.63	0.0003

* Total number of amplifiable molecules is given in brackets.
$\dagger$ Ratio to control group.
$\ddagger$ Student's test and probability for difference from control group.
PIR = Post-irradiation

Table 4.3

Table to show the percentage of repeat gains and losses amongst the total set of unique ESTR mutations. Data is taken from the locus Ms6-hm in brain, bone marrow, and sperm tissues taken from inbred BALB/c male mice of ages 8 weeks and 15 weeks. Also shown are the chi-squared test results for homogeneity within groups, and their corresponding *P*-values.

Tissue, Group	Gains (%)	Losses (%)	Total	x^2 (df)*	$P^\dagger$
Sperm					
Control	26 (66.7)	13 (33.3)	39		
1 week PIR	12 (63.2)	7 (36.8)	19		
8 weeks PIR	19 (51.4)	18 (48.6)	37		
In utero IR	34 (69.4)	15 (30.6)	49		
Total	91 (63.2)	53 (36.8)	144	3.24 (3)	0.3559
Bone marrow					
Control	19 (47.5)	21 (52.5)	40		
1 week PIR	11 (78.6)	3 (21.4)	14		
8 weeks PIR	20 (66.7)	10 (33.3)	30		
In utero IR	20 (48.8)	21 (51.2)	41		
Total	70 (56.0)	55 (44.0)	125	6.32 (3)	0.0970
Brain					
Control	15 (53.6)	13 (46.4)	28		
1 week PIR	5 (38.5)	8 (61.5)	13		
8 weeks PIR	7 (50.0)	7 (50.0)	14		
In utero IR	25 (65.8)	13 (34.2)	38		
Total	52 (55.9)	41 (44.1)	93	3.37 (3)	0.3379
All tissues					
Control	60 (56.1)	47 (43.9)	107		
1 week PIR	28 (60.9)	18 (39.1)	46		
8 weeks PIR	46 (56.8)	35 (43.2)	81		
In utero IR	79 (61.7)	49 (38.3)	128		
Total	213 (58.8)	149 (41.2)	362	0.99 (3)	0.8026
All treatments					
Sperm	91 (63.2)	53 (36.8)	144		
Bone marrow	70 (56.0)	55 (44.0)	125		
Brain	52 (55.9)	41 (44.1)	93		
Total	213 (58.8)	149 (41.2)	362	1.87 (2)	0.3921

* Chi-square test for homogeneity within group (degrees of freedom)
† Probability
PIR = Post-irradiation
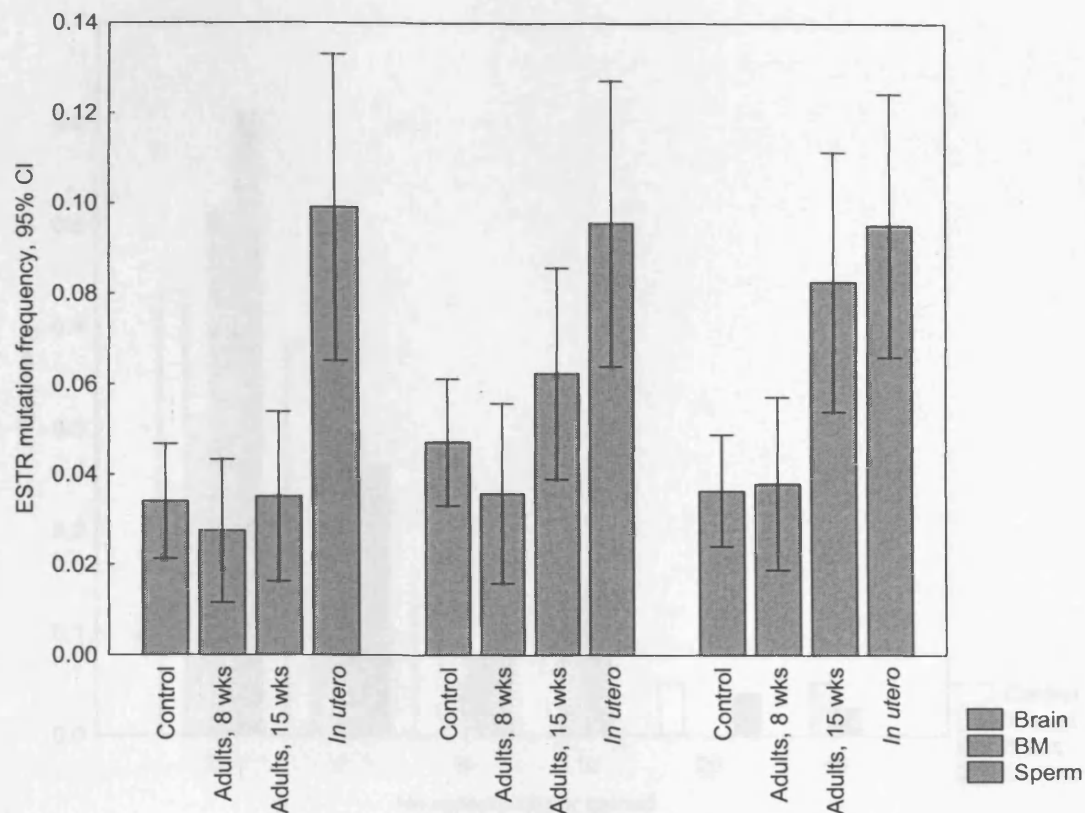
Figure 4.1
Graph to show the frequency of unique mutations at the ESTR locus Ms6-hm in brain, bone marrow, and sperm tissues taken from inbred BALB/c male mice of ages 8 weeks and 15 weeks.
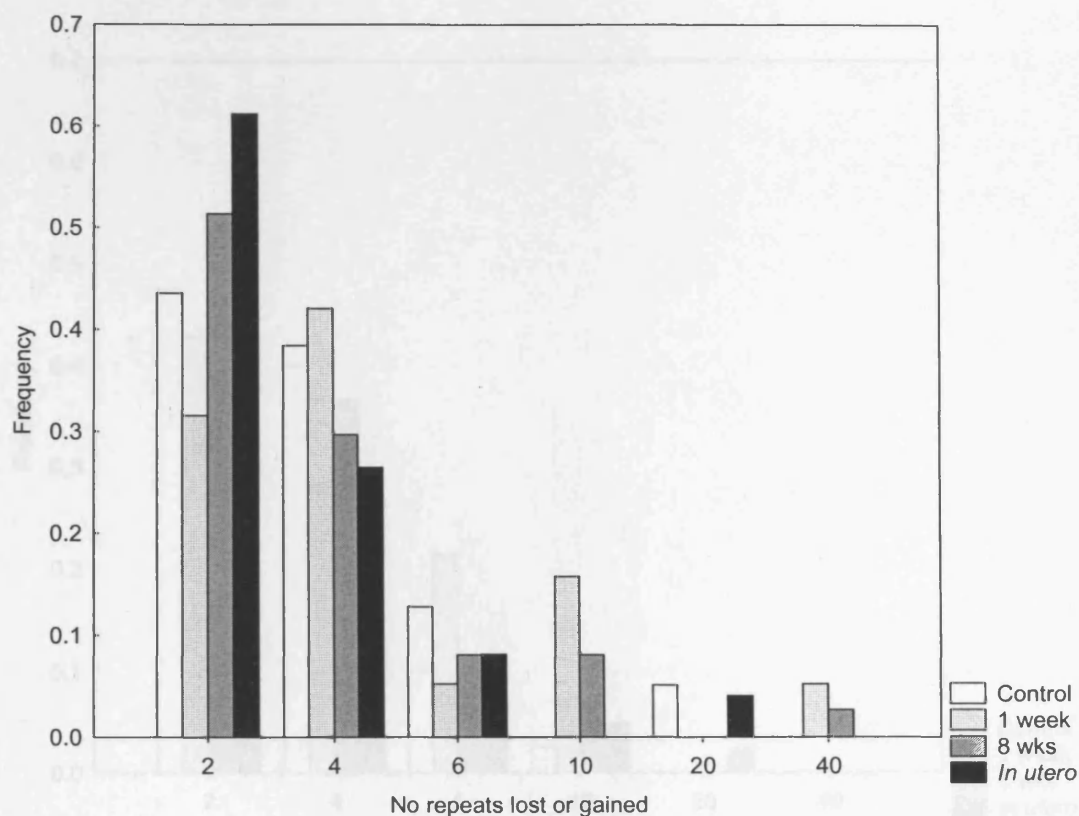
Figure 4.2
Graph to show the spectrum of repeats lost or gained for each of the unique mutations arising at the ESTR locus Ms6-hm in sperm from one week post-irradiation, eight weeks post-irradiation, *in utero*-irradiated, and control inbred BALB/c male mice. Gains and losses of equal size changes were pooled together. The number of repeats lost or gained are binned as ± 2–3 repeats (2), ± 4–5 repeats (4), 6–9 repeats (6), 10–19 repeats (10), 20–39 repeats (20), and 40 + repeats (40). The Kruskal-Wallis Test shows no significant differences between the groups, with a *P*-value of 0.1173.
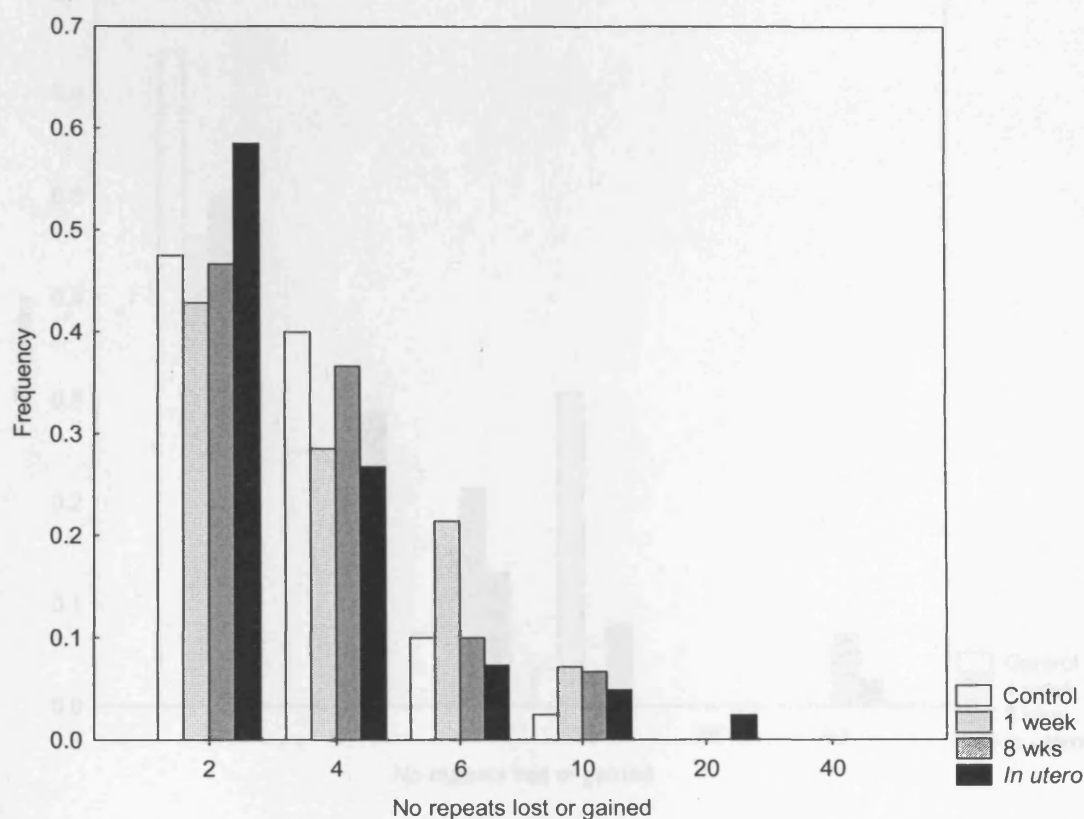
Figure 4.3
Graph to show the spectrum of repeats lost or gained for each of the unique mutations arising at the ESTR locus Ms6-hm in bone marrow from one week post-irradiation, eight weeks post-irradiation, *in utero*-irradiated, and control inbred BALB/c male mice. Gains and losses of equal size changes were pooled together. The number of repeats lost or gained are binned as ± 2–3 repeats (2), ± 4–5 repeats (4), 6–9 repeats (6), 10–19 repeats (10), 20–39 repeats (20), and 40 + repeats (40). The Kruskal-Wallis Test shows no significant differences between the groups, with a *P*-value of 0.6308.

Figure 4.4

Graph to show the spectrum of repeats lost or gained for each of the unique mutations arising at the ESTR locus Ms6-hm in brain from one week post-irradiation, eight weeks post-irradiation, *in utero*-irradiated, and control inbred BALB/c male mice. Gains and losses of equal size changes were pooled together. The number of repeats lost or gained are binned as ± 2–3 repeats (2), ± 4–5 repeats (4), 6–9 repeats (6), 10–19 repeats (10), 20–39 repeats (20), and 40 + repeats (40). The Kruskal-Wallis Test shows no significant differences between the groups, with a *P*-value of 0.2324.

Figure 4.5
Graph to show the spectrum of repeats lost or gained for each of the unique mutations arising at the ESTR locus Ms6-hm as analysed by treatment for all tissues. Gains and losses of equal size changes were pooled together. The tissues studied were bone marrow, brain, and sperm, and the treatments analysed were one week post-irradiation, eight weeks post-irradiation, *in utero*-irradiated, and control inbred BALB/c male mice. The number of repeats lost or gained are binned as ± 2–3 repeats (2), ± 4–5 repeats (4), 6–9 repeats (6), 10–19 repeats (10), 20–39 repeats (20), and 40 + repeats (40).
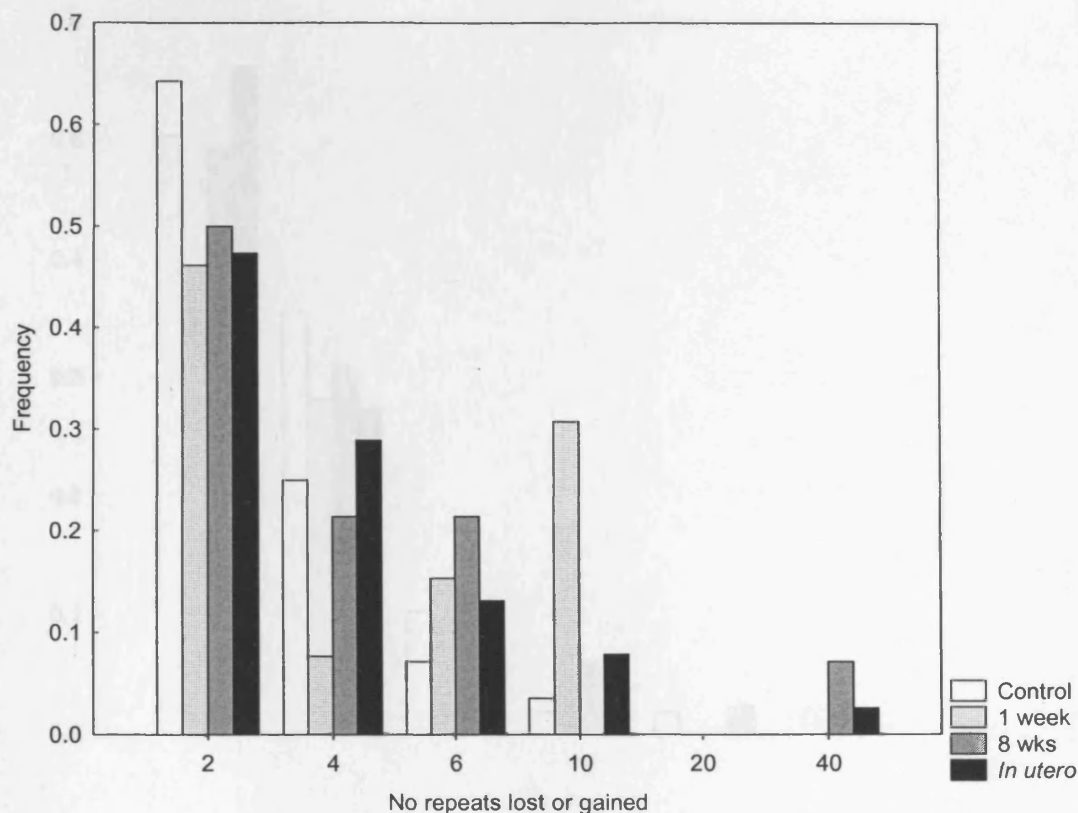The Kruskal-Wallis Test shows no significant differences between the groups, with a *P*-value of 0.0793.

Figure 4.6
Graph to show the spectrum of repeats lost or gained for each of the unique mutations arising at the ESTR locus Ms6-hm as analysed by tissue for all treatments. The tissues studied were bone marrow, brain, and sperm, and the treatments analysed were one week post-irradiation, eight weeks post-irradiation, *in utero*-irradiated, and control inbred BALB/c male mice. The number of repeats lost or gained are binned as ± 2–3 repeats (2), ± 4–5 repeats (4), 6–9 repeats (6), 10–19 repeats (10), 20–39 repeats (20), and 40 + repeats (40).
The Kruskal-Wallis Test shows no significant differences between the groups, with a *P*-value of 0.9475)
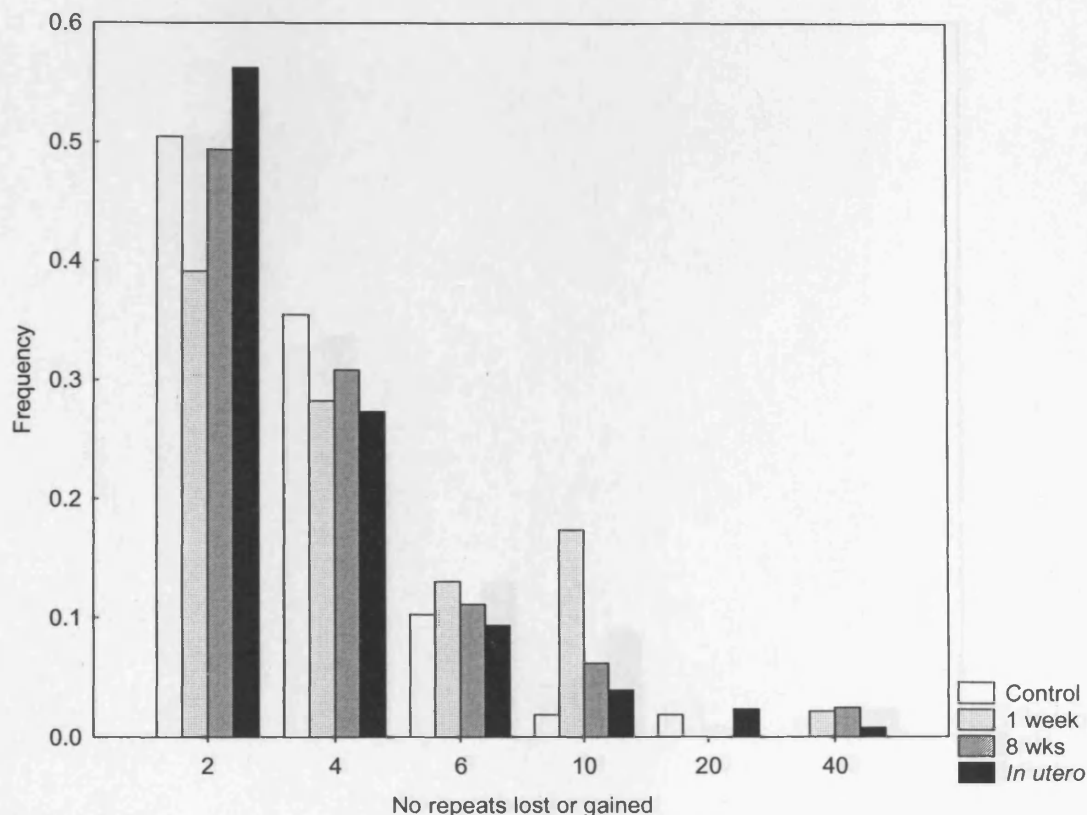
Figure 4.7
Picture of an X-ray autoradiograph of an SM-PCR Southern blot probed for the
ESTR locus Ms6-hm from an inbred BALB/c male mouse with no mutants.

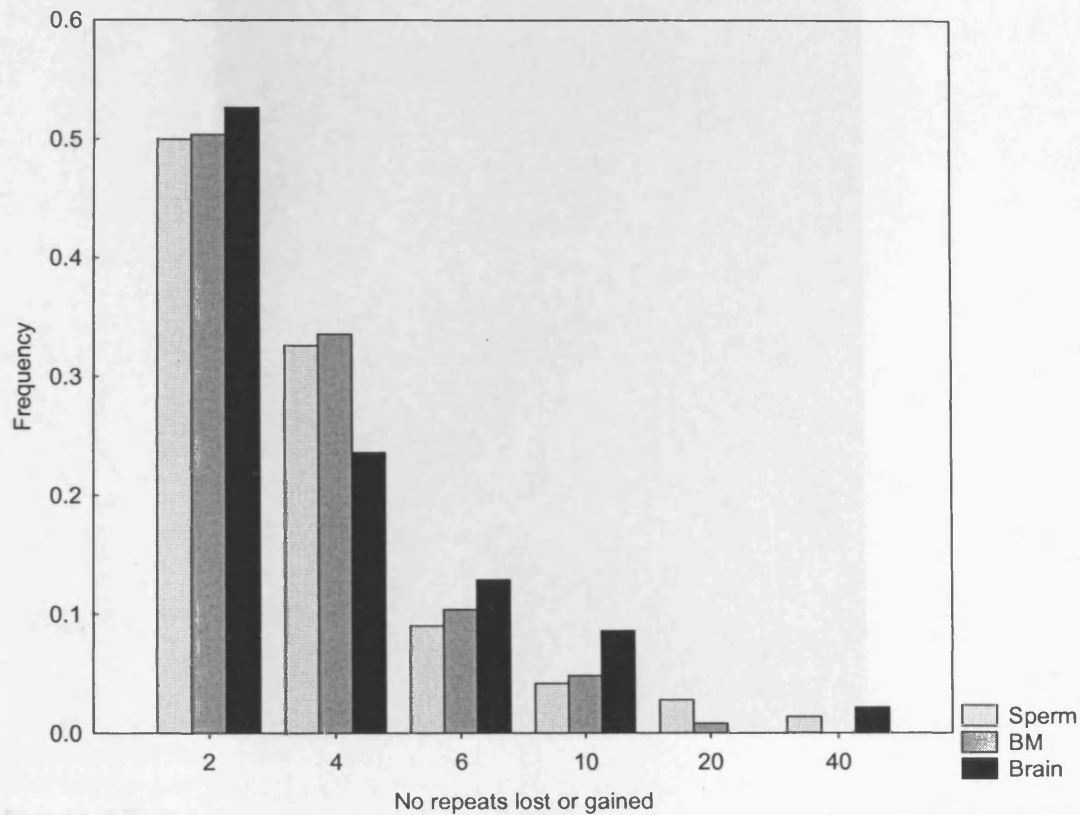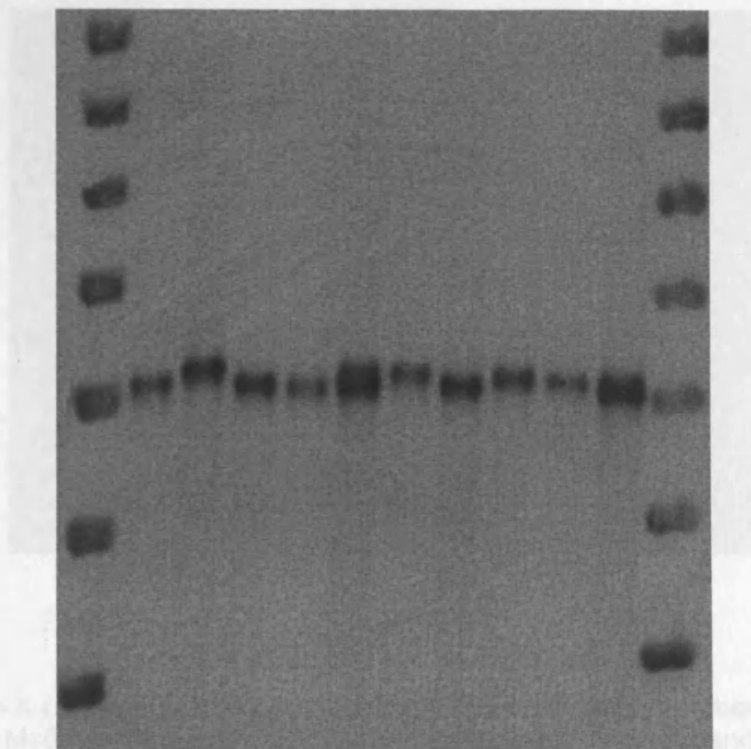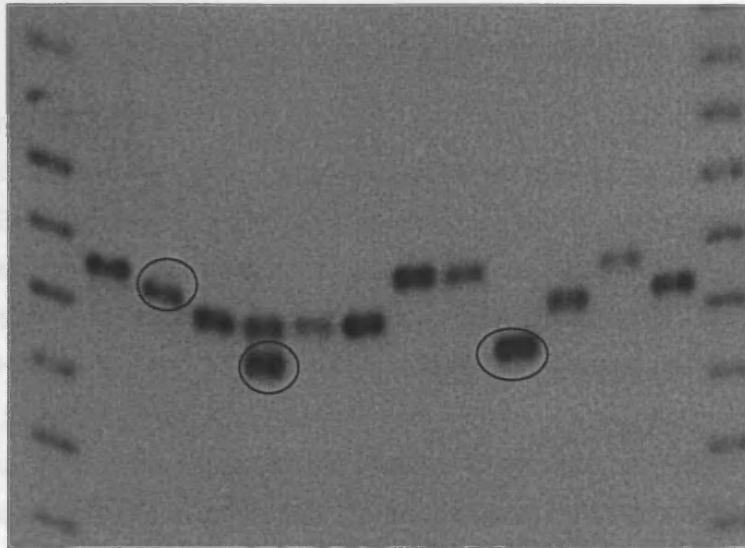**Figure 4.8**

Picture of an X-ray autoradiograph of an SM-PCR Southern blot probed for the ESTR locus Ms6-hm from an inbred BALB/c male mouse. Mutant bands were scored as those which deviated a distance of 1 mm or more from the parental alleles and are circled. This distance is equivalent to approximately 10 base-pairs (or 2 repeat Ms6-hm repeat units) for BALB/c mice.

Chapter 5: Conclusion

5.1 Summary of Results

In this thesis, two separate studies were conducted to test the hypothesis that mouse ESTR mutation is attributed to DNA replication-mediated events. Both of these involved looking for correlations between the mitotic index of a tissue and the ESTR mutation frequency. If, as predicted, mutation induction is dependent on events at DNA replication, then the more cell divisions there are in a system, the more ESTR mutations it will accumulate.

In the first study, the effects of advancing age on ESTR spontaneous mutation frequency were investigated. Three tissues of varying proliferative status in adults were selected: brain (low mitotic index), bone marrow (intermediate mitotic index) and sperm (high mitotic index). If our hypothesis was correct, then advancing age would cause an increase in the frequency of ESTR mutation induction in sperm, but should have no effect on the brain. The results suggest that this is indeed the case, with sperm displaying significantly higher ESTR mutation frequencies in 48 and 96 week old mice compared to those aged 12 and 26 weeks, and brain showing no evidence of an increase in ESTR mutation frequency with age. The bone marrow, with its heterogenous population of dividing and non-dividing cells, perhaps might be expected to show an increase in ESTR mutation frequency with age, but in this study there were no significant changes with age; despite a slight trend of mutation frequency elevation. This would suggest that the bone marrow cell population consists mainly of non-dividing cells.

In the second study, the effects of ionising radiation on ESTR mutation frequency were assessed in brain, bone marrow, and sperm, in two scenarios: the effects of irradiation on prenatally-developing tissues, and the short-term delayed effects of irradiation. In the first part of this study, it was found that *in utero* exposure to ionising radiation induces a statistically significant increase in ESTR mutation frequency in each of the analysed tissues, which is particularly interesting in the case of the brain which in adult mice is largely post-mitotic, and will only be actively dividing during embryogenesis. This cohort alone provides arguably the strongest support of all the data in this thesis that ESTR mutation induction is dependent on a DNA-replication-mediated mechanism. There was also found to be a small but statistically insignificant increase in ESTR mutation frequency in post-irradiated bone marrow, but no sign of any increase in the brain. Together, this study indicates that ESTRs mutate via DNA-replication-associated process that can become

destabilised further by exposure to ionising radiation. The cause of this destabilisation is not known, and beyond the scope of the experiments in this thesis.

5.2 Replication-Mediated ESTR Mutation

The unifying conclusion of both sets of experimental data presented in this thesis is the involvement of DNA replication in mutation induction at the $(GGGCA)_n$ pentanucleotide ESTR locus, Ms6-hm. This conclusion is supported from observations elsewhere (Dubrova, *et al.*, 1998; Barber, *et al.*, 2000; Barber, *et al.*, 2002; Dubrova, *et al.*, 2002; Barber, *et al.*, 2004; Burr, *et al.*, 2005; Burr, *et al.*, 2006), where the prevailing theory is of mutagenic replication slippage caused by fork stalling.

The proposed model of mutagenic replication slippage would require the formation of slipped-strand secondary structures during chromatin structural alterations that temporarily release DNA single-strands from their bound duplex state. Such secondary structures have been demonstrated to arise at Ms6-hm *in vitro* in the form of quadruplex structures (Weitzmann, *et al.*, 1998; Katahira, *et al.*, 1999; Fukuda, *et al.*, 2002), and whilst they have yet to be demonstrated *in vivo*, there is evidence that quadruplexes form *in vivo* at structurally-similar telomeric repeats (Paeschke, *et al.*, 2005).

The opportunity for quadruplex formation at ESTRs will arise mainly through duplex unwinding at the array during replication fork progression. This, coupled to the uninterrupted nature of ESTR repeat elements, will provide plenty of scope for intra-strand folding to occur across the array, and so presents ample opportunities for quadruplex formation. This makes it plausible that slippage could readily occur at ESTRs, in a manner possibly akin to the model of replication-induced instability proposed by Mirkin (2006), which postulated that slipped-strand structures could cause replication pausing by interfering with the progression of the replisome. Furthermore, in this context, it is interesting to note that the unwinding of ESTR quadruplexes *in vitro* by the DNA-binding protein UP1 can reverse replication stalling and restart replication (Fukuda, *et al.*, 2002).

More support for the involvement of replication fork stalling has come from a study into the effects of DNA repair deficiencies on ESTR mutation frequencies. Barber *et al.*, (2004) reported elevated ESTR mutation frequencies in both NHEJ-deficient *scid* mice and a SSB repair-deficient PARP knockout strain. They concluded that the lack of effective DNA repair mechanisms in these strains would increase the global genomic incidence of DNA lesions, and it was postulated that

this would lead to prolonged cell-cycle arrest and thus promote replication fork pausing with subsequent mutagenic slippage (Barber, *et al.*, 2004).

As well as causing problems at the replication fork, secondary structure formation can also be the target for cellular excision repair pathways. Data from CAG•CTG trinucleotide repeats in mice supports a MMR-mediated mechanism of DNA repeat mutation (Manley, *et al.*, 1999; Kovtun and McMurray, 2001; Gomes-Pereira, *et al.*, 2004), whilst in *Escherichia coli* it seems that NER can destabilise repeat arrays (Oussatcheva, *et al.*, 2001). At ESTR loci, Burr *et al.* (2007) observed significantly higher spontaneous mutation rates in homozygous knockout $MSH2^{-/-}$ males compared to wild-type ($MSH2^{+/+}$) and heterozygous ($MSH2^{+/-}$) mice, which suggests that MMR in fact stabilises the ESTR arrays in a process not yet understood. If replication-slippage is the predominant mode of ESTR mutation induction, it could be speculated that MMR has a role in the removal of slipped-structures and their gap-repair synthesis, and so in the absence of the MMR pathway the quadruplexes could persist unhindered at the replication fork and contribute towards replication-slippage mutagenesis.

Other possible modes of ESTR mutation include meiotic and mitotic recombination, and sister chromatid exchanges. Meiotic recombination does not appear to be a big contributor to ESTR mutation induction, given the high somatic instability of ESTRs (Kelly, *et al.*, 1989; Gibbs, *et al.*, 1993), and the lack of a correlation between meiotic crossover events and ESTR mutation frequency (Barber, *et al.*, 2000). This contrasts with minisatellites, which have been shown by small pool (SP-) and minisatellite variant repeat (MVR-) PCR to exhibit both complex internal repeat shuffling (as indicative of germline gene-conversion-type events), and size gains from simple reduplication events (as characteristic of replication slippage and / or sister chromatid exchanges) (Jeffreys, *et al.*, 1994). Unfortunately the procedure of MVR-PCR cannot be applied to ESTRs due to their homogenous internal array of repeat units, and so similar insight cannot be gathered.

Mitotic recombination also appears not to be a major cause of ESTR mutation. It has been suggested that recombination is associated with large size changes, whereas smaller size changes are attributed to replication slippage (Jeffreys, *et al.*, 1988a). Thus, if mitotic recombination was driving ESTR mutation induction, the mutation spectra would be expected to reveal a significant proportion of large mutation events. However, the spectra data in this thesis all show narrow size distributions, with mutations clustering mainly around the ±2–4 repeats range. This would suggest that ESTR mutation by replication slippage is the primary

mechanism, with possible recombination-induced mutations appearing as sporadic large insertion and deletion events.

With all things considered from above, it would appear that DNA replication is the principal cause of ESTR mutation, and this hypothesis would be consistent with the data presented in this thesis.

5.3 Ionising Radiation-Induced ESTR Mutation Induction

The second component of this thesis was to assess the frequency of ionising-radiation-induced ESTR mutation frequency in prenatally developing tissues, and in adult mice of different ages post-irradiation. Several studies have shown that ESTR loci respond to irradiation with an elevated mutation rate (Dubrova, *et al.*, 1993; Sadamoto, *et al.*, 1994; Fan, *et al.*, 1995; Niwa, *et al.*, 1996; Dubrova, *et al.*, 1998; Barber, *et al.*, 2000; Dubrova, *et al.*, 2000a; Dubrova, *et al.*, 2000b; Dubrova and Plumb, 2002; Yauk, *et al.*, 2002; Somers, *et al.*, 2004), and analyses of ESTR mutation spectra of irradiated and non-irradiated animals have revealed striking similarities between the two, indicating that while the mutation frequency increases following irradiation, the underlying mutation mechanism remains the same but is operating at an elevated rate (Dubrova, *et al.*, 1998; Barber, *et al.*, 2000; Barber, *et al.*, 2002; Dubrova, *et al.*, 2002; Barber, *et al.*, 2004; Burr, *et al.*, 2005; Burr, *et al.*, 2006). The nature of this mechanism has been hypothesised to be replication-dependent, with further support coming from the age-related study in this thesis. The data from the irradiation study also suggest an intimate link between DNA replication and ESTR mutation induction by demonstrating that cell division proficient systems generate higher frequencies of ESTR mutation.

The most compelling evidence for this came from the analysis of ESTR mutation frequencies in *in utero*-irradiated brain tissues. Given the likely direct role of DNA replication on spontaneous ESTR mutation and the observed elevation of this process following irradiation, it follows that in any tissue system marked by the same inherent rate of cell division there should be the same frequency of ESTR mutation within an irradiated group, and the same (but lower relative to exposed animals) ESTR mutation frequency within the unexposed cohort. Based on this hypothesis, the brain provides an ideal tissue to study given its differing rates of cell division between its actively dividing prenatal state, and its mitotically-inactive post-natal state. It would be expected that prenatally-developing brain would have the same mutation frequency (whether spontaneous or ionising radiation-induced) as all the other tissues given that embryogenesis is characterised by a uniformly high rate of cell division across all tissues. However, in adult mice when brain tissue becomes

largely non-dividing, the ESTR mutation frequency would be expected to be lower than other tissues of higher proliferation status; even after ionising radiation exposure. The data from this thesis directly support both of these ideas, with Chapter 4 reporting comparable levels of ESTR mutation induction in all the *in utero*-irradiated tissues, whilst Chapter 3 demonstrated that the spontaneous ESTR mutation frequency increases with age only in the mitotically-proficient sperm and not in the mitotically-inactive brain. Moreover, when eight-weeks post-irradiation brain samples were compared to control brain samples there was no change in ESTR mutation frequency, but when they were analysed against *in utero*-irradiated brain they had significantly lower ESTR mutation frequencies. This demonstrates that ionising radiation exposure alone is not sufficient to induce ESTR mutations, but rather mutation induction primarily requires an interaction between DNA damage and replication.

A final piece of evidence from this thesis to suggest that DNA replication-mediated events are causing ESTR mutation induction comes from analysis of the male germline and the timing of ionising radiation-induced mutation induction. The results in Chapter 4 reiterate the observations of previous papers (Dubrova, *et al.*, 1998; Barber, *et al.*, 2000) in suggesting that actively-dividing spermatogonial-irradiated stem cells have significantly higher ESTR mutation frequencies than the non-dividing, terminally-differentiated spermatozoa-irradiated sperm cells, but contradict other work (Sadamoto, *et al.*, 1994; Fan, *et al.*, 1995; Niwa, *et al.*, 1996). In support of the spermatogonial stage of ESTR mutation induction, sperm analyses from Chapter 3 reported that spontaneous ESTR mutation frequencies increase significantly with age in the actively-dividing male germline, and the source of these mutations must be the spermatogonial stem cells, given that these cells persist throughout the life of the mouse (constantly producing new germ cell progenitors), whereas mature sperm are absorbed back into the testes if not used after about one week in the epididymis to be replaced by fresh sperm (Adler, 1996). It is thus concluded that events at DNA replication are driving ESTR mutation induction, and that a destabilising radiation-induced factor is causing the increased frequency of ESTR mutation induction in irradiated tissues. The exact nature of this 'destabilising signal' is not fully understood.

5.4 The Radiation-Induced Damage Signal

The nature of the ionising-radiation-induced DNA-damaging factor hypothesised to cause destabilisation of ESTR loci remains unclear, and was not addressed by the experiments in this thesis. But recent evidence from

transgenerational studies is pointing towards an epigenetic mode of ESTR mutation. Dubrova *et al.* (2000b) and Barber *et al.* (2002) have demonstrated persistently elevated ESTR mutation frequencies in each of the offspring of F_1 and F_2 litters derived from a common irradiated male. This pattern of inheritance was non-Mendelian, and so could not be explained by gene mutations. Instead it was proposed to be the result of an as-of-yet undefined transmissible 'damage signal', and in recent years a number of potential candidates for this signal have emerged, including DNA methylation, histone modifications, and RNA-mediated transactions.

One of the main epigenetic routes to instability could lie in heritable DNA methylation and histone modifications. DNA methylation is well established as a stably inherited epigenetic modification (Rakyan, *et al.*, 2003), but studies have revealed that ionising radiation exposure can induce methylation at certain promoters (Kovalchuk, *et al.*, 2004), and a more general global trend of hypomethylation (Pogribny, *et al.*, 2004), and interestingly, the same is true in the context of ageing, with ageing cells showing a genome-wide hypomethylation (Wilson and Jones, 1983; Richardson, 2002), and promoter hypermethylation (Toyota, *et al.*, 1999; Issa, 2000). When this is considered alongside the findings that DNA hypomethylation can induce chromosomal instability (Eden, *et al.*, 2003), it becomes plausible that heritable and age-related patterns of DNA methylation could contribute towards ESTR instability.

Further evidence for the involvement of DNA methylation in transgenerational instability comes from studies on chemical mutagenesis. Rats exposed to the drug 5-azacytidine were demonstrated to have altered states of sperm DNA methylation (Doerksen, *et al.*, 2000), whilst paternal exposure to cyclophosphamide can disrupt patterns of DNA methylation and histone acetylation during epigenetic programming in the rat pre-implantation embryo (Barton, *et al.*, 2005). But the biggest clue to date that mutagenic exposure can result in transgenerational alterations in methylation status came from an investigation into the transgenerational effects of the endocrine disruptors vinclozolin and methoxychlor, which reported transgenerational alterations in methylation up to the F_4 generation (Anway, *et al.*, 2005). It remains to be seen if a similar transgenerational methylation effect is present following ionising radiation exposure.

In addition to DNA methylation, RNA has recently been implicated as a key epigenetic factor that can cause heritable phenotypic effects. In one study, mutant RNAs were shown to be the causative agent behind non-Mendelian inheritance at the mouse *Kit* locus (Rassoulzadegan, *et al.*, 2006), whilst in another report, RNA molecules were observed as the causative agents of paramutation in maize

(Alleman, *et al.*, 2006). It is possible that these inherited RNAs could mediate transgenerational gene expression by manipulating chromatin domain structure through an RNAi-like mechanism similar to that involved in the maintenance of heterochromatin regions (Fukagawa, *et al.*, 2004), but this remains speculation, and currently cannot be linked to transgenerational DNA repeat instability.

5.5 Future Perspectives

The data from this thesis suggest that events at DNA replication are the principal determinants of ESTR mutation induction, but what still remains unclear is how ionising radiation exposure could destabilise the replication fork in a heritable manner. Determining what this signal is will be of keen interest in forthcoming years.

Recent observations suggest that epigenetic factors could be a potential source of this 'damage signal'. Anway *et al.* (2005) showed that chemical mutagens can induce a heritable change in genomic methylation patterns, while Alleman *et al.* (2006) and Rassoulzadegan *et al.* (2006) each implicated RNA molecules as important transgenerational phenotypic transmitters. Thus it would be reasonable to assume that the ESTR transgenerational instability observed by Dubrova *et al.* (2000b) and Barber *et al.* (2002) was influenced by a similar epigenetically-inherited factor that could be proposed to interfere with DNA replication and induce mutations via stalling of the replication fork.

As well as methylation and RNA, it would be interesting to know if histone modifications could be altered in response to irradiation and if this pattern of modifications could be maintained (possibly through the altered behaviour of *de novo* histone modifying complexes) transgenerationally. Changes to histone modification patterns could have important regulatory consequences for local DNA transactions, as argued by the Histone Code hypothesis (Strahl ad Allis, 2000). It would also be interesting to track the behaviour of PcG/trxG proteins in the context of ESTR mutation frequency to see if these heritable repressors and activators of gene transcription could have important effects. Answering these questions of how epigenetic factors interplay and influence phenotypes such as the mutator-phenotype will be one of the most interesting challenges of the near future.

References

Abraham, R. T. (2001). Cell cycle checkpoint signaling through the ATM and ATR kinases. *Genes and Development* **15**: 2177-2196. [Review].

Acharya, S., Foster, P. L., Brooks, P., and Fishel, R. (2003). The Coordinated Functions of the *E. coli* MutS and MutL Proteins in Mismatch Repair. *Molecular Cell* **12**: 233-246.

Adler, I. D. (1996). Comparison of the duration of spermatogenesis between male rodents and humans. *Mutation Research* **352**: 169-172.

Aggarwal, B. D. and Calvi, B. R. (2004). Chromatin regulates origin activity in Drosophila follicle cells. *Nature* **430**: 372-376.

Alleman, M., Sidorenko, L., McGinnis, K., Seshadri, V., Dorweiler, J. E., White, J., Sikkink, K., and Chandler, V. L. (2006). An RNA-dependent RNA polymerase is required for paramutation in maize. *Nature* **442**: 295-298.

Anway, M. D., Cupp, A. S., Uzumcu, M., and Skinner, M. K. (2005). Epigenetic transgenerational actions of endocrine disruptors and male fertility. *Science* **308**:1466-1469.

Aparicio, O. M., Stout, A. M., and Bell, S. P. (1999). Differential assembly of Cdc45p and DNA polymerases at early and late origins of DNA replication. *Proceedings of the National Academy of Sciences of the United States of America* **96**: 9130-9135.

Aponte, P. M., van Bragt, M. P. A., de Rooij, D. G., and van Pelt, A. M. M. (2005). Spermatogonial stem cells: characteristics and experimental possibilities. *Acta Pathologica, Microbiologica et Immunologica Scandinavica* **113**: 727-742. [Review]

Au, K. G., Welsh, K., and Modrich, P. (1992). Initiation of methyl-directed mismatch repair. *Journal of Biological Chemistry* **267**: 12142-12148.

Azzam, E., De Toledo, S., Gooding, T., and Little, J. (1998). Intercellular communication is involved in the bystander regulation of gene expression in human cells exposed to very low fluences of alpha particles. *Radiation Research* **150**: 497–504.

Bakkenist, C. J., and Kastan, M. B. (2003). DNA damage activates ATM through intermolecular autophosphorylation and dimer dissociation. *Nature* **421**: 499-506.

Banin, S., Moyal, L., Shieh, S., Taya, Y., Anderson, C. W., Chessa, L., Smorodinsky, N. I., Prives, C., Reiss, Y., Shiloh, Y., and Ziv, Y. (1998). Enhanced phosphorylation of p53 by ATM in response to DNA damage. *Science* **281**: 1674-1677.

Bannister, A. J., Zegerman, P., Partridge, J. F., Miska, E. A., Thomas, J. O., Allshire, R. C. and Kouzarides, T. (2001). Selective recognition of methylated lysine 9 on histone H3 by the HP1 chromo domain. *Nature* **410**: 120-124.

Bao, S., Tibbetts, R. S., Brumbaugh, K. M., Fang, Y., Richardson, D. A., Ali, A., Chen, S. M., Abraham, R. T., and Wang, X-F. (2001). ATR/ATM-mediated phosphorylation of human Rad17 is required for genotoxic stress responses. *Nature* **411**: 969-974.

Barber, R. C., Plumb, M. A., Smith, A. G., Cesar, C. E., Boulton, E., Jeffreys, A. J., and Dubrova, Y. E. (2000). No correlation between germline mutation at repeat DNA and meiotic crossover in male mice exposed to X-rays and cisplatin. *Mutation Research* **457**: 79-91.

Barber, R., Plumb, M. A., Boulton, E., Roux, I., and Dubrova, Y. E. (2002). Elevated mutation rates in the germ line of first- and second-generation offspring of irradiated male mice. *Proceedings of the National Academy of Sciences of the United States of America* **99**: 6877-6882.

Barber, R. C., Miccoli, L., van Buul, P. P. W., Burr, K. L-A., van Duyn-Goedhart, A., Angulo, J. F., and Dubrova, Y. E. (2004). Germline mutation rates at tandem repeat loci in DNA-repair deficient mice. *Mutation Research* **554**: 287-295.

Barber, R .C., Hickenbotham, P., Hatch, T., Kelly, D., Topchiy, N., Almeida, G. M., Jones, G. D., Johnson, G. E., Parry, J. M., Rothkamm, K., and Dubrova, Y. E. (2006). Radiation-induced transgenerational alterations in genome stability and DNA damage. *Oncogene* **25**:7336-7342.

Barton, T. S., Robaire, B., and Hales, B. F. (2005). Epigenetic programming in the preimplantation rat embryo is disrupted by chronic paternal cyclophosphamide exposure. *Proceedings of the National Academy of Sciences of the United States of America* **102**: 7865-7870.

Baudat, F., Manova, K., Yuen, J. P., Jasin, M., and Keeney, S. (2000). Chromosome synapsis defects and sexually dimorphic meiotic progression in mice lacking Spo11. *Molecular Cell* **6**: 989-998.

Baumann, P., and West, S. C. (1998). Role of the human RAD51 protein in homologous recombination and double-strand break repair. *Trends in Biochemical Sciences* **23**: 247-251. [Review].

Beckman, K. B., and Ames, B. N. (1997). Oxidative decay of DNA. *Journal of Biological Chemistry*. **272**: 19633-19636. [Review].

Bell, S. P., and Dutta, A. (2002). DNA replication in eukaryotic cells. *Annual Review of Biochemistry* **71**: 333-374. [Review]

Belyakov, O. V., Malcolmson, A. M., Folkard, M., Prise, K. M., and Michael, B. D. (2001). Direct evidence for a bystander effect of ionizing radiation in primary human fibroblasts. *British Journal of Cancer* **84**: 674–679.

Benson, F. E., Baumann, P., and West, S. C. (1998). Synergistic actions of Rad51 and Rad52 in recombination and DNA repair. *Nature* **391**: 401-404.

Bermudez, V. P., Lindsey-Boltz, L. A., Cesare, A. J., Maniwa, Y., Griffith, J. D., Hurwitz, J., and Sancar, A. (2003). Loading of the human 9-1-1 checkpoint complex onto DNA by the checkpoint clamp loader hRad17-replication factor C complex *in vitro*. *Proceedings of the National Academy of Sciences of the United States of America* **100**: 1633–1638.

Blackburn, E. H. (2001). Switching and signalling at the telomere. *Cell* **106**: 661-673.

Blat, Y., Protacio, R., Hunter, N., and Kleckner, N. (2002). Physical and functional interactions among basic chromosome organizational features govern early steps of meiotic chiasma formation. *Cell* **111**: 791-802.

Bird, A. (2002a). DNA methylation patterns and epigenetic memory. *Genes and Development*. **16**: 6–21. [Review].

Bird, A. W., Yu, D. Y., Pray-Grant, M. G., Qiu, Q., Harmon, K. E., Megee, P. C., Grant, P. A., Smith, M. M., and Christman, M. F. (2002b). Acetylation of histone H4 by Esa1 is required for DNA double-strand break repair. *Nature* **419**: 411–415.

Boeger, H., Griesenbeck, J., Stratton J. S., Kornberg, R. D. (2003). Nucleosomes unfold completely at a transcriptionally active promoter. *Molecular Cell* **11**: 1587-1598.

Bois, P., Stead, J. D. H., Bakshi, S., Williamson, J., Neumann, R., Moghadaszadeh, B., and Jeffreys, A. J. (1998a). Isolation and characterization of mouse minisatellites. *Genomics* **50**: 317-330.

Bois, P., Williamson, J., Brown, J., Dubrova, Y. E., and Jeffreys, A. J. (1998b). A novel unstable mouse VNTR family expanded from SINE B1 elements. *Genomics* **49**: 122-128.

Bois, P. R., Southgate, L., and Jeffreys, A. J. (2001). Length of uninterrupted repeats determines instability at the unstable mouse expanded simple tandem repeat family MMS10 derived from independent SINE B1 elements. *Mammalian Genome* **12**: 104-111.

Boyer, L. A., Plath, K., Zeitlinger, J., Brambrink, T., Medeiros, L. A., Lee, T. I., Levine, S. S., Wernig, M., Tajonar, A., Ray, M. K., Bell, G. W., Otte, A. P., Vidal, M., Gifford, D. K., Young, R. A., and Jaenisch, R. (2006). Polycomb complexes repress developmental regulators in murine embryonic stem cells. *Nature* **441**: 349–353.

Bozhenok, L., Wade, P. A., and Varga-Weisz, P. (2002). WSTF-ISW1 chromatin remodelling complex targets heterochromatic replication foci. *EMBO Journal* **21**: 2231-2241.

Briggs, S. D., Bryk, M., Strahl, B. D., Cheung, W. L., Davie, J. K., Dent, S. Y., Wimston, F., and Allis, C. D. (2001). Histone H3 lysine 4 methylation is mediated by Set1 and required for cell growth and rDNA silencing in Saccharomyces cerevisiae. *Genes and Development* **15**: 3286-3295.

Brinkmann, B., Klintschar, M., Neuhaber, F., Huhne, J., and Rolf, B. (1998). Mutation rate in human microsatellites: influence of the structure and length of the tandem repeat. *American Journal of Human Genetics* **62**: 1408-1415.

Brohede, J., Arnheim, N., and Ellegren, H. (2004). Single-molecule analysis of the hypermutable tetranucleotide repeat locus *D21S1245* through sperm genotyping: A heterogenous pattern of mutation but no clear male age effect. *Molecular Biology and Evolution* **21**: 58-64.

Brooks, P. J. (2002). DNA repair in neural cells: basic science and clinical implications. *Mutation Research* **509**: 93-108. [Review].

Burr, K. L-A., Smith, A. G. and Dubrova, Y. E. (2005). p53 deficiency does not affect mutation rate in the mouse germline. *Oncogene* **24**: 4315–4318.

Burr, K. L-A., Velasco-Miguel, S., Duvvuri, V. S., McDaniel, L. D., Friedberg, E. C., and Dubrova, Y. E. (2006). Elevated mutation rates in the germline of *Polk* mutant male mice. *DNA Repair* **5**: 860-862.

Burr, K. L-A., van Duyn-Goedhart, A., Hickenbotham, P., Monger, K., van Buul, P. P. W., and Dubrova, Y. E. (2007). The effects of MSH2 deficiency on spontaneous and radiation-induced mutation rates in the mouse germline. *Mutation Research* **617**: 147-151.

Calsou, P., Delteil, C., Frit, P., Drouet, J., and Salles, B. (2003). Coordinated assembly of Ku and p460 subunits of the DNA-dependent protein kinase on DNA ends is necessary for XRCC4-ligase IV recruitment. *Journal of Molecular Biology* **326**: 93-103.

Cameron, H. A. and McKay, R. D. (2001). Adult neurogenesis produces a large pool of new granule cells in the dentate gyrus. *Journal of Comparative Neurology* **435**: 406-417.

Campuzano, V., Montermini, L., Molto, M. D., Pianese, L., Cossee, M., Cavalcanti, F., Monros, E., Rodius, F., Duclos, F., Monticelli, A., Zara, F., Canizares, J., Koutnikova, H., Bidichandani, S. I., Gellera, C., Brice, A., Trouillas, P., De Michele, G., Filla, A., De Frutos, R., Palau, F., Patel, P. I , Di Donato, S., Mandel, J. L., Cocozza, S., Koenig, M., and Pandolfo, M. (1996). Friedrich's ataxia: autosomal recessive disease caused by an intronic GAA triplet repeat expansion. *Science* **271**: 1423-1427.

Canman, C. E., Lim, D. S., Cimprich, K. A., Taya, Y., Tamai, K., Sakaguchi, K., Appella, E., Kastan, M. B., and Siliciano, J. D. (1998). Activation of the ATM kinase by ionising radiation and phosphorylation of p53. *Science* **281**: 1677-1679.

Capelli, E., Taylor, R., Cervasco, M., Abbondandolo, A., Caldecott, K., and Frosina, G. (1997). Involvement of XRCC1 and DNA ligase III gene products in DNA base excision repair. *Journal of Biological Chemistry* **272**: 23970-23975.

Carson C. T., Schwartz, R. A., Stracker, T. H., Lilley, C .E., Lee, D. V., and Weitzman, M. D. (2003). The Mre11 complex is required for ATM activation and the G2/M checkpoint. *EMBO Journal* **22**:6610-6620.

Cary, R. B., Peterson, S. R., Wang, J., Bear, D. G., Bradbury, E. M., and Chen, D. J. (1997). DNA looping by Ku and the DNA-dependent protein kinase. *Proceedings of the National Academy of Sciences of the United States of America* **94**: 4267-4272.

Chadee, D. N. Hendzel, M. J., Tylipski, C. P., Allis, C. D., Bazett-Jones, D. P., Wright, J. A., and Davie, J. R. (1999). Increased Ser-10 phosphorylation of histone H3 in mitogens-stimulated and oncogene-transformed mouse fibroblasts. *Journal of Biological Chemistry* **274**: 24914-24920.

Chang, W. and Little, J. (1992). Persistently elevated frequency of spontaneous mutations in progeny of CHO clones surviving X-irradiation: association with delayed reproductive death phenotype. *Mutation Research* **270**: 191–199.

Chen, D., Ma, H., Hong, H., Koh, S. S., Huang, S. M., Schurter, B. T., Aswad, D. W., and Stallcup, M. R. (1999). Regulation of transcription by a protein methyltransferase. *Science* **284**: 2174-2177.

Chen, H. Y., Sun, J. M., Zhang, Y., Davie, J. R., and Meistrich, M. L. (1998). Ubiquitination of histone H3 in elongating spermatids of rat testes. *Journal of Biological Chemistry* **273**: 13165-13169.

Cheshier, S. H., Morrison, S. J., Liao, X., and Weissman, I. L. (1999). In vivo proliferation and cell cycle kinetics of long-term self-renewing hematopoietic stem cells. *Proceedings of the National Academy of Sciences of the United States of America* **96**: 3120-3125.

Clark, R. M., De Biase, I., Malykhina, A. P., Al-Mahdawi, S., Pook, M., and Bidichandani, S. I. (2007). The GAA triplet-repeat is unstable in the context of the human FXN locus and displays age-dependent expansions in cerebellum and DRG in a transgenic mouse model. *Human Genetics* **120**: 633-640.

Clarke, A. R., Purdie, C. A., Harrison, D. J., Morris, R. G., Bird, C. C., Hooper, M. L., and Wyllie, A. H. (1993). Thymocyte apoptosis induced by p53-dependent and independent pathways. *Nature* **362**: 849-852.

Clutton, S., Townsend, K., Walker, C., Ansell, J., and Wright, E. (1996). Radiation-induced genomic instability and persisting oxidative stress in primary bone marrow cultures. *Carcinogenesis* **17**: 1633–1639.

Collins, K. and Mitchell, J. R. (2002). Telomerase in the human organism. *Oncogene* **21**: 564-579.

Collins, N., Poot, R. A., Kukimoto, I., Garcia-Jimenez, C., Dellaire, G., and Varga-Weisz, P. (2002). An ACF1-ISW1 chromatin-remodelling complex is required for DNA replication through heterochromatin. *Nature Genetics* **32**: 627-632.

Cook, P. R. (1997). The transcriptional basis of chromosome pairing. *Journal of Cell Science* **110**: 1033-1040. [Review].

Cortez, D., Wang, Y., Qin, J., and Elledge, S. J. (1999). Requirement of ATM-dependent phosphorylation of brca1 in the DNA damage response to double-strand breaks. *Science* **286**: 1162-1166.

Crosio, C., Cermakian, N., Allis, C. D., and Sassone-Corsi, P. (2000). Light induces chromatin modification in cells of the mammalian circadian clock. *Nature Neuroscience* **3**: 1241-1247.

Cuthbert, G. L., Daujat, S., Snowden, A. W., *et al.* (2004). Histone deimination antagonizes arginine methylation. *Cell* **118**: 545-553.

Dahmann, C., Diffley, J. F., and Nasmyth, K. A. (1995). S-phase-promoting cyclin-dependent kinases prevent re-replication by inhibiting the transition of replication origins to a pre-replicative state. *Current Biology* **5**: 1257-1269.

de Magalhaes, J. P. (2005). Open-minded scepticism: inferring the causal mechanisms of human ageing from genetic perturbations. *Ageing Research Reviews* **4**: 1-22. [Review].

De Nadal, E., Zapater, M., Alepuz, P. M., Sumoy, L., Mas, G., and Posas, F. (2004). The MAPK Hog1 recruits Rpd3 histone deacetylase to activate osmoresponsive genes. *Nature* **427**: 370-374.

de Ruijter, A. J., van Gennip, A. H., Caron, H. N., Kemp, S. and van Kuilenberg, A. B. (2003). Histone deacetylases (HDACs): characterisation of the classical HDAC family. *Biochemical Journal* **370**: 737-749. [Review].

Dere, R., Napierala, M., Ranum, L. P., and Wells, R. D. (2004). Hairpin structure-forming propensity of the (CCTG•CAGG) tetranucleotide repeats contributes to the genetic instability associated with myotonic dystrophy type 2. *Journal of Biological Chemistry* **279**: 41715-41726.

Dernberg, A. F., McDonald, K., Moulder, G., Barstead, R., Dresser, M., and Villeneuve, A. M. (1998). Meiotic recombination in *C. elegans* initiates by a conserved mechanism and is dispensable for homologous chromosome synapsis. *Cell* **94**: 387-394.

Doerksen, T., Benoit, G., and Trasler, J. M. (2000). Deoxyribonucleic acid hypomethylation of male germ cells by mitotic and meiotic exposure to 5-azacytidine is associated with altered testicular histology. *Endocrinology* **141**: 3235-3244.

Dou, Y., Milne, T. A., Tackett, A. J., Smith, E. R., Fukuda, A., Wysocka, J., Allis, C. D., Chait, B. T., Hess, J. L., and Roeder, R. G. (2005). Physical association and coordinate function of the H3 K4 methyltransferase MLL1 and the H4 K16 acetyltransferase MOF. *Cell* **121**: 873–885.

Dover, J., Schneider, J., Tawiah-Boateng, M. A., Wood, A., Dean, K., Johnston, M. and Shilatifard, A. (2002). Methylation of histone H3 by COMPASS requires ubiquitination of histone H2B by Rad6. *Journal of Biological Chemistry* **277**: 28368–28371.

Drummond, J. T., Li, G. M., Longley, M. J., and Modrich, P. (1995). Isolation of an hMSH2-p160 heterodimer that restores DNA mismatch repair to tumor cells. *Science* **268**: 1909-1912.

Dubrova, Y. E., Jeffreys, A. J., and Malashenko, A. M. (1993). Mouse minisatellite mutations induced by ionising radiation. *Nature Genetics* **5**: 92-94.

Dubrova, Y. E., Nesterov, V. N., Krouchinsky, N. G., Ostapenko, V. A., Neumann, R., Neil, D. L., and Jeffreys, A. J. (1996). Human minisatellite mutation rate after the Chernobyl accident. *Nature* **380**: 683-686.

Dubrova, Y. E., Plumb, M., Brown, J., Fennelly, J., Bois, P., Goodhead, D., and Jeffreys, A. J. (1998). Stage specificity, dose response, and doubling dose for mouse minisatellite germ-line mutation induced by acute radiation. *Proceedings of the National Academy of Sciences of the United States of America* **95**: 6251-6255.

Dubrova, Y. E., Plumb, M., Brown, J., Boulton, E., Goodhead, D., and Jeffreys, A. J. (2000a). Induction of minisatellite mutations in the mouse germline by low-dose chronic exposure to gamma-radiation and fission neutrons. *Mutation Research* **453**: 17-24.

Dubrova, Y. E., Plumb, M., Gutierrez, B., Boulton, E., and Jeffreys, A. J. (2000b). Genome stability - transgenerational mutation by radiation. *Nature* **405**: 37-37.

Dubrova, Y. E., Bersimbaev, R. I., Djansugurova, L. B., Tankimanova, M. K., Mamyrbaeva, Z., Mustonen, R., Lindholm, C., Hulten, M., and Salomaa, S. (2002). Nuclear weapons tests and human germline mutation rate. *Science* **295**: 1037.

Dubrova, Y. E., and Plumb, M. A. (2002). Ionising radiation and mutation induction at mouse minisatellite loci. The story of the two generations. *Mutation Research* **499**: 143-150.

Dubrova, Y. E. (2005). Radiation-induced mutation at tandem repeat DNA loci in the mouse germline: spectra and doubling doses. *Radiation Research* **163**: 200-207. [Review].

Dufour, E., and Larsson, N. G. (2004). Understanding aging: revealing order out of chaos. *Biochimica et Biophysica Acta* **1658**: 122-132. [Review].

Dupuy, B. M., Stenersen, M., Egeland, T., and Olaisen, B. (2004). Y-chromosomal microsatellite mutation rates: differences in mutation rate between and within loci. *Human Mutation* **23**: 117-124.

Eden, A., Gaudet, F., Waghmare, A., and Jaenisch, R. (2003). Chromosomal instability and tumors promoted by DNA hypomethylation. *Science* **300**: 455.

Eijpe, M., Heyting, C., Gross, B., and Jessberger, R. (2000). Association of mammalian SMC1 and SMC3 proteins with meiotic chromosomes and synaptonemal complexes. *Journal of Cell Science* **113**: 673-682.

Ellegren, H. (2004). Microsatellites: simple sequences with complex evolution. *Nature Reviews Genetics* **5**: 435-445. [Review].

Eriksson, P. S., Perfilieva, E., Björk-Eriksson, T., Alborn, A-M., Nordborg, C., Peterson, D. A. and Gage, F. H. Neurogenesis in the adult human hippocampus. *Nature Medicine* **4**: 1313-1317.

Evans, M. D., Dizdaroglu, M., and Cooke M. S. (2004). Oxidative DNA damage and disease: induction, repair and significance. *Mutation Research* **567**: 1-61. [Review].

Falck, J., Mailand, N., Syljuasen, R. G., Bartek, J., and Lukas, J. (2001). The ATM-Chk2-Cdc25A checkpoint pathway guards against radioresistant DNA synthesis. *Nature* **410**: 842-847.

Fan, Y. J., Wang, Z., Sadamoto, S., Ninomiya, Y., Kotomura, N., Kamiya, K., Dohi, K., Kominami, R., and Niwa, O. (1995). Dose-response of a radiation induction of a germline mutation at a hypervariable mouse minisatellite locus. *International Journal of Radiation Biology* **68**: 177-183.

Favor, J. and Neuhäuser-Klaus, A. (1994). Genetic mosaicism in the house mouse. *Annual Review of Genetics* **28**: 27-47. [Review].

Feinberg, A. P., and Vogelstein, B. (1983). A technique for radiolabeling DNA restriction endonuclease fragments to high specific activity. *Analytical Biochemistry* **132**: 6-13.

Feinberg, A. P., and Vogelstein, B. (1984). "A technique for radiolabeling DNA restriction endonuclease fragments to high specific activity". Addendum. *Analytical Biochemistry* **137**: 266-267.

Finch, J. T., and Klug, A. (1976). Solenoidal model for superstructure of chromatin. *Proceedings of the National Academy of Sciences of the United States of America* **73**: 1897-1901.

Fletcher, R. J., Bishop, B. E., Leon, R. P., Sclafani, R. A., Ogata, C. M., and Chen, X. S. (2003). The structure and function of MCM from archaeal M.thermoautotrophicum. *Nature Structural Biology* **10**: 160-167.

Fojtik, P., and Vorlickova, M. (2001). The fragile X chromosome (GCC) repeat folds into a DNA tetraplex at neutral pH. *Nucleic Acids Research* **29**: 4684-4890.

Fortune, M. T., Vassilopoulos, C., Coolbaugh, M. I., Siciliano, M., and Monckton, D. G. (2000). Dramatic, expansion-biased, age-dependent, tissue-specific somatic mosaicism in a transgenic mouse model of triplet repeat instability. *Human Molecular Genetics* **9**: 439-445.

Fraga, M. F., Ballestar, E., Paz, M. F., Ropero, S., Setien, F., Ballestar, M. L., Heine-Suner, D., Cigudosa, J. C., Urioste, M., Benitez, J., Boix-Chornet, M., Sanchez-Aguilera, A., Ling, C., Carlsson, E., Poulsen, P., Vaag, A., Stephan, Z. Spector, T.D., Wu, Y. Z., Plass, C., and Esteller, M. (2005). Epigenetic differences arise during the lifetime of monozygotic twins. *Proceedings of the. National Academy of Sciences of the United States of America* **102**:10604–10609.

Freidberg, E. C., Walker, G. C., and Siede, W. (1995). DNA repair and mutagenesis. ASM Press, Washington D. C. pp 1-58.

Freudenreich, C. H., Kantrow, S. M., and Zakian V. A. (1998). Expansion and length-dependent fragility of CTG repeats in yeast. *Science* 279: 853-856.

Fukagawa, T., Nogami, M., Yoshikawa, M., Ikeno, M., Okazaki, T., Takami, Y., Nakayama, T., and Oshimura, M. (2004). Dicer is essential for formation of the heterochromatin structure in vertebrate cells. *Nature Cell Biology* 6: 784-791.

Fukuda, H., Katahira, M., Tsuchiya, N., Enokizono, Y., Sugimura, T., Nagao, M., and Nakagama, H. (2002). Unfolding of quadruplex structure in the G-rich strand of the minisatellite repeat by the binding protein UP1. *Proceedings of the National Academy of Sciences of the United States of America* **99**: 12685-12690.

Fung, J. C., Rockmill, B., Odell, M., and Roeder, G. S. (2004). Imposition of crossover interference through the non-random distribution of synapsis initiation complexes. *Cell* **116**: 795-802.

Gage, F. H. (2000). Mammalian neural stem cells. *Science* **287**: 1433-1438. [Review]

Gardner, M. J., Snee, M. P., Hall, A. J., Powell, C. A., Downes, S., and Terrell, J. D. (1990). Results of case-control study of leukaemia and lymphoma among young people near Sellafield nuclear plant in West Cumbria. *British Medical Journal* **300**: 423-429

Genschel, J., Littman, S. J., Drummond, J. T., and Modrich, P. (1998). Isolation of MutSβ from human cells and comparison of the mismatch repair specificities of MutSβ and MutSα. *Journal of Biological Chemistry* **273**: 19895-19901.

Gibbs, M., Collick, A., Kelly, R. G., and Jeffreys, A. J. (1993). A tetranucleotide repeat mouse minisatellite displaying substantial somatic instability during early preimplantation development. *Genomics* **17**: 121-128.

Gibbs, P. E., McDonald, J., Woodgate, R., and Lawrence, C. W. (2005). The relative roles *in vivo* of Saccharomyces cerevisiae Pol eta, Pol zeta, Rev1 protein and Pol32 in the bypass and mutation induction of an abasic site, T-T (6-4) photoadduct and T-T *cis*-syn cyclobutane dimer. *Genetics* **169**: 575-582.

Giménez-Abián, J. F., Clarke, D. C., Mullinger, A. M., Downes, C. S., and Johnson, R. T. (1995). A postprophase topoisomerase II-dependent chromatid core separation step in the formation of metaphase chromosomes. *Journal of Cell Biology* **131**: 7-17.

Goldberg, M., Stucki, M., Falck, J., D'Amours, D., Rahman, D., Pappin, D., Bartek, J., and Jackson, S. P. (2003). MDC1 is required for the intra-S-phase DNA damage checkpoint. *Nature* **421**: 952-956.

Goldmark, J. P., Fazzio, T. G., Estep, P. W., Church, G. M. and Tsukiyama, T. (2000). The Isw2 chromatin remodeling complex represses early meiotic genes upon recruitment by Ume6p. *Cell* **103**: 423–433.

Gomes-Pereira, M., Fortune, T., and Monckton, D. G. (2001). Mouse tissue culture models of unstable triplet repeats: *in vitro* selection for larger alleles, mutational expansion bias and tissue specificity, but no association with cell division rates. *Human Molecular Genetics* **10**: 845-854.

Gomes-Pereira M., Fortune M. T., Ingram L., McAbney J. P., and Monckton D. G. (2004). *Pms2* is a genetic enhancer of trinucleotide (CAG.CTG) repeat somatic mosaicism: implications for the mechanism of triplet repeat expansion. *Human Molecular Genetics* **13**: 1815–1825.

Gordenin, D. A., Kunkel, T. A., and Resnick, M. A. (1997). Repeat expansion – all in a flap? *Nature Genetics* **16**: 116-118.

Goyal, R., Reinhardt, R. and Jeltsch, A. (2006) Accuracy of DNA methylation pattern preservation by the Dnmt1 methyltransferase. *Nucleic Acids Research* **34**: 1182-1188.

Greaves, M. (1996). *The new biology of Leukaemia*. Leukaemia. E.S.L. Henderson, T. A. Greaves, M. F. Philadelphia, Wb Saunders Company.

Green, C. M., and Almouzni, G. (2003). Local action of the chromatin assembly factor CAF-1 at sites of nucleotide excision repair *in vivo*. *EMBO Journal* **22**: 5163-5174.

Grimaud, C., Bantignies, F., Pal-Bhadra, M., Ghana, P., Bhadra, U., and Cavalli, G. (2006). RNAi Components Are Required for Nuclear Clustering of Polycomb Group Response Elements. Cell 124, 957–971.

Gruss, C., Wu, J., Koller, T., and Sogo, J. M. (1993). Disruption of the nucleosomes at the replication fork. *EMBO Journal* **12**: 4533-4545.

Gu, Y., Kai, M., and Kusama, T. (1997). The embryonic and fetal effects in ICR mice irradiated in the various stages of the pre-implantation period. *Radiation Research* **147**: 735-740.

Guillon, H., Baudat, F., Grey, C., Liskay, R. M., and de Massy, B. (2005). Crossover and noncrossover pathways in mouse meiosis. *Molecular Cell* **20**: 563-573.

Guo, G., Wang, W., and Bradley, A. (2004). Mismatch repair genes identified using genetic screens in Blm-deficient embryonic stem cells. *Nature* **429**: 891-895.

Habraken, Y., Sung, P., Prakash, L., and Prakash, S. (1998). ATP-dependent assembly of a ternary complex consisting of a DNA mismatch and the yeast MSH2-MSH6 and MLH1-PMS1 protein complexes. *Journal of Biological Chemistry* **273**: 9837-9841.

Hake, S., Xiao, A., and Allis, C. (2004). Linking the epigenetic 'language' of covalent histone modifications to cancer. *British Journal of Cancer* **90**: 761–769.

Harley, H. G., Brook, J. D., Rundle, S. A., Crow, S., Reardon, W., Buckler, A. J., Harper, P. S., Housman, D. E., and Shaw, D. J. (1992). Expansion of an unstable DNA region and phenotypic variation in myotonic dystrophy. *Nature* **355**: 545-546.

Harper, J. W., Adami, G. R., Wei, N., Keyomarsi, K., and Elledge, S. J. (1993). The p21 Cdk-interacting protein Cip1 is a potent inhibitor of G1 cyclin-dependent kinases. *Cell* **75**: 805-816.

Hayley, C. B., Futcher, A. B., and Greider, C. W. (1990). Telomeres shorten during ageing of human fibroblasts. *Nature* **345**: 458-460.

Hedenskog, M., Sjogren, M., Cederberg, H. and Rannug, U. (1997). Induction of germline-length mutations at the minisatellites PC-1 and PC-2 in male mice exposed to polychlorinated biphenyls and diesel exhaust emissions. *Environmental and Molecular Mutagenesis* **30**: 254-259.

Hoege, C., Pfander, B., Moldovan, G. L., Pyrowolakis, G., and Jentsch, S. (2002). RAD6-dependent DNA repair is linked to modification of PCNA by ubiquitin and SUMO. *Nature* **419**: 135-141.

Hopfner, K-P., Karcher, A., Shin, D. S., Craig, L., Arthur, L. M., Carney, J. P., and Tainer, J. A. (2000). Structural biology of Rad50 ATPase: ATP-driven conformational control in DNA double-strand break repair and the ABC-ATPase superfamily. *Cell* **101**: 789-800.

Hunter, N., and Kleckner, N. (2001). The single-end invasion: an asymmetric intermediate at the double-strand break to double-Holliday junction transition of meiotic recombination. *Cell* **106**: 59-70.

Huntington's Disease Collaborative Research Group. (1993). A novel gene containing a trinucleotide repeat that is expanded and unstable on Huntington's Disease chromosomes. *Cell* **72**: 971–983.

ICRP. (2003). Biological Effects after Prenatal Irradiation. *Annals of the ICRP, ICRP Publication 90*. Pergamon. ed. Valentin, J. pp 11–20 and 23–40.

Inoue, M., Kamiya, H., Fujikawa, K., Ootsuyama, Y., Murata-Kamiya, N., et al. (1998). Induction of chromosomal gene mutations in *Escherichia coli* by direct incorporation of oxidatively damaged nucleotides. New evaluation method for mutagenesis by damaged DNA precursors in vivo. *Journal of Biological Chemistry* **276**: 15155-15163.

Ishimi, Y. (1997). A DNA helicase activity is associated with an MCM4, -6, and -7 protein complex. *Journal of Biological Chemistry* **272**: 24508-24513.

Issa, J. P. (2000). CpG-island methylation in ageing and cancer. *Current Topics in Microbiology and Immunology* **249**: 101-118. [Review].

Jankowski, C., Nasar F., and Nag, D. K. (2000). Meiotic instability of CAG repeat tracts occurs by double-strand break repair in yeast. *Proceedings of the National Academy of Sciences of the United States of America* **97**: 2134–2139.

Jeffreys, A. J., Wilson, V., Kelly, R., Taylor, B. A., and Bulfield, G. (1987). Mouse DNA 'fingerprints': analysis of chromosome localization and germ- line stability of hypervariable loci in recombinant inbred strains. *Nucleic Acids Research* **15**: 2823-2836.

Jeffreys, A. J., Royle, N. J., Wilson, V., and Wong, Z. (1988a). Spontaneous mutation rates to new length alleles at tandem-repetitive hypervariable loci in human DNA. *Nature* **332**: 278-281.

Jeffreys, A. J., Wilson, V., Neumann, R., and Keyte, J. (1988b). Amplification of human minisatellites by the polymerase chain reaction: towards DNA fingerprinting of single cells. *Nucleic Acids Research* **16**: 10953-10971.

Jeffreys, A. J., MacLeod, A., Tamaki, K., Neil, D. L., and Monckton, D. G. (1991). Minisatellite repeat coding as a digital approach to DNA typing. *Nature* **354**: 204-209.

Jeffreys, A. J., Tamaki, K., MacLeod, A., Monckton, D. G., Neil, D. L., and Armour, J. A. (1994). Complex gene conversion events in germline mutation at human minisatellites. *Nature Genetics* **6**: 136-145.

Jeffreys, A. J., and Neumann, R. (1997). Somatic mutation processes at a human minisatellite. *Human Molecular Genetics* **6**: 129-136.

Jeffreys, A. J., Neumann, R., and Wilson, V. (1990). Repeat unit sequence variation in minisatellites: a novel source of DNA polymorphism for studying variation and mutation by single molecule analysis. *Cell* **60**: 473-485.

Kadhim, M., Macdonald, D., Goodhead, D., Lorimore, S., Marsden, S., and Wright, E. (1992). Transmission of chromosomal instability after plutonium alpha-particle irradiation. *Nature* **355**: 738-740.

Kaeberlein, M., McVey, M., and Guarente, L. (1999). The SIR2/3/4 complex and SIR2 alone promote longevity in *Saccharomyces cerevisiae*. *Genes and Development* **13**: 2570-2580.

Kang, S., Jaworski, A., Ohshima, K., and Wells, R. D. (1995). Expansion and deletion of CTG repeats from human disease genes are determined by the direction of replication in *E. coli*. *Nature Genetics* **10**: 213-218.

Katahira, M., Fukuda, H., Kawasumi, H., Sugimura, T., Nakagama H., and Nagao, M. (1999). Intramolecular quadruplex formation of the G-rich strand of the mouse hypervariable minisatellite Pc-1. *Biochemical and Biophysical Research Communications* **264**: 327-333.

Kaufman, M. H., and Bard, J. B. L. (1999). *The Anatomical Basis of Mouse Develpoment*. Academic Press, Harcourt Brace and Company, Publishers. pp 33

Kazazian Jr, H. H. (1999). An estimated frequency of endogenous insertional mutations in humans. *Nature Genetics* **22**: 130.

Keeney, S., Giroux, C. N., and Kleckner, N. (1997). Meiosis-specific DNA double- strand breaks are catalysed by Spo11, a member of a widely conserved protein family. *Cell* **88**: 375-384.

Kellerer, A. M. (2000). Risk estimates for radiation-induced cancer - the epidemiological evidence. *Radiation and Environmental Biophysics* **39**: 17-24.

Kelly, R., Bulfield, G., Collick, A., Gibbs, M., and Jeffreys, A. J. (1989). Characterization of a highly unstable mouse minisatellite locus: evidence for somatic mutation during early development. *Genomics* **5**: 844-856.

Kelly, R., Gibbs, M., Collick, A., and Jeffreys, A. J. (1991). Spontaneous mutation at the hypervariable mouse minisatellite locus *Ms6-hm* - Flanking DNA-sequence and analysis of germline and early somatic mutation events. *Proceedings of the Royal Society of London Series B-Biological Sciences* **245**: 235-245

Keshava, N., and Ong, T-m. (1999). Occupational exposure to genotoxic agents. *Mutation Research* **437**: 175-194. [Review].

Kim, T. H., Barrera, L. O., Zheng, M., Qu, C., Singer, M. A., Richmond, T. A., Wu, Y., Green, R. D., and Ren, B. (2005). A high-resolution map of active promoters in the human genome. *Nature* **436**: 876–880.

Kimura, K., Rybenikov, V. V., Crisona, N. J., Hirano, T., and Cozzarelli, N. R. (1999). 13S condensin actively reconfigures DNA by introducing global positive writhe: implications for chromosome condensation. *Cell* **98**: 239-248.

Kirkpatrick, D. T., Wang, Y. H., Dominska, M., Griffith, J. D., and Petes, T. D. (1999). Control of meiotic recombination and gene expression in yeast by a simple repetitive DNA sequence that excludes nucleosomes. *Molecular and Cellular Biology* **19**:7661–7671.

Kolesnick, R., and Fuks, Z. (2003). Radiation and ceramide-induced apoptosis. *Oncogene* **22**: 5897–906.

Koshland, D. and Strunnikov, A. (1996). Mitotic chromosome condensation. *Annual Review of Cell and Developmental Biology* **12**: 305-333. [Review].

Kouzarides, T., (2002). Histone methylation in transcriptional control. *Current. Opinion in Genetics and Development.* **12**:198–209. [Review].

Kovalchuk, O., Burke, P., Besplug, J., Slovack, M., Filkowski, J., and Pogribny, I. (2004). Methylation changes in muscle and liver tissues of male and female mice exposed to acute and chronic low-dose X-ray-irradiation. *Mutation Research* **548**: 75–84.

Kovtun I. V., and McMurray C. T. (2001). Trinucleotide expansion in haploid germ cells by gap repair. *Nature Genetics* **27**: 407–411.

Kraus, W. L. and Lis, J. J. (2003). PARP goes transcription. *Cell* **113**: 677-683.

Kremer, E. J., Pritchard, M., Lynch, M., Yu, S., Holman, K., Baker, E., Warren, S. T., Schlessinger, D., Sutherland, G. R., and Richards, R. I. (1991). Mapping of DNA instability at the fragile X to a trinucleotide repeat sequence p(CCG)n. *Science* **252**: 1711-1714.

Kubota, Y., Nash, R. A., Klungland, A., Schär, P., Barnes, D. E., and Lindahl, T. (1996). Reconstitution of DNA base-excision repair with purified human proteins: interaction between DNA polymerase β and the XRCC1 protein. *EMBO Journal* **15**: 6662-6670.

Kuhn, H.G., Dickinson-Anson, H. and Gage, F.H. Neurogenesis in the dentate gyrus of the adult rat: Age-related decrease of neuronal progenitor proliferation. *Journal of Neuroscience* **16**: 2027–2033 (1996).

Kumagai, A., and Dunphy, W. G. (2000). Claspin, a novel protein required for the activation of Chk1 during a DNA replication checkpoint response in Xenopus egg extracts. *Molecular Cell* **6**: 839-849.

Kunst, C. B. and Warren, S. T. (1994). Cryptic and polar variation of the fragile X repeat could result in predisposing normal alleles. *Cell* **77**: 853-861.

Lachner, M., O'Carroll, D., Rea, S., Mechtler, K. and Jenuwein, T. (2001). Methylation of histone H3 lysine 9 creates a binding site for HP1 proteins. *Nature* **410**: 116-120.

Lalioti, M. D., Scott, H. S., Buresi, C., Rossier, C., Bottani, A., Morris, M. A., Malafosse, A., and Antonarakis, S. E. (1997). Dodecamer repeat expansion in cystatin B gene in progressive myoclonus epilepsy. *Nature* **386**: 847-851.

La-Spada, A. R., Roling, D. B., Harding, A. E., Warner, C. L., Spiegel, R., Hausmanowa-Petrusewicz, I., Yee, W. C., and Fischbeck, K. H. (1992). Meiotic stability and genotype-phenotype correlation of the trinucleotide repeat in X-linked spinal and bulbar muscular atrophy. *Nature Genetics* **2**: 301-304.

Lee, J. H., and Paull, T. T. (2005). ATM activation by DNA double-strand breaks through the Mre11-Rad50-Nbs1 complex. *Science* **308**: 551-554.

Lehnert, B. and Goodwin, E. (1997). Extracellular factor(s) following exposure to alpha particles can cause sister chromatid exchanges in normal human cells. *Cancer Research* **57**: 2164–2171.

Lewin, B. (2000). DNA is the genetic material. In *Genes VII*, B. Lewin, ed. (Oxford, Oxford University Press), pp. 95.

Li, C. J., Vassilev, A., and DePamphilis, M. L. (2004). Role for Cdk1 (Cdc2)/cyclin A in preventing the mammalian origin recognition complex's largest subunit (Orc1) from binding to chromatin during mitosis. *Molecular Cell Biology* **24**: 5875-5886.

Li, G. and Modrich, P. (1995). Restoration of mismatch repair to nuclear extracts of H6 colorectal tumour cells by a heterodimer of human MutL homologues. *Proceedings of the National Academy of Sciences of the United States of America* **92**: 1950-1954.

Lia, A-S., Seznec, H., Hofmann-Radvanyi, H., Radvanyi, F., Duros, C., Saquet, C., Blanche, M., Junien, C., and Gourdon, G. (1998). Somatic instability of the CTG repeat in mice transgenic for the myotonic dystrophy region is age dependent but not correlated to the relative intertissue transcription levels and proliferative capacities. *Human Molecular Genetics* **7**: 1285-1291.

Lim, D. S., Kim, S. T., Xu, B., Maser, R. S., Lin, J., Petrini, J. H., and Kastan, M. B. (2000). ATM phosphorylates p95/nbs1 in an S-phase checkpoint pathway. *Nature* **404**: 613-617.

Lindahl, T. (1993). Instability and decay of the primary structure of DNA. *Nature* **362**: 709-715.

Ling, H., Boudsocq, F., Plosky, B. S., Woodgate, R., and Yang, W. (2003). Replication of a *cis*-syn thymine dimer at atomic resolution. *Nature* **424**: 1083-1087.

Liquori, C. L., Ricker, K., Moseley, M. L., Jacobsen, J. F., Kress, W., Naylor, S. L., Day, J. W., and Ranum, L. P. (2001). Myotonic dystrophy type 2 caused by a CCTG expansion in intron 1 of ZNF9. *Science* **293**: 864-867.

Liu, Y., Oakeley, E. J., Sun, L., and Jost, J. P. (1998). Multiple domains are involved in the targeting of the mouse DNA methyltransferase to the DNA replication foci. *Nucleic Acids Research* **26**: 1038–1045.

Liu, Z. G., Baskaran, R., Lea-Chou, E. T., Wood, L. D., Chen, Y., Karin M, and Wang, J. Y. (1996). Three distinct signalling responses by murine fibroblasts to genotoxic stress. *Nature* **384**: 273–276.

Lo, W. S., Duggan, L., Emre., N. C., Belotserkovskya, R., Lane, W. S., Shiekhattar, R., and Berger, S. L. (2001). Snf1 – a histone kinase that works in concert with the histone acetyltransferase Gcn5 to regulate transcription. *Science* **293**: 1142-1146.

Loeb, L., Loeb, K., and Anderson, J. (2003). Multiple mutations and cancer. *Proceedings of the National Academy of Sciences of the United States of America* **100**: 776–781.

Lorenzetti, D., Watase, K., Xu, B., Matzuk, M. M., Orr, H. T., and Zoghbi, H. Y. (2000). Repeat instability and motor incoordination in mice with a targeted expanded CAG repeat in the *Sca1* locus. *Human Molecular Genetics* **9**: 779-785.

Lorimore, S.A., Coates, P. J., Scobie, G. E., Milne, G., and Wright, E. G. (2001). Inflammatory-type responses after exposure to ionizing radiation *in vivo*: a mechanism for radiation-induced bystander effects? *Oncogene* **20**: 7085-7095.

Lowe, S. W., Schmitt, E. M., Smith, S. W., Osborne, B. A., and Jacks, T. (1993). p53 is required for radiation-induced apoptosis in mouse thymocytes. *Nature* **362**: 847-849.

Lu, B. Y., Emtage, P. C., Duyf, B. J., Hilliker, A. J., and Eissenberg, J. C. (2000). Heterochromatin protein 1 is required for the normal expression of two heterochromatin genes in *Drosophila*. *Genetics* **155**: 699-708.

Luger, K., Mader, A. W., Richmond, R. K. Sargent, D. F. and Richmond, T. J. (1997). Crystal structure of the nucleosome core particle at 2.8 Å resolution. *Nature* **389**: 251-260

Ma, Y., Pannicke, U., Schwarz, K., and Lieber, M. R. (2002). Hairpin opening and overhang processing by an Artemis/DNA-dependent protein kinase complex in nonhomologous end joining and V(D)J recombination. *Cell* **108**: 781-794.

Mahadevan, L. C., Willis, A. C., and Barratt, M. J. (1991). Rapid histone H3 phosphorylation in response to growth factors, phorbol esters, okadaic acid, and protein synthesis inhibitors. *Cell* **65**: 775-783.

Maiorno, D., Moreau, J., and Mechali, M. (2000). XCDT1 is required for the assembly of ore-replicative complexes in Xenopus laevis. *Nature* **404**: 622-625.

Maki, H. and Sekiguchi, M. (1992). MutT protein specifically hydrolyses a potent mutagenic substrate for DNA synthesis. *Nature* **355**: 273-275.

Manley K., Shirley T. L., Flaherty L., and Messer A. (1999). Msh2 deficiency prevents *in vivo* somatic instability of the CAG repeat in Huntington disease transgenic mice. *Nature Genetics* **23**: 471–473.

Martínez-Balbás, M. A., Dey, A., Rabindran, S. K., Ozato, K., and Wu, C. (1995). Displacement of sequence-specific transcription factors from mitotic chromatin. *Cell* **83**: 29-38.

Matsumoto, Y., Kim, K., Hurwitz, J., Gray, R., Levin, D. S., Tomkinson, A. E., and Park, M. S. Reconstitution of proliferating cell nuclear antigen-dependent repair of apurinic/apyrimidinic sites with purified human proteins. *Journal of Biological Chemistry* **274**:33703-33708.

Matsuoka, S., Huang, M., and Elledge, S. J. (1998). Linkage of ATM to cell cycle regulation by the Chk2 protein kinase. *Science* **282:** 1893-1897.

Matsuura, T., Yamagata, T., Burgess, D. L., Rasmussen, A., Grewal, R. P., Watase, K., Khajavi, M., McCall, A. E., Davis, C. F., Zu, L., Achari, M., Pulst, S. M., Alonso, E., Noebels, J. L., Nelson, D. L., Zoghbi, H. Y., and Ashizawa, T. (2000). Large expansion of the ATTCT pentanucleotide repeat in spinocerebellar ataxia type 10. *Nature Genetics* **26**: 191-194.

McCulloch, S. D., Kokoska, R. J., Masutani, C., Iwai, S., Hanaoka, F., and Kunkel, T. A. (2004). Preferential *cis*-syn thymine dimer bypass by DNA polymerase η occurs with biased fidelity. *Nature* **428**: 97-100.

McGarry, T. J. and Kirschner, M. W. (1998). Germinin, an inhibitor of DNA replication, is degraded during mitosis. *Cell* **93**: 1043-1053.

Metgar, D., and Willis, C. (2000). Evidence for the adaptive evolution of mutation rates. *Cell* **101**: 581-584.

Mimura, S., Masuda, T., Matsui, T., and Takisawa, H. (2000). Central role for cdc45 in establishing an initiation complex of DNA replication in Xenopus egg exracts. *Genes and Cells* **5**: 439-452.

Mirkin, S. M. (2006). DNA structures, repeat expansions, and human hereditary disorders. *Current Opinion in Structural Biology* **16**: 351-358.

Mizuguchi, G., Shen, X., Landry, J., Wu, W. H., Sen, S., and Wu, C. (2004). ATP-driven exchange of histone H2AZ variant catalysed by SWR1 chromatin remodelling complex. *Science* **303**: 343-348.

Modrich, P. (2006). Mechanisms in eukaryotic mismatch repair. *Journal of Biological Chemistry* **281**: 30305-30309. [Review].

Morrison, A. J., Highland, J., Krogan, N. J., Arbel-Eden, A., Greenblatt, J. F., Haber, J. E., and Shen, X. (2004). INO80 and gamma-H2AX interaction links ATP-dependent chromatin remodelling to DNA damage repair. *Cell* **119**: 767-775.

Mothersill, C., Crean, M., Lyons, M., McSweeney, J., Mooney, R., O'Reilly, J., and Seymour, C. B. (1998). Expression of delayed toxicity and lethal mutations in the progeny of human cells surviving exposure to radiation and other environmental mutagens. *International Journal of Radiation Biology* **74**: 673-680.

Mouse Genome Sequencing Consortium. (2002). Initial sequencing and comparative analysis of the mouse genome. *Nature* **420**: 520-562.

Mu, D., Park, C-H., Matsunaga, T., Hsu, D. S., Reardon, J. T., and Sancar, A. (1995). Reconstitution of human DNA repair excision nuclease in a highly defined system. *Journal of Biological Chemistry* **270**: 2415-2418.

Müller, W-U., and Streffer, C. (1990). Lethal and teratogenic effects after exposure to X-rays at various times of early murine gestation. *Teratology* **42**: 643-650

Nakamura, J., and Swenberg, J. A. (1999). Endogenous apurinic/apyrimidinic sites in genomic DNA of mammalian tissues. *Cancer Research* **59**: 2522-2526.

Narita, M., Nunez, S., Heard, E., Lin, A. W., Hearn, S. A., Spector, D. L., Hannon, G. J., and Lowe, S. W. (2003). Rb-mediated heterochromatin formation and silencing of E2F target genes during cellular senescence. *Cell* **113**:703-716.

Neidle, S., and Parkinson, G. N. (2003). The structure of telomeric DNA. *Current Opinion in Structural Biology* **13**: 275-283.

New, J. H., Sugiyama, T., Zaitseva, E., and Kowalczylkowski, S. C. (1998). Rad52 protein stimulates DNA strand exchange by Rad51 and replication protein A. *Nature* **391**: 407–409.

Nguyen, V. Q., Co, C., and Li, J. J. (2001). Cyclin-dependent kinases prevent DNA re-replication through multiple mechanisms. *Nature* **411**: 1068-1073.

Nickel, B. E., and Davie, J. R. (1989). Structure of polyubiquitinated histone H2A. *Biochemistry* **28**: 964-968.

Nishitani, H., Lygerou, Z., Nishimoto, T., and Nurse, P. (2000). The Cdt1 protein is required to license DNA for replication in fission yeast. *Nature* **404**: 625-628.

Niwa, O., Fan, Y. J., Numoto, M., Kamiya, K., and Kominami, R. (1996). Induction of a germline mutation at a hypervariable mouse minisatellite locus by ^{252}Cf radiation. *Journal of Radiation Research* **37**: 217-224.

O'Donovan, A., Davies, A. A., Moggs, J. G., West, S. C., and Wood, R. D. (1994). XPG endonuclease makes the 3' incision in human DNA nucleotide excision repair. *Nature* **371**: 432-435.

Ogi, T., Shinkai, Y., Tanaka, K., and Ohmori, H. (2002). Pol κ protects mammalian cells against the lethal and mutagenic effects of benzo(a)pyrene. *Proceedings of the National Academy of Sciences of the United States of America* **99**: 15548-15553.

Okano, M., Xie, S., and Li, E. (1998). Cloning and characterization of a family of novel mammalian DNA (cytosine-5) methyltransferases. *Nature Genetics* **19**: 219–220.

Okano, M., Bell, D. W., Haber, D. A., and Li, E. (1999). DNA methyltransferases Dnmt3a and Dnmt3b are essential for de novo methylation and mammalian development. *Cell* **99**: 247–257.

Owen, B. A., Yang, Z., Lai, M., Gajek, M., Badger, J. D. II., Hayes, J. J., Edelmann, W., Kucherlapati, R., Wilson, T. M., and McMurray, C. T. (2005). (CAG)n-hairpin DNA binds to Msh2-Msh3 and changes properties of mismatch recognition. *Nature Structural Biology* **12**: 663-670.

Oussatcheva, E. A., Hashem, V. I., Zou, Y., Sinden, R. R., and Potaman, V. N. (2001). Involvement of the nucleotide excision repair protein UvrA in instability of CAG•CTG repeat sequences in *Escherichia coli*. *Journal of Biological Chemistry* **276**: 30878-30884.

Padmore, R., Cao, L., and Kleckner, N. (1991). Temporal comparison of recombination and synaptonemal complex formation during meiosis in *S. cerevisiae*. *Cell* **66**: 1239-1256.

Paeschke, K., Simonsson, T., Postberg, J., Rhodes, D., and Lipps, H. J. (2005). Telomere end-binding proteins control the formation of G-quadruplex DNA structures in vivo. *Nature Structural and Molecular Biology* **12**: 847–854.

Palombo, F., Gallinari, P., Iaccarino, I., Lettieri, T., Hughes, M., D'Arrigo, A., Truong, O., Hsuan, J. J., and Jiricny, J. (1995). GTBP, a 160-kilodalton protein essential for mismatch-binding activity in human cells. *Science* **268**, 1912-1914.

Palombo, F., Iaccarino, I., Nakajima, E., Ikejima, M., Shimada, T., and Jiricny, J. (1996). hMutSβ, a heterodimer of hMSH2 and hMSH3, binds to insertion/deletion loops in DNA. *Current Biology* **6**: 1181-1184.

Pampfer, S., and Streffer, C. (1988). Prenatal death and malformations after irradiation of mouse zygotes with neutrons or X-rays. *Teratology* **37**: 599-607.

Pampfer, S., and Streffer, C. (1989). Increased chromosome aberration levels in cells from mouse fetuses after zygote X-irradiation. *International Journal of Radiation Biology* **55**: 85-92.

Pape,T., Meka, H., Chen, S., Vicentini, G., van Heel, M., and Onesti, S. (2003). Hexameric ring structure of the full-length archaeal MCM protein complex. *EMBO Reports* **4**: 1079-1083.

Park, E. M., Shigenaga, M. K., Degan, P., Korn, T. S., Kitzler, J. W., Wehr, C. M., Kolachana, P., and Ames, B. N. (1992). Assay of excised oxidative DNA lesions: isolation of 8-oxoguanine and its nucleoside derivatives from biological fluids with a monoclonal antibody column. *Proceedings of the National Academy of Sciences of the United States of America* **89**: 3375-3379.

Pascucci, B., Stucki, M., Zophoni, sO. J, Dogliotti, E., and Hubscher, U. (1999). Long-patch base excision repair with purified human proteins. *Journal of Biological Chemistry* **274**: 33696-33702.

Paull, T. T., and Gellert, M. (1998). The 3' to 5' exonuclease activity of Mre11 facilitates repair of DNA double-strand breaks. *Molecular Cell* **1**: 969-979.

Pearson, C. E., Tam, M., Wang, Y. H., Montgomery, S. E., Dar, A. C., Cleary, J. D., and Nichol, K. (2002). Slipped-strand DNAs formed by long (CAG)•(CTG) repeats: slipped-out repeats and slip-out junctions. *Nucleic Acids Research* **30**: 4534-4547.

Peoples, T. L., Dean, E., Gonzalez, O., Lambourne, L., and Burgess, S. M. (2002). Close, stable homolog juxtaposition during meiosis in budding yeast is dependent on meiotic

recombination, occurs independently of synapsis, and is distinct from DSB-independent pairing contacts. *Genes and Development* **16**: 1682-1695.

Piatti, S., Bohm, T., Cocker, J. H., Diffley, J. F., and Nasmyth, K. (1996). Activation of S-phase-promoting CDKs in late G1 defines a "point of no return" after which Cdc6 synthesis cannot promote DNA replication in yeast. *Genes and Development* **10**: 1516-1531.

Pogribny, I., Raiche, J., Slovack, M., and Kovalchuk, O. (2004). Dose-dependence, sex- and tissue-specificity, and persistence of radiation-induced genomic DNA methylation changes. *Biochemical and Biophysical Research Communications* **320**: 1253-1261.

Poot, R. A., Bozhenok, L., van den Berg, D. L., Steffensen, S., Ferreira, F., Grimaldi, M., Gilbert, N., Ferreira, J., and Varga-Weisz, P. D. (2004). The Williams syndrome transcription factor target interacts with PCNA to target chromatin remodelling by ISWI to replication foci. *Nature Cell Biology* **6**: 1236-1244.

Potaman, V. N., Oussatcheva, E. A., Lyubchenko, Y. L., Shylyakhteno, L. S., Bidichandani, S. I., Ashizawa, T., and Sinden, R. R. (2004). Length-dependent structure formation in Freidreich ataxia $(GAA)_n \cdot (TTC)_n$ repeats at neutral pH. *Nucleic Acids Research* **32**: 1224-1231.

Prakash, S., Johnson, R. E., and Prakash, L. (2005). Eukaryotic translesion synthesis DNA polymerases: specificity of structure and function. *Annual Review of Biochemistry* **74**: 317-353. [Review].

Prasad, R., Dianov, G. L., Bohr, V. A., and Wilson, S. H. (2000). FEN1 stimulation of DNA polymerase β mediates an excision step in mammalian long patch base excision repair. *Journal of Biological Chemistry* **275**: 4460-4466.

Rakyan, V. K., Chong, S., Champ, M. E., Cuthbert, P. C., Morgan, H. D., Luu, K. V., and Whitelaw, E. (2003). Transgenerational inheritance of epigenetic states at the murine Axin(Fu) allele occurs after maternal and paternal transmission. *Proceedings of the National Academy of Sciences of the United States of America* **100**: 2538-2543.

Ramsahoye, B. H., Biniszkiewicz, D., Lyko, F., Clark, V., Bird, A. P., and Jaenisch, R. (2000). Non-CpG methylation is prevalent in embryonic stem cells and may be mediated by DNA methyltransferase 3a. *Proceedings of the National Academy of Sciences of the United States of America* **97**: 5237-5242.

Rassoulzadegan, M., Grandjean, V., Gounon, P., Vincent, S., Gillot, I. and Cuzin, F. (2006). RNA-mediated non-mendelian inheritance of an epigenetic change in the mouse. *Nature* **441**: 469-474.

Remus, D., Beall, E. L., and Botchan, M. R. (2004). DNA topology, not DNA sequence, is a critical determinant for *Drosophila* ORC-DNA binding. *EMBO Journal* **23**: 897-907.

Richardson, B. C. (2002). Role of DNA methylation in the regulation of cell function: autoimmunity, ageing and cancer. *Journal of Nutrition* **132**: 2401S-2405S.

Riedl, T., Hanaoka, F., and Egly, J. M. (2003). The comings and goings of nucleotide excision repair factors on damaged DNA. *EMBO Journal* **22**: 5293-5303.

Robertson, K. D., and Wolffe, A. P. (2000). DNA methylation in health and disease. *Nature Reviews Genetics* **1**: 11–19. [Review].

Robzyk, K., Recht, J., and Osley, M. A. (2000). Rad6-dependent ubiquitination of histone H2B in yeast. *Science* **287**: 501-504.

Rockmill, B., Sym, B., Scherthan, H., and Roeder, G. S. (1995). Roles for two RecA homologs in promoting chromosome synapsis. *Genes and Development* **9**: 2684-2695.

Rogakou, E. P., Pilch, D. R., Orr, A. H., Ivanova, V. S., and Bonner, W. M. (1998). DNA double-stranded breaks induce histone H2AX phosphorylation on serine 139. *Journal of Biological Chemistry* **273**: 5858-5868.

Romanienko, P. J. and Camerini-Otero, R. D. (2000). The mouse Spo11 gene is required for meiotic chromosome synapsis. *Molecular Cell* **6**: 975-987.

Rooney, S., Alt, F. W., Lombard, D., Whitlow, S., Eckersdorff, M., Fleming, J., Fugmann, S., Ferguson, D. O., Schatz, D. G., and Sekiguchi, J. (2003). Defective DNA repair and increased genomic instability in Artemis-deficient murine cells. *Journal of Experimental Medicine* **197**: 553-565.

Roth, S. Y., Denu, J. M. and Allis, C. D. (2001). Histone acetyltransferases. *Annual Review of Biochemistry* **70**: 81-120. [Review].

Rouleau, M., Aubin, R. A., Poirier, G. G. (2004). Poly(ADP-ribosyl)ated chromatin domains: access granted. *Journal of Cell Science* **117**: 815-825. [Review]

Russell, W. L., Kelly, E. M., Hunsicker, P. R., Bangham, J. W., Maddux, S. C., and Phipps, E. L. (1979). Specific-locus test shows ethylnitrosourea to be the most potent mutagen in the mouse. *Proceedings of the National Academy of Sciences of the United States of America* **76**: 5818-5819.

Sadamoto, S., Suzuki, S., Kamiya, K., Kominami, R., Dohi, K., and Niwa, O. (1994). Radiation induction of germline mutation at a hypervariable mouse minisatellite locus. *International Journal of Radiation Biology* **65**: 549-557.

Samadashwily, G. M., Raca, G., and Mirkin, S. M. (1997). Trinucleotide repeats affect DNA replication *in vivo*. *Nature Genetics* **17**: 298-304.

Sambrook, J., and Russell, D. W. (2001). Molecular Cloning: A Laboratory Manual. Cold Spring Harbor Laboratory Press, Cold Spring Harbor, New York.

Sanchez, Y., Wong, C., Thoma, R. S., Richman, R., Wu, Z., Piwnica-Worms, H., and Elledge, S.J. (1997). Conservation of the Chk1 checkpoint pathway in mammals: Linkage of DNA damage to Cdk regulation through Cdc25. *Science* **277**: 1497-1501.

Santos-Rosa, H., Schneider, R., Bannister, A. J., Sherriff, J., Bernstein, B. E., Emre, N. C., Schreiber, S. L., Mellor, J., and Kouzarides, T. (2002). Active genes are tri-methylated at K4 of histone H3. *Nature* **419**: 407-411.

Schwacha, A., and Kleckner, N. (1995). Identification of double Holliday junctions as intermediates in meiotic recombination. *Cell* **83**: 783-791.

Searle, A. G. (1974). Mutation induction in mice. In *Advances in Radiation Biology*, eds. Lett, J. T., Adler, H., and Zelle, M. (Academic Press, New York), pp. 131-207.

Selby, C. P., and Sancar, A. (1993). Molecular mechanism of transcription-repair coupling. *Science* **260**: 53-58.

Sharan, S. K., Morimatsu, M, Albrecht, U., Lim, D. S., Regel, E., Dinh, C., Sands, A., Eichele, G., Hasty, P., and Bradley, A. (1997). Embryonic lethality and radiation hypersensitivity mediated by Rad51 in mice lacking Brca2. *Nature* **386**: 804-810.

Shi, Y., Lan, F., Matson, C., Mulligan, P., Whetstine, J., Cole, P., Casero, R., and Shi, Y. (2004). Histone demethylation mediated by the nuclear amine oxidase homolog LSD1. *Cell* **119**: 941-953.

Shiomi, Y., Shinozaki, A., Nakada, D., Sugimoto, K., Usukura, J., Obuse, C., and Tsurimoto, T. (2002). Clamp and clamp loader structures of the human checkpoint protein complexes, Rad9-1-1 and Rad17-RFC. *Genes to Cells* **7**: 861-868.

Shivji, M. K. K., Podust, V. N., Huebscher, U., and Wood, R. D. (1995). Nucleotide excision repair DNA synthesis by DNA polymerase epsilon in the presence of PCNA, RFC, and RPA. *Biochemistry* **34**: 5011 – 5017

Sijbers, A. M., de Laat, W. L., Ariza, R. A., Biggerstaff, M., Wei, Y. F., Moggs, J. G., Carter, K. C., Shell, B. K., Evans, E., de Jong, M. C., Rademakers, S., de Rooij, J., Jaspers, N. G. J., Hoeijmakers, J. H. J., and Wood, R. (1996). Xeroderma pigmentosum group F caused by a defect in a structure-specific DNA repair endonuclease. *Cell* **86**: 811-822.

Smith, L., Plug, A., and Thayer, M. (2001). Delayed replication timing leads to delayed mitotic chromosome condensation and chromosomal instability of chromosome translocations. *Proceedings of the National Academy of Sciences of the United States of America* **98**: 13300–13305.

Somers, C. M., Yauk, C. L., White, P. A., Parfett, C. L. J., and Quinn, J. S. (2002). Air pollution induces heritable DNA mutations. *Proceedings of the National Academy of Sciences of the United States of America* **99**: 15904-15907.

Somers, C. M., Sharma, R., Quinn, J. S., and Boreham, D. R. (2004). Gamma radiation-induced heritable mutations at repetitive DNA loci in out-bred mice. *Mutation Research* **568**: 69-78.

Southern, E. (1979). Measurement of DNA length by gel electrophoresis. *Analytical Biochemistry* **100**: 319-323.

Strahl, B. D. and Allis, D. (2000). The language of covalent histone modifications. *Nature* **403**: 41-45.

Strasser, A., O'Connor, L., Dixit, V. M. (2000). Apoptosis signalling. *Annual Review of Biochemistry* **69**:217-245. [Review].

Su, S.-S., and Modrich, P. (1986). *Escherichia coli mutS*-encoded protein binds to mismatched DNA base pairs. *Proceedings of the National Academy of Sciences of the United States of America* **83**: 5057–5061.

Sudakin, V., Ganoth, D., Dahan, A., Heller, H., Hershko, J., Luca, F. C., Ruderman, J. V., and Hershko, A. (1995). The cyclosome, a large complex containing cyclin-selective ubiquitin-ligase activity, targets cyclins for destruction at the end of mitosis. *Molecular Biology of the Cell* **6**: 185-197.

Sugasawa, K., Ng, J. M. Y., Masutani, C., Iwai, S., van der Spek, P., J., Eker, A. P. M., Hanaoka, F., Bootsma, D., Hoeijmakers, J. H. J. (1998). Xeroderma pigmentosum group C protein complex is the initiator of global genome nucleotide excision repair. *Molecular Cell* **2**: 223-232.

Sugawara, N., Ira, G., and Haber, J. F. (2000). DNA length dependence of the single-strand annealing pathway and the role of *Saccharomyces cerevisiae* RAD59 in double-strand break repair. *Molecular and Cellular Biology* **20**: 5300-5309.

Sullivan, E. K., Weirich, C. S., Guyon, J. R., Sif, S., and Kingston, R. E. (2001). Transcriptional activation domains of human heat shock factor 1 recruit human SWI/SNF. *Molecular and Cellular Biology* **21**: 5826-5837.

Sun, Z. W. and Allis, C. D. (2002). Ubiquitination of histone H2B regulates H3 methylation and gene silencing in yeast. *Nature* **418**: 104-108

Sung, P., and Robberson, D. L. (1995). DNA strand exchange mediated by a RAD51-ssDNA nucleoprotein filament with polarity opposite to that of RecA. *Cell* **82**: 453-461.

Svejstrup, J. Q. (2002). Mechanisms of transcription-coupled DNA repair. *Nature Reviews Molecular Cell Biology* **3**: 21-29. [Review].

Tanaka, T., Fuchs, J., Loidl, J., and Nasmyth, K. (2000). Cohesin ensures bipolar attachment of microtubules to sister centromeres and resists their precocious separation. *Nature Cell Biology* **2**: 492-499.

Theiler, K. (1989). *The House Mouse: Atlas of Embryonic Development.* New York: Springer-Verlag.

Thoma, F., Koller, T., and Klug, A. (1979). Involvement of histone H1 in the organisation of the nucleosome and the salt-dependent superstructures of chromatin. *Journal of Cell Biology* **83**: 402-427.

Tillib, S., Petruk, S., Sedkov, Y., Kuzin, A., Fujioka, M., Goto, T., and Mazo, A. (1999). Trithorax- and Polycomb-group response elements within an Ultrabithorax transcription maintenance unit consist of closely situated but separable sequences, *Molecular and Cellular Biology* **19**: 5189–5202

Tini, M., Benecke, A., Um, S. J., Torchia, J., Evans, R. M., and Chambon, P. (2002). Association of CBP/p300 acetylase and thymine DNA glycosylase links DNA repair and transcription. *Molecular Cell* **9**: 265-277.

Toyota, M., Ahuja, N., Ohe-Toyota, M., Herman, J. G., Baylin S. B., and Issa, J. P. CpG island methylator phenotype in colorectal cancer. (1999). *Proceedings of the National Academy of Sciences of the United States of America* **96**: 8681–8686.

Tsukamoto, Y., Kato, J-i., and Ikeda, H. (1997). Silencing factors participate in DNA repair and recombination in Saccharomyces cerevisiae. *Nature* **388**: 900-903.

Tsurimoto, T. and Stillman, B. (1991). Replication factors required for SV40 DNA replication *in vitro.* II, Switching of DNA polymerase alpha and delta during initiation of leading and lagging strand synthesis. *Journal of Biological Chemistry* **266**: 1961-1968.

Tulin, A. and Spradling, A. (2003). Chromatin loosening by poly(ADP-ribose) polymerase (PARP-1) at *Drosophila* puff loci. *Science* **299**: 560-562.

Uhlmann, F., Wernic, D., Poupart, M. A., Koonin, E. V., and Nasmyth, K. (2000). Cleavage of cohesin by the CD clan protease separin triggers anaphase in yeast. *Cell* **103**: 375-386.

Uma Devi, P., Baskar, R., and Hande, M. P. (1994). Effect of exposure to low-dose gamma radiation during late organogenesis in the mouse fetus. *Radiation Research* **138**: 133-138.

Uma Devi, P., and Hossain, M. (2000a). Induction of tumours in the Swiss albino mouse by low dose foetal irradiation. *International Journal of Radiation Biology* **76**: 95-99.

Uma Devi, P., and Hossain, M. (2000b). Induction of chromosomal instability in mouse haemopoietic cells by fetal irradiation. *Mutation Research* **456**: 33-37.

Umar, A., Buermeyer, A. B., Simon, J. A., Thomas, D. C., Clark, A. B., Liskay, R. M., and Kunkel, T. A. (1996). Requirement for PCNA in DNA mismatch repair at a step preceding DNA resynthesis. *Cell* **87**: 65-73.

UNSCEAR (2000). Sources and Effects of Ionizing Radiation. Volume 1: Sources. (New York, United Nations)

Ura, K., Araki, M., Saeki, H., Masutani, C., Ito, T., Iwai, S., Mizukoshi, T., Kaneda, Y., and Hanaoka, F. (2001). ATP-dependent chromatin remodeling facilitates nucleotide excision repair of UV-induced DNA lesions in synthetic dinucleosomes. *EMBO Journal* **20**: 2004–2014.

Usui, T., Ohta, T., Oshiumi, H., Tomizawa, J-i., Ogawa, H., and Ogawa, T. (1998). Complex formation and functional versatility of Mre11 of budding yeast in recombination. *Cell* **95**: 705-716.

van Attikum, H., Fritsch, O., Hohn, B., and Gasser, S. M. (2004). Recruitment of the INO80 complex by H2A phosphorylation links ATP-dependent chromatin remodelling with DNA double-strand break repair. *Cell* **119**: 777-788.

Van Hooser, A., Goodrich, D. W., Allis, C. D., Brinkley, B. R., and Mancini, M. A. (1998). Histone H3 phosphorylation is required for the initiation, but not maintenance, of mammalian chromosome condensation. *Journal of Cell Science* **111**: 3497-3506.

Verreault, A., Kaufmann, P. D., Kobayashi, R., and Stillman, B. (1996). Nucleosome assembly by a complex of CAF-1 and acetylated histones H3/H4. *Cell* **87**: 95-104.

Vilarino-Guell, C., Smith, A. G., and Dubrova, Y. E. (2003). Germline mutation induction at mouse repeat DNA loci by chemical mutagens. *Mutation Research* **526**: 63-73

Vilkaitis, G., Suetake, I., Klimasauskas, S. and Tajima, S. (2005). Processive methylation of hemimethylated CpG sites by mouse Dnmt1 DNA methyltransferase. *Journal of Biological Chemistry* **280**: 64–72.

Volker, M., Mone, M. J., Karmakar, P., van Hoffen, A., Schul, W., Vermeulen, W., Hoeijmakers, J. H., van Driel, R., van Zeeland, A. A., and Mullenders, L. H. (2001). Sequential assembly of the nucleotide excision repair factors *in vivo*. *Molecular Cell* **8**: 213-224.

Walker, J. R., Corpina, R. A., and Goldberg, J. (2001). Structure of the Ku heterodimer bound to DNA and its implications for double-strand break repair. *Nature* **412**: 607-614.

Walter, J. and Newport, J. (2000). Initiation of eukaryotic DNA replication: origin unwinding, and sequential chromatin association of Cdc45, RPA, and DNA polymerase α. *Molecular Cell* **5**: 617-627.

Wang, B., Matsuoka, S., Carpenter, P. B., and Elledge, S. J. (2002). 53BP1, a mediator of the DNA damage checkpoint. *Science* **298**: 1435-1438.

Wang, G. and Vasquez, K. M. (2006). Non-B DNA structure-induced genetic instability. *Mutation Research* **598**: 103-119. [Review].

Wang, W., Wu, J., Zhang, Z., and Tong, T. (2001). Characterisation of regulatory elements on the promoter region of p16 (INK4a) that contribute to overexpression of p16 in senescent fibroblasts. *Journal of Biological Chemistry* **276**: 48655-48661.

Wang, Y., Wysocka, J., Sayegh, J., Lee, Y-H, Perlin, J. R., Leonelli, L., Sonbuchner, L. S., McDonald, C. H., Cook, R. G., Dou, Y., Roeder, R. G., Clarke, S., Stallcup, M. R., Allis, C. D., and Coonrod, S. A. (2004). Human PAD4 regulates histone arginine methylation levels via demethylimination. *Science* **306**: 279-283.

Warner, H. R. (2005). Longivity genes: from primitive organisms to humans. *Mechanisms of Ageing and Development* **126**: 235-242. [Review].

Weber, J. L., and Wong, C. (1993). Mutation of human short tandem repeats. *Human Molecular Genetics* **2**: 1123-1128.

Weirich-Schwaiger, H., Weirich, H. G., Gruber, B., Schweiger, M., and Hirsch-Kauffmann, M. (1994). Correlation between senescence and DNA repair in cells from young and old individuals and in premature aging syndromes. *Mutation Research* **316**: 37-48.

Weitzmann, M. N., Woodford, K. J., and Usdin, K. (1998). The mouse Ms6-hm hypervariable microsatellite forms a hairpin and two unusual tetraplexes. *Journal of Biological Chemistry* **46**: 30742-30749.

Wells, R. D. (2007). Non-B DNA conformations, mutagenesis and disease. *Trends in Biochemical Science* **32**: 271-278. [Review].

Wilson, V. L., and Jones, P. A. (1983). DNA methylation decreases in ageing but not in immortal cells. *Science* **220**: 1055-1057.

Wohlschlegel, J. A., Dhar, S. K., Prokhorova, T. A., Dutta, A., and Walter, J. C. (2002). Xenopus Mcm10 binds to origins of replication after Mcm2-7 and stimulates origin binding of Cdc45. *Molecular Cell* **9**: 233-240.

Wojciechowska, M., Bacolla, A., Larson, J. E., and Wells, R. D. (2005). The myotonic dystrophy type 1 triplet repeat sequence induces gross deletions and inversions. *Journal of Biological Chemistry* **280**: 941-952.

Wright, W. E., and Shay, J. W. (2000). Telomere dynamics in cancer progression and prevention: fundamental differences in human and mouse telomere biology. *Nature Medicine* **6**: 849-851.

Wu, L. J., Randers-Pehrson, G., Xu, A., Waldren, C. A., Geard, C. R., Yu, Z., and Hei, T. K. (1999). Targeted cytoplasmic irradiation with alpha particles induces mutations in mammalian cells. *Proceedings of the National Academy of Sciences of the United States of America* **96**: 4959-4964.

Wu, X., Wilson, T. E., and Lieber, M. R. (1999). A role for FEN-1 in nonhomologous DNA end joining: the order of strand annealing and nucleolytic processing events. *Proceedings of the National Academy of Sciences of the United States of America* **96**: 1303-1308.

Xu, B., Kim, S.-T., and Kastan, M. B. (2001). Involvement of Brca1 in S-phase and G_2-phase checkpoints after ionizing irradiation. *Molecular and Cellular Biology* **21**: 3445-3450.

Yamaguchi, M., Dao, V., and Modrich, P. (1998). MutS and MutL activate DNA helicase II in a mismatch-dependent manner. *Journal of Biological Chemistry* **273**: 9197–9201.

Yamane, K., Wu, X., and Chen, J. (2002) A DNA damage-regulated BRCT-containing protein, TopBP1, is required for cell survival. *Molecular and Cellular Biology* **22**: 555–566.

Yauk, C. L., and Quinn, J. S. (1996). Multilocus DNA fingerprinting reveals high rate of heritable genetic mutation in herring gulls nesting in an industrialized urban site. *Proceedings of the National Academy of Sciences of the United States of America* **93**: 12137-12141.

Yauk, C. L., Dubrova, Y. E., Grant, G. R., and Jeffreys, A. J. (2002). A novel single molecule analysis of spontaneous and radiation-induced mutation at a mouse tandem repeat locus. *Mutation Research* **500**: 147-156.

Yoder, J. A., Soman, N. S., Verdine, G. L., and Bestor, T. H. (1997). DNA (cytosine-5)-methyltransferases in mouse cells and tissues. Studies with a mechanism-based probe. *Journal of Molecular Biology* **270**: 385–395.

Yu, H. G., and Koshland, D. E. (2003). Meiotic condensin is required for proper chromosome compaction, SC assembly, and resolution of recombination-dependent chromosome linkages. *Journal of Cell Biology* **163**: 937-947.

Yu, Y., Teng, Y., Liu, H., Reed, S. H., and Waters, R. (2005). UV irradiation stimulates histone acetylation and chromatin remodelling at a repressed yeast locus. *Proceedings of the National Academy of Sciences of the United States of America* **102**: 8650–8655.

Zhang, Y. and Reinberg, D. (2001). Transcription regulation by histone methylation: interplay between different covalent modifications of the core histone tails. *Genes and Development* **15**: 2343–2360.

Zheng, N., Monckton, D. G., Wilson, G., Hagemeister, F., Chakraborty, R., Connor, T. H., Siciliano, M. J., and Meistrich, M. L. (2000). Frequency of minisatellite repeat number changes at the MS205 locus in human sperm before and after cancer chemotherapy. *Environmental and Molecular Mutagenesis* **36**: 134-145.

Zou, L. and Stillman, B. (2000). Assembly of a Complex Containing Cdc45p, Replication Protein A, and Mcm2p at Replication Origins Controlled by S-Phase Cyclin-Dependent Kinases and Cdc7p-Dbf4p Kinase. *Molecular and Cellular Biology* **20**: 3086-3096.

Zou, L., Liu, D., and Elledge, S. J. (2003). Replication protein A-mediated recruitment and activation of Rad17 complexes. *Proceedings of the National Academy of Sciences of the United States of America* **100**: 13827-13832.